New logotropic model based on a complex scalar field
with a logarithmic potential

Pierre-Henri Chavanis[*]

Laboratoire de Physique Théorique, Université de Toulouse, CNRS, UPS, Toulouse, France

We introduce a new logotropic model based on a complex scalar field with a logarithmic potential that unifies dark matter and dark energy. The scalar field satisfies a nonlinear wave equation generalizing the Klein-Gordon equation in the relativistic regime and the Schrödinger equation in the nonrelativistic regime. This model has an intrinsically quantum nature and returns the Λ cold dark matter (CDM) model in the classical limit $\hbar \to 0$. It involves a new fundamental constant of physics $A/c^2 = 2.10 \times 10^{-26} \, \mathrm{g\,m^{-3}}$ responsible for the late accelerating expansion of the Universe and superseding the Einstein cosmological constant Λ. The logotropic model is almost indistinguishable from the ΛCDM model at large (cosmological) scales but solves the CDM crisis at small (galactic) scales. It also solves the problems of the fuzzy dark matter model. Indeed, it leads to cored dark matter halos with a universal surface density $\Sigma_0^{\mathrm{th}} = 5.85(A/4\pi G)^{1/2} = 133 \, M_\odot/\mathrm{pc}^2$. This universal surface density is predicted from the logotropic model without adjustable parameter and turns out to be close to the observed value $\Sigma_0^{\mathrm{obs}} = 141_{-52}^{+83} \, M_\odot/\mathrm{pc}^2$. We also argue that the quantities $\Omega_{\mathrm{dm},0}$ and $\Omega_{\mathrm{de},0}$, which are usually interpreted as the present proportions of dark matter and dark energy in the ΛCDM model, are equal to $\Omega_{\mathrm{dm},0}^{\mathrm{th}} = \frac{1}{1+e}(1 - \Omega_{\mathrm{b},0}) = 0.2559$ and $\Omega_{\mathrm{de},0}^{\mathrm{th}} = \frac{e}{1+e}(1 - \Omega_{\mathrm{b},0}) = 0.6955$ in very good agreement with the measured values $\Omega_{\mathrm{dm},0}^{\mathrm{obs}} = 0.2589$ and $\Omega_{\mathrm{de},0}^{\mathrm{obs}} = 0.6911$ (their empirical ratio 2.669 is close to the Euler number $e = 2.71828\ldots$). We point out, however, important difficulties with the logotropic model, similar to those encountered by the generalized Chaplygin gas model. These problems are related to the difficulty of forming large-scale structures due to an increasing speed of sound as the Universe expands. We discuss potential solutions to these problems, stressing in particular the importance to perform a nonlinear study of structure formation.

I. INTRODUCTION

The nature of dark matter (DM) and dark energy (DE) is still unknown and remains one of the greatest mysteries of cosmology. In a previous paper [1] (see also [2–4]), we have introduced an exotic fluid, called the logotropic dark fluid (LDF), that unifies DM and DE in the spirit of a generalized Chaplygin gas model.[1] The LDF is characterized by the equation of state [1–4]

$$P = A \ln\left(\frac{\rho_m}{\rho_P}\right), \tag{1}$$

where $\rho_m = nm$ is the rest-mass density, $\rho_P = 5.16 \times 10^{99} \, \mathrm{g/m^3}$ is the Planck density, and $A/c^2 = 2.10 \times 10^{-26} \, \mathrm{g\,m^{-3}}$ is a constant interpreted as a new

fundamental constant of physics superseding the Einstein cosmological constant Λ. For $\rho_m < \rho_P$, the pressure of the LDF is negative.[2] At early times, the pressure is negligible with respect to the energy density and the LDF behaves like the pressureless cold dark matter (CDM) model. At later times, the negative pressure of the LDF becomes efficient and explains the acceleration of the Universe that we observe today. We obtained very encouraging results [1–4]. At large (cosmological) scales, the logotropic model is almost indistinguishable from the ΛCDM model up to the present time for what concerns the evolution of the homogeneous background. The two models will differ in about 25 Gyr when the logotropic model will start to exhibit a phantom behavior, i.e., the energy density will increase with the scale factor, leading to a super–de Sitter era where the scale factor increases

---

[2]The logotropic model is not valid in the primordial Universe so that, in practice, the LDF exhibits a negative pressure, as required to explain the acceleration of the Universe today.

as $a \sim e^{t^2}$.[3] At small (galactic) scales, the logotropic model is able to solve the small-scale crisis of the CDM model. Indeed, contrary to the pressureless CDM model, the logotropic equation of state provides a pressure gradient that can balance the gravitational attraction and prevent gravitational collapse. As a result, logotropic DM halos present a central core rather than a cusp, in agreement with the observations. In addition, a very nice property of the logotropic equation of state is that it generates DM halos with a universal surface density. Its predicted value $\Sigma_0^{\text{th}} = 5.85(A/4\pi G)^{1/2} = 133 \, M_\odot/\text{pc}^2$ turns out to be close to the observed value $\Sigma_0^{\text{obs}} = 141_{-52}^{+83} \, M_\odot/\text{pc}^2$ [15–17]. This is remarkable because there is no adjustable parameter in our model [1–4]. The logotropic model implies that the mass of dwarf galaxies enclosed within a sphere of fixed radius $r_u = 300$ pc has a universal value $M_{300}^{\text{th}} = 1.82 \times 10^7 \, M_\odot$, i.e., $\log(M_{300}^{\text{th}}/M_\odot) = 7.26$, in agreement with the observations giving $\log(M_{300}^{\text{obs}}/M_\odot) = 7.0_{-0.4}^{+0.3}$ [18]. The logotropic model also reproduces the Tully-Fisher relation $M_b \propto v_h^4$, where M_b is the baryonic mass and v_h is the circular velocity at the halo radius, and predicts a value of the ratio $(M_b/v_h^4)^{\text{th}} = 46.4 \, M_\odot \, \text{km}^{-4} \, \text{s}^4$ which is close to the observed value $(M_b/v_h^4)^{\text{obs}} = 47 \pm 6 \, M_\odot \, \text{km}^{-4} \, \text{s}^4$ [19].

In the present paper, we introduce a related, but different, logotropic model. We develop a field theory based on the Klein-Gordon (KG) equation in general relativity for a complex scalar field (SF) with a logarithmic potential.[4] In the fast oscillation regime, which is equivalent to the Thomas-Fermi (TF) approximation $\hbar \to 0$, this complex SF generates a logotropic equation of state similar to Eq. (1) except that the rest-mass density ρ_m is replaced by a pseudo-rest-mass density ρ related to the squared modulus of the SF. This new logotropic model is similar to the previous one (conserving its main virtues), except that it does not display a phantom behavior in the future but rather a late de Sitter era. Indeed, the energy density always decreases as the Universe expands and tends to a constant $\epsilon_{\min}$ like in the ΛCDM model but with a slightly different value. Correspondingly, the speed of sound is real and always smaller than the speed of light while, in the original logotropic model [1–4], the speed of sound was diverging at the entry of the phantom regime before becoming imaginary. Therefore, the new logotropic model avoids

some pathologies of the original logotropic model such as a phantom behavior (violation of the dominant-energy condition $P/\epsilon > -1$ and little rip) and a superluminal or imaginary speed of sound. It rather asymptotically approaches a well-behaved de Sitter era. Therefore, the new logotropic model interpolates a regime of dust-dominated Universe to a vacuum-energy-dominated Universe, providing an explanation for the possible accelerating phase today: For small values of the scale factor, the LDF exhibits the same behavior as a pressureless fluid; for large values of the scale factor, it approaches the equation of state of a cosmological constant.

The logotropic complex SF model is based on a nonlinear KG equation involving a logarithmic potential whose strength is measured by the logotropic constant A. We argue that this constant does not correspond to a particular characteristic of the SF (such as its mass m or self-interaction constant λ) but that it has a fundamental and universal nature.[5] In our model, this constant is responsible for the accelerating expansion of the Universe and, at the same time, for the universality of the surface density of DM halos. In the nonrelativistic limit, the nonlinear KG equation reduces to a nonlinear Schrödinger equation which has the form of a generalized Gross-Pitaevskii (GP) equation with a logarithmic potential.

The aim of this paper is to develop the logotropic complex SF model in detail and to compare it with other models such as the original logotropic model, the ΛCDM model, and the fuzzy dark matter (FDM) model. The paper is organized as follows. In Sec. II, we summarize the theory developed in [20–22] for a spatially homogeneous complex SF with an arbitrary potential $V(|\varphi|^2)$ evolving in an expanding background. We consider in particular the fast oscillation regime, equivalent to the TF approximation, where the equations can be simplified and where the SF behaves as a fluid with a barotropic equation of state $P(\rho)$ determined by the SF potential. In Sec. III, we consider a logarithmic potential and show that it leads to a logotropic equation of state. In Sec. IV, we determine the rest-mass density and the internal energy of the LDF which represent DM and DE, respectively. In Sec. V, we study the evolution of the LDF, stressing that it behaves as DM in the early Universe and as DE in the late Universe. In Sec. VI, we determine the fundamental constant A (and the equivalent dimensionless constant B) of our model from cosmological considerations. We argue that the quantities $\Omega_{\text{dm},0}$ and $\Omega_{\text{de},0}$, which are usually interpreted as the present proportions of DM and DE in the ΛCDM model, are equal to

---

[3]By contrast, in the ΛCDM model, the energy density tends to a constant ϵ_Λ leading to a de Sitter era where the scale factor increases as $a \sim e^t$. Note that the increase of the energy density ϵ with a in the logotropic model is slow—logarithmic. As a result, there is no future finite time singularity (no "big rip") [13]. The energy density becomes infinite in infinite time. This is called "little rip" [14].

[4]Most authors describe DM and DE by a real SF. Here, we consider a complex SF based on the general formalism developed in [20–22] for an arbitrary potential. It could be called the CSF model.

[5]This term should be present in all SF theories even though it may be negligible in certain cases. In other words, a SF with a purely logarithmic potential is considered to be massless and noninteracting. We can then introduce specific attributes of the SF such as a mass term $\frac{1}{2}m^2|\varphi|^2$ and a self-interaction term like a quartic potential $\frac{1}{4}\lambda|\varphi|^4$.

$\Omega^{\text{th}}_{\text{dm},0} = \frac{1}{1+e}(1 - \Omega_{\text{b},0}) = 0.2559$ and $\Omega^{\text{th}}_{\text{de},0} = \frac{e}{1+e}(1 - \Omega_{\text{b},0}) = 0.6955$ in very good agreement with the measured values $\Omega^{\text{obs}}_{\text{dm},0} = 0.2589$ and $\Omega^{\text{obs}}_{\text{de},0} = 0.6911$ (their empirical ratio 2.669 is close to the Euler number $e = 2.71828...$). In Sec. VII, we write the equations of the problem in dimensionless form and study the cosmic evolution of the LDF. We show that the ΛCDM model is recovered in the limit $B \to 0$ which corresponds to $\hbar \to 0$. Therefore, the ΛCDM model can be viewed as the classical limit of the logotropic model (it corresponds to a dark fluid with a constant pressure $P = -\epsilon_\Lambda$ or to a complex SF with a constant potential $V = \epsilon_\Lambda$). In Sec. VIII, we determine the effective proportions of DM and DE in the logotropic model. In Secs. IX and X, we study the evolution of the deceleration parameter and speed of sound. We show that the speed of sound increases from $c_s = 0$ to $c_s = c$ as the Universe expands. In Sec. XI, we study the evolution of the scale factor. In Sec. XII, we determine the total SF potential including the rest-mass term and the potential term and discuss the motion of the SF in this potential in relation to the phenomenon of spintessence. In Sec. XIII, we determine the validity of the fast oscillation regime. We first show that it imposes the condition $m \gg m_\Lambda$ on the mass of the SF, where $m_\Lambda = (\Lambda\hbar^2/3c^4)^{1/2} = 1.20 \times 10^{-33}$ eV/c^2 is the cosmon mass. We then show that the SF undergoes a stiff matter era (in the slow oscillation regime) prior to the DM and DE eras. We also argue that the fast oscillation regime ceases to be valid at very late times and we determine the dynamical phase diagram of the logotropic model. In Sec. XIV, we discuss the analogies and the differences between the logotropic model and the ΛCDM model. We show that the asymptotic energy density ϵ_{min} in the logotropic model is slightly larger than the asymptotic energy density ϵ_Λ in the ΛCDM model. They differ by a factor 1.02. We also show that the logotropic model leads to DM halos with a universal surface density consistent with the observations, while the CDM model leads to cuspy density profiles that are not observed. In Sec. XV, we go beyond the TF approximation and describe DM halos in terms of the logotropic GP equation. Their equilibrium state is determined by a quantum Lane-Emden equation of index $n = -1$. Quantum logotropic DM halos have a quantum core (soliton), an inner logotropic envelope where the density decreases as $\rho \sim r^{-1}$ (responsible for the constant surface density of DM halos), and an outer Navarro-Frenk-White (NFW) envelope where the density decreases as r^{-3}, or an outer isothermal envelope where the density decreases as r^{-2}. The classical logotropic model is recovered in the TF approximation $\hbar \to 0$. On the other hand, the FDM model is recovered in the limit $B \to 0$. We mention that the inner logotropic envelope solves the problems of the FDM model reported in our previous papers [23–25] (see also [26,27]). In Sec. XVI, we study the Jeans instability of an expanding logotropic Universe by using a nonrelativistic approach. We show that the speed of sound and the comoving Jeans length increase as the Universe expands. As a result, the density contrast first increases like in the ΛCDM model, then undergoes damped oscillations. This is the same behavior as in the generalized Chaplygin gas (GCG) model and the opposite behavior as in the FDM model. We explain that this behavior poses problems for the formation of structures and we discuss possible solutions that have been invoked in the context of the GCG model. In particular, we stress the importance to perform a nonlinear study of structure formation. The Appendices provide complements to our main results. In Appendix A, we recall the motivations of the logotropic model and explain that it can be regarded as the simplest generalization of the ΛCDM model. In Appendix B, in line with [21], we show that different types of logotropic models can be introduced depending on whether the pressure is specified in terms of the energy density, the rest-mass density, or the pseudo-rest-mass density (the present model corresponds to a logotropic model of type III in the terminology of [21]). In Appendix C, we extend certain results of the Jeans instability study to the case of DM with a linear equation of state. In Appendix D, we discuss different equivalent versions of the ΛCDM model. In Appendix E, we discuss the main properties of the ΛFDM model. In Appendix F, we describe the structure of logotropic DM halos. In Appendix G, we determine the typical mass of the DM particle in the quantum logotropic model.

II. COMPLEX SF THEORY

In this section, we recall the basic equations governing the cosmological evolution of a spatially homogeneous complex SF with an arbitrary self-interaction potential in a Friedmann-Lemaître-Robertson-Walker (FLRW) universe. We also recall how these equations can be simplified in the fast oscillation regime (equivalent to the classical or TF approximation) that will be considered in the following sections. We refer to our previous papers [20–22] and references therein for a more detailed discussion.

A. Spatially homogeneous SF

Let us consider a complex SF φ with a self-interaction potential $V(|\varphi|^2)$ described by the KG equation. For a spatially homogeneous SF $\varphi(t)$ evolving in an expanding background, the KG equation takes the form[6]

$$\frac{1}{c^2}\frac{d^2\varphi}{dt^2} + \frac{3H}{c^2}\frac{d\varphi}{dt} + \frac{m^2c^2}{\hbar^2}\varphi + 2\frac{dV}{d|\varphi|^2}\varphi = 0, \quad (2)$$

where $H = \dot{a}/a$ is the Hubble parameter and $a(t)$ is the scale factor. The second term in Eq. (2) is the Hubble drag. The rest-mass term (third term) can be written as φ/λ_C^2,

---

[6]See, e.g., Refs. [20–22,28–31] and Sec. XV for the general expression of the KG equation valid for possibly inhomogeneous systems.

where $\lambda_C = \hbar/mc$ is the Compton wavelength defined with the mass m of the SF. The total potential including the rest-mass term and the self-interaction term reads

$$V_{\text{tot}}(|\varphi|^2) = \frac{m^2 c^2}{2\hbar^2}|\varphi|^2 + V(|\varphi|^2). \qquad (3)$$

The energy density $\epsilon(t)$ and the pressure $P(t)$ of the SF are given by

$$\epsilon = \frac{1}{2c^2}\left|\frac{d\varphi}{dt}\right|^2 + \frac{m^2 c^2}{2\hbar^2}|\varphi|^2 + V(|\varphi|^2), \qquad (4)$$

$$P = \frac{1}{2c^2}\left|\frac{d\varphi}{dt}\right|^2 - \frac{m^2 c^2}{2\hbar^2}|\varphi|^2 - V(|\varphi|^2). \qquad (5)$$

The equation of state parameter is defined by $w = P/\epsilon$.

The Friedmann equations determining the evolution of the homogeneous background are

$$\frac{d\epsilon}{dt} + 3H(\epsilon + P) = 0 \qquad (6)$$

and

$$H^2 = \frac{8\pi G}{3c^2}\epsilon - \frac{kc^2}{a^2} + \frac{\Lambda}{3}, \qquad (7)$$

where Λ is the cosmological constant and k determines the curvature of space. The universe may be closed ($k > 0$), flat ($k = 0$), or open ($k < 0$). In this paper, we consider a flat universe ($k = 0$) in agreement with the inflation paradigm [32] and the observations of the cosmic microwave background (CMB) [33,34]. On the other hand, we set $\Lambda = 0$ because the acceleration of the expansion of the Universe will be taken into account in the potential of the SF (see below). The Friedmann equation (7) then reduces to the form

$$H^2 = \frac{8\pi G}{3c^2}\epsilon. \qquad (8)$$

The Friedmann equations can be derived from the Einstein field equations by using the FLRW metric [35]. The energy conservation equation (6) can also be obtained from the KG equation (2) by using Eqs. (4) and (5) (see Appendix G of [21]).[7] Once the SF potential $V(|\varphi|^2)$ is given, the Klein-Gordon-Friedmann (KGF) equations provide a complete set of equations that can in principle be solved to obtain the evolution of the Universe, assuming that the energy density is entirely due to the SF. To complete the description one can introduce radiation and baryonic matter as independent species but, for simplicity, we shall not consider their effect here.

B. Charge of the SF

Writing the complex SF as

$$\varphi = |\varphi|e^{i\theta}, \qquad (9)$$

where $|\varphi|$ is the modulus of the SF and θ is its argument (angle), inserting this decomposition into the KG equation (2) and separating the real and imaginary parts, we obtain the following pair of equations:

$$\frac{1}{c^2}\left(2\frac{d|\varphi|}{dt}\frac{d\theta}{dt} + |\varphi|\frac{d^2\theta}{dt^2}\right) + \frac{3H}{c^2}|\varphi|\frac{d\theta}{dt} = 0, \qquad (10)$$

$$\frac{1}{c^2}\left[\frac{d^2|\varphi|}{dt^2} - |\varphi|\left(\frac{d\theta}{dt}\right)^2\right] + \frac{3H}{c^2}\frac{d|\varphi|}{dt}$$
$$+ \frac{m^2 c^2}{\hbar^2}|\varphi| + 2\frac{dV}{d|\varphi|^2}|\varphi| = 0. \qquad (11)$$

Equation (10) can be rewritten as a conservation equation

$$\frac{d}{dt}\left(a^3|\varphi|^2\frac{d\theta}{dt}\right) = 0. \qquad (12)$$

Introducing the pulsation $\omega = -\dot{\theta}$, we get

$$\omega = \frac{Q\hbar c^2}{a^3|\varphi|^2}, \qquad (13)$$

where Q is a constant of integration which represents the conserved charge of the complex SF [20–22,28,29,36,37] (see Sec. II G).[8] Note that this equation is exact. On the other hand, in the fast oscillation regime $\omega = d\theta/dt \gg H = \dot{a}/a$ where the pulsation is high with respect to the Hubble expansion rate, Eq. (11) reduces to

$$\omega^2 = \frac{m^2 c^4}{\hbar^2} + 2c^2\frac{dV}{d|\varphi|^2}. \qquad (14)$$

For a free field ($V = 0$), the pulsation ω is proportional to the mass of the SF ($\omega = mc^2/\hbar$) and the fast oscillation condition reduces to $mc^2/\hbar \gg H$. Combining Eqs. (13) and (14), we obtain

$$\frac{Q^2\hbar^2 c^4}{a^6|\varphi|^4} = \frac{m^2 c^4}{\hbar^2} + 2c^2\frac{dV}{d|\varphi|^2}. \qquad (15)$$

This equation relates the modulus $|\varphi|$ of the SF to the scale factor a in the fast oscillation regime. The pulsation ω of the SF is then given by Eq. (13) or (14).

---

[7]Inversely, the KG equation (2) can be obtained from the energy conservation equation (6).

[8]The conservation of the charge results from the global $U(1)$ symmetry of the Lagrangian of a complex SF. There is no such conservation law for a real SF.

C. Spintessence

According to Eqs. (11) and (13) we have

$$\frac{d^2|\varphi|}{dt^2} + 3H\frac{d|\varphi|}{dt} + \frac{m^2c^4}{\hbar^2}|\varphi| + 2c^2\frac{dV}{d|\varphi|^2}|\varphi| - \frac{Q^2\hbar^2c^4}{a^6|\varphi|^3} = 0,$$ (16)

where H is given by Eq. (8). This equation is exact. It determines the evolution of the modulus of the complex SF. It differs from the KG equation of a real SF by the presence of the last term and the fact that φ is replaced by $|\varphi|$. The energy density and the pressure are given by

$$\epsilon = \frac{1}{2c^2}\left(\frac{d|\varphi|}{dt}\right)^2 + \left(\frac{\omega^2}{2c^2} + \frac{m^2c^2}{2\hbar^2}\right)|\varphi|^2 + V(|\varphi|^2), \quad (17)$$

$$P = \frac{1}{2c^2}\left(\frac{d|\varphi|}{dt}\right)^2 + \left(\frac{\omega^2}{2c^2} - \frac{m^2c^2}{2\hbar^2}\right)|\varphi|^2 - V(|\varphi|^2). \quad (18)$$

Equation (16) can be written as

$$\frac{d^2R}{dt^2} + 3H\frac{dR}{dt} = -c^2\frac{dV_{\text{tot}}}{dR} + \omega^2R,$$ (19)

where $R = |\varphi|$ and $\omega = Q\hbar c^2/(a^3R^2)$. This equation is similar to the equation of motion of a damped particle of position $R(t)$ moving in a potential $c^2V_{\text{tot}}(R) - (1/2)\omega^2R^2$. The last term coming from the "angular motion" of the complex SF can be interpreted as a "centrifugal force" whose strength depends on the charge of the complex SF [37]. The presence of the centrifugal force for a complex SF is a crucial difference with respect to a real SF (that is not charged) because the fast oscillation approximation leading to Eq. (14) or (15) corresponds to the equilibrium $c^2V'_{\text{tot}}(R) = \omega^2R$ between the centrifugal force and the force associated with the total SF potential V_{tot} (see Sec. V A of [20]). When this condition is satisfied, the phase of the SF rotates rapidly while its modulus remains approximately constant. This is what Boyle *et al.* [38] call "spintessence." There is no relation such as Eq. (14) or (15) for a real SF.

Remark.—For a complex SF in the fast oscillation regime, only the phase θ of the SF oscillates (spintessence). The modulus $|\varphi|$ of the SF evolves slowly (adiabatically) without oscillating. By contrast, for a real SF in the fast oscillation regime, $\varphi(t)$ oscillates rapidly by taking positive and negative values. In this connection, we note that Arbey *et al.* [36] study a complex SF but consider a fast oscillation regime different from spintessence where the complex SF behaves as a real SF. In the present paper, when considering the fast oscillation regime of a complex SF, we shall implicitly assume that it corresponds to the spintessence regime.

D. Equation of state in the fast oscillation regime

To establish the equation of state of the SF in the fast oscillation regime, we can proceed as follows [20,28,39–42].

Multiplying the KG equation (2) by φ^* and averaging over a time interval that is much longer than the field oscillation period ω^{-1}, but much shorter than the Hubble time H^{-1}, we obtain

$$\frac{1}{c^2}\left\langle\left|\frac{d\varphi}{dt}\right|^2\right\rangle = \frac{m^2c^2}{\hbar^2}\langle|\varphi|^2\rangle + 2\left\langle\frac{dV}{d|\varphi|^2}|\varphi|^2\right\rangle. \quad (20)$$

This relation constitutes a sort of virial theorem. On the other hand, for a spatially homogeneous SF, the energy density and the pressure are given by Eqs. (4) and (5). Taking the average value of the energy density and pressure, using Eq. (20), and making the approximation

$$\left\langle\frac{dV}{d|\varphi|^2}|\varphi|^2\right\rangle \simeq V'(\langle|\varphi|^2\rangle)\langle|\varphi|^2\rangle, \quad (21)$$

we get

$$\langle\epsilon\rangle = \frac{m^2c^2}{\hbar^2}\langle|\varphi|^2\rangle + V'(\langle|\varphi|^2\rangle)\langle|\varphi|^2\rangle + V(\langle|\varphi|^2\rangle), \quad (22)$$

$$\langle P\rangle = V'(\langle|\varphi|^2\rangle)\langle|\varphi|^2\rangle - V(\langle|\varphi|^2\rangle). \quad (23)$$

The equation of state parameter is then given by

$$w = \frac{P}{\epsilon} = \frac{V'(\langle|\varphi|^2\rangle)\langle|\varphi|^2\rangle - V(\langle|\varphi|^2\rangle)}{\frac{m^2c^2}{\hbar^2}\langle|\varphi|^2\rangle + V'(\langle|\varphi|^2\rangle)\langle|\varphi|^2\rangle + V(\langle|\varphi|^2\rangle)}. \quad (24)$$

We note that the averages are not strictly necessary in Eqs. (22)–(24) since the modulus of the SF changes slowly with time.

Remark.—Equations (22) and (23) can also be obtained from Eqs. (17) and (18) by using Eq. (14) and neglecting the term $(d|\varphi|/dt)^2$.

E. Equation of state in the slow oscillation regime: Kination and stiff matter era

In the so-called "kination regime" [43] where the kinetic term dominates the potential term in Eqs. (4) and (5), we obtain the stiff equation of state $P = \epsilon$ where the speed of sound $c_s = (P'(\epsilon))^{1/2}c$ equals the speed of light. This equation of state applies in particular to a free massless SF ($m = V = 0$) or when $H \sim |\dot{\varphi}|/|\varphi|$ is large. The stiff matter era associated with the kination regime may take place in the very early Universe before other eras associated with the fast oscillation regime ($\omega \gg H$). The stiff matter era usually corresponds to a slow oscillation regime ($\omega \ll H$). In that case, the SF cannot even complete one cycle of spin within one Hubble time so that it just rolls down the potential well, without oscillating. Therefore, the comparison of ω and H determines whether the SF oscillates or rolls (see Sec. XIII). For the stiff equation of state $P = \epsilon$, using the Friedmann equations (6) and (8), one easily gets

$\epsilon \propto a^{-6}$, $a \propto t^{1/3}$, and $\epsilon \sim c^2/24\pi G t^2$. One can also show that $|\varphi| \sim (3c^4/4\pi G)^{1/2}(-\ln a)$ [29].

F. Hydrodynamic variables and TF approximation

Instead of working with the SF $\varphi(t)$, we can use hydrodynamic variables (see our previous works [20–22,29–31] for a general hydrodynamic description valid for possibly inhomogeneous systems). We define the pseudo-rest-mass density by

$$\rho = \frac{m^2}{\hbar^2}|\varphi|^2. \qquad (25)$$

We stress that it is only in the nonrelativistic limit $c \to +\infty$ that ρ has the interpretation of a rest-mass density (in this limit, we have $\epsilon \sim \rho c^2$). In the relativistic regime, ρ does not have a clear physical interpretation but it can always be defined as a convenient notation. We note that the total potential (3) can be written as

$$V_{\text{tot}}(\rho) = \frac{1}{2}\rho c^2 + V(\rho). \qquad (26)$$

We now write the SF in the de Broglie form

$$\varphi(t) = \frac{\hbar}{m}\sqrt{\rho(t)}e^{iS_{\text{tot}}(t)/\hbar}, \qquad (27)$$

where ρ is the pseudo-rest-mass density and $S_{\text{tot}} = (1/2)i\hbar \ln(\varphi^*/\varphi)$ is the total action of the SF. The total energy of the SF (including its rest-mass energy mc^2) is

$$E_{\text{tot}}(t) = -\frac{dS_{\text{tot}}}{dt}. \qquad (28)$$

Substituting Eq. (27) into the KG equation (2) and taking the imaginary part, we obtain the conservation equation [20]

$$\frac{d}{dt}(\rho E_{\text{tot}}a^3) = 0. \qquad (29)$$

It expresses the conservation of the charge of the SF.[9] It can be integrated into

$$\frac{E_{\text{tot}}}{mc^2} = \frac{Qm}{\rho a^3}, \qquad (30)$$

where Q is the charge of the SF. These equations are equivalent to Eqs. (12) and (13).[10] Next, substituting

Eq. (27) into the KG equation (2), taking the real part, and making the TF approximation $\hbar \to 0$, we obtain the Hamilton-Jacobi (or Bernoulli) equation [20]

$$E_{\text{tot}}^2 = m^2c^4 + 2m^2c^2V'(\rho). \qquad (31)$$

This equation is equivalent to Eq. (14). It can be rewritten as

$$E_{\text{tot}} = mc^2\sqrt{1 + \frac{2}{c^2}V'(\rho)}. \qquad (32)$$

We note that Eq. (31) requires

$$1 + \frac{2}{c^2}V'(\rho) > 0, \qquad (33)$$

corresponding to $V'_{\text{tot}}(\rho) > 0$. Combining Eqs. (30) and (32), we obtain

$$\rho\sqrt{1 + \frac{2}{c^2}V'(\rho)} = \frac{Qm}{a^3}, \qquad (34)$$

which is equivalent to Eq. (15). Finally, writing Eqs. (4) and (5) in terms of hydrodynamic variables, making the TF approximation $\hbar \to 0$, and using the Hamilton-Jacobi (or Bernoulli) equation (31), we get [20]

$$\epsilon = \rho c^2 + V(\rho) + \rho V'(\rho), \qquad (35)$$

$$P = \rho V'(\rho) - V(\rho), \qquad (36)$$

which are equivalent to Eqs. (22) and (23). Equation (36) determines the equation of state $P(\rho)$ for a given potential $V(\rho)$.[11] Inversely, for a given equation of state, the potential is given by

$$V(\rho) = \rho \int \frac{P(\rho)}{\rho^2}d\rho. \qquad (37)$$

The correspondences with the results of the previous sections show that the fast oscillation regime ($\omega \gg H$) is equivalent to the TF or semiclassical approximation ($\hbar \to 0$). We note that we cannot directly take $\hbar = 0$ in the KG equation (this is why we have to average over the oscillations) while we can take $\hbar = 0$ in the hydrodynamic equations (see Refs. [20–22] for more details). This is an interest of the hydrodynamic representation of the SF. It can be shown [21,22,44] that Eqs. (35) and (36) remain valid for a spatially inhomogeneous SF in the TF

---

[9]The density of charge is proportional to ρE_{tot} (see [31] and footnote 4 of [20]).

[10]To make the link between the SF variables and the hydrodynamical variables, we use $|\varphi| = (\hbar/m)\sqrt{\rho}$, $\theta = S_{\text{tot}}/\hbar$, and $\omega = E_{\text{tot}}/\hbar$.

[11]We can add a term of the form $A\rho$ in the potential without changing the pressure. This adds a term $2A\rho$ in the energy density. If we add a constant term C (cosmological constant) in the potential, this adds a term C in the energy density and a term $-C$ in the pressure.

approximation.[12] They determine the equation of state $P = P(\epsilon)$ of the SF in parametric form. The equation of state parameter can be written as

$$w = \frac{P}{\epsilon} = \frac{\rho V'(\rho) - V(\rho)}{\rho c^2 + V(\rho) + \rho V'(\rho)}, \qquad (38)$$

which is equivalent to Eq. (24). We note that the condition from Eq. (33) implies $w > -1$ so that a complex SF in the fast oscillation regime has never a phantom behavior. The pseudo squared speed of sound is

$$c_s^2 = P'(\rho) = \rho V''(\rho), \qquad (39)$$

while the true squared speed of sound is

$$c_s^2 = P'(\epsilon) = \frac{\rho V''(\rho)}{c^2 + 2V'(\rho) + \rho V''(\rho)}. \qquad (40)$$

Remark.—We note that Eq. (34) can be obtained directly from the energy equation (6) with Eqs. (35) and (36) [29]. Indeed, combining these equations we obtain

$$[c^2 + 2V'(\rho) + \rho V''(\rho)]\frac{d\rho}{dt} = -3H[\rho c^2 + 2\rho V'(\rho)], \quad (41)$$

leading to

$$\int \frac{c^2 + 2V'(\rho) + \rho V''(\rho)}{\rho c^2 + 2\rho V'(\rho)} d\rho = -3 \ln a. \qquad (42)$$

Equation (42) integrates to give Eq. (34).

G. Rest-mass density and internal energy

The rest-mass density $\rho_m = nm$ (proportional to the charge density) of a spatially homogeneous SF is given by [21,22]

$$\rho_m = \rho \frac{E_{\text{tot}}}{mc^2} = \rho \frac{\hbar\omega}{mc^2} = -\rho \frac{\dot{S}_{\text{tot}}}{mc^2}. \qquad (43)$$

It is equal to $\rho_m = J_0/c$, where $J_0 = -\rho\partial_0 S_{\text{tot}}/m$ is the time component of the current of charge. This formula is general for a homogeneous SF, being valid beyond the TF approximation. According to Eq. (30), we have

$$\rho_m = \frac{Qm}{a^3}. \qquad (44)$$

The rest-mass density (or the charge density) decreases as a^{-3}. This expresses the conservation of the charge of the SF or, equivalently, the conservation of the boson number

(provided that antibosons are counted negatively).[13] In the TF approximation, using the Hamilton-Jacobi (or Bernoulli) equation (32), we find that the relation between the rest-mass density ρ_m and the pseudo-rest-mass density ρ is

$$\rho_m = \rho\sqrt{1 + \frac{2}{c^2}V'(\rho)}. \qquad (45)$$

From the knowledge of $P(\rho)$ we can then obtain $P = P(\rho_m)$. It can be shown [21,22] that Eq. (45) remains valid for an inhomogeneous SF in the TF approximation.

The energy density can be written as

$$\epsilon = \rho_m c^2 + u(\rho_m), \qquad (46)$$

where the first term is the rest-mass energy and the second term is the internal energy. The internal energy is related to the equation of state $P(\rho_m)$, expressed in terms of the rest-mass density, by[14]

$$u(\rho_m) = \rho_m \int \frac{P(\rho_m)}{\rho_m^2} d\rho_m. \qquad (47)$$

It is argued in [1] that the rest-mass density ρ_m represents DM and that the internal energy $u(\rho_m)$ represents DE. This provides an interesting interpretation of these two mysterious components. From Eqs. (35), (45), and (46), we obtain

$$u = \rho c^2 + V(\rho) + \rho V'(\rho) - \rho c^2\sqrt{1 + \frac{2}{c^2}V'(\rho)}. \quad (48)$$

Therefore, the rest-mass density (DM) is determined by Eq. (45) and the internal energy density (DE) is determined by Eq. (48). We can then obtain $u = u(\rho_m)$. Equation (48) remains valid for an inhomogeneous SF in the TF approximation [21,22].

Remark.—Owing to our interpretation of DM and DE, we can write

$$\rho_m c^2 = \frac{\Omega_{\text{m},0}\epsilon_0}{a^3} \qquad (49)$$

and

$$\epsilon = \frac{\Omega_{\text{m},0}\epsilon_0}{a^3} + u\left(\frac{\Omega_{\text{m},0}\epsilon_0}{c^2 a^3}\right), \qquad (50)$$

---

[12]Equation (36) is also valid for a nonrelativistic SF in the general case, i.e., for a possibly spatially inhomogeneous SF beyond the TF approximation [21,24].

[13]Inversely, Eq. (43) can be directly obtained from Eq. (30) by using Eq. (44).

[14]This relation can be obtained by integrating the first law of thermodynamics at $T = 0$ which reads $d(\epsilon/\rho_m) = -Pd(1/\rho_m)$ [1]. Combining the first law of thermodynamics at $T = 0$ written as $d\epsilon/d\rho_m = (P + \epsilon)/\rho_m$ with the energy conservation equation $d\epsilon/dt + 3H(\epsilon + P) = 0$, we get $d\rho_m/dt + 3H\rho_m = 0$, which integrates to give $\rho_m \propto a^{-3}$ [1].

where ϵ_0 is the present energy density of the Universe and $\Omega_{m,0}$ is the present proportion of DM. We can then solve the Friedmann equation (8) with Eq. (50) to obtain the temporal evolution of the scale factor $a(t)$. We note that, in this interpretation, the constant Qmc^2 (which is proportional to the charge of the SF) is equal to the present energy density of DM $\epsilon_{m,0} = \Omega_{m,0}\epsilon_0$ [compare Eqs. (44) and (49)]. Therefore, we have the relation

$$Qmc^2 = \Omega_{m,0}\epsilon_0. \tag{51}$$

H. Two-fluid model

In our model, we have a single SF (or a single dark fluid). Still, the energy density (46) is the sum of two terms, a rest-mass term ρ_m which mimics DM and an internal energy term $u(\rho_m)$ which mimics DE. It is interesting to consider a two-fluid model which leads to the same results as the single dark fluid model, at least for what concerns the evolution of the homogeneous background. In this two-fluid model, one fluid corresponds to pressureless DM with an equation of state $P_m = 0$ and a density $\rho_m c^2 = \Omega_{m,0}\epsilon_0/a^3$ determined by the energy conservation equation for DM, and the other fluid corresponds to DE with an equation of state $P_{de}(\epsilon_{de})$ and an energy density $\epsilon_{de}(a)$ determined by the energy conservation equation for DE. We can obtain the equation of state of DE yielding the same results as the one-fluid model by taking

$$P_{de} = P(\rho_m), \qquad \epsilon_{de} = u(\rho_m). \tag{52}$$

In other words, the equation of state $P_{de}(\epsilon_{de})$ of DE in the two-fluid model corresponds to the relation $P(u)$ in the single-fluid model. Explicit examples of the correspondence between the one-fluid model and the two-fluid model are given in [21,22] and in Sec. IV. We note that, although the one- and two-fluid models are equivalent for the evolution of the homogeneous background, they may differ for what concerns the formation of the large-scale structures of the Universe and for inhomogeneous systems in general.

III. LOGARITHMIC POTENTIAL AND LOGOTROPIC EQUATION OF STATE

The previous equations are general. We now apply them to a specific model of the Universe called the logotropic model. We assume that DM and DE are the manifestation of a single substance and that this substance can be described by a complex SF (or an exotic dark fluid) governed by a KG equation with a logarithmic potential of the form

$$V(|\varphi|^2) = -A \ln\left(\frac{m^2|\varphi|^2}{\hbar^2\rho_P}\right) - A. \tag{53}$$

Using the hydrodynamic variables introduced previously, the SF potential can be written as

$$V(\rho) = -A \ln\left(\frac{\rho}{\rho_P}\right) - A, \tag{54}$$

where A/c^2 and ρ_P are two positive constants with the dimensions of a mass density. We will give the physical meaning and the value of these constants in Sec. VI. In the fast oscillation regime, using Eq. (36), we find that the pressure is given by[15]

$$P = A \ln\left(\frac{\rho}{\rho_P}\right). \tag{55}$$

This equation is similar to the logotropic equation of state [see Eq. (1)] introduced in our previous papers [1–4]. However, as we shall see, the present model is substantially different from the model of Refs. [1–4]. In particular, we stress that ρ represents here the pseudo-rest-mass density defined by Eq. (25), not the true rest-mass density $\rho_m = nm$ used in Refs. [1–4]. It is only in the nonrelativistic limit that they coincide. The relation between the different logotropic models is discussed in Appendix B (see also [21]).

For the logarithmic potential (54) the equations of the problem valid in the fast oscillation regime [see Eqs. (32)–(35)] are

$$\rho\sqrt{1 - \frac{2A}{\rho c^2}} = \frac{Qm}{a^3}, \tag{56}$$

$$\epsilon = \rho c^2 - A \ln\left(\frac{\rho}{\rho_P}\right) - 2A, \tag{57}$$

$$\frac{E_{tot}}{mc^2} = \sqrt{1 - \frac{2A}{\rho c^2}}. \tag{58}$$

They depend on three parameters A, Qm, and ρ_P. The first equation can be solved explicitly giving

$$\rho c^2 = A + \sqrt{A^2 + \frac{(Qmc^2)^2}{a^6}}. \tag{59}$$

On the other hand, eliminating ρ between Eqs. (55) and (57), we find that the equation of state $P(\epsilon)$ is given under the inverse form $\epsilon(P)$ by

$$\epsilon = \rho_P c^2 e^{P/A} - P - 2A. \tag{60}$$

Finally, the equation of state parameter is given by

---

[15]Conversely, we could start from the equation of state (55) and integrate Eq. (37) to obtain the potential $V(\rho)$.

$$w = \frac{P}{\epsilon} = \frac{A \ln(\frac{\rho}{\rho_P})}{\rho c^2 - A \ln(\frac{\rho}{\rho_P}) - 2A}. \tag{61}$$

We note from Eq. (55) that $P > 0$ when $\rho > \rho_P$ and $P < 0$ when $\rho < \rho_P$. The pressure vanishes ($P = w = 0$) when $\rho = \rho_P$. We will see that the logotropic model is valid for $\rho \ll \rho_P$. Therefore, in practice, the pressure of the LDF is always negative.

IV. REST-MASS DENSITY AND INTERNAL ENERGY

According to Eqs. (45) and (54), the rest-mass density ρ_m of the LDF is related to its pseudo-rest-mass density ρ by

$$\rho_m = \rho \sqrt{1 - \frac{2A}{\rho c^2}}. \tag{62}$$

This equation can be inverted to give

$$\rho = \frac{A}{c^2} + \sqrt{\frac{A^2}{c^4} + \rho_m^2}, \tag{63}$$

where ρ_m is given by Eq. (44). Using Eqs. (48), (54), and (63), we find that the internal energy is given by

$$u = -A + \sqrt{A^2 + \rho_m^2 c^4} - \rho_m c^2$$
$$- A \ln\left[\frac{A}{\rho_P c^2} + \sqrt{\frac{A^2}{\rho_P^2 c^4} + \frac{\rho_m^2}{\rho_P^2}}\right]. \tag{64}$$

Finally, according to Eqs. (55) and (63), we obtain the equation of state of the SF in terms of the rest-mass density as

$$P = A \ln\left[\frac{A}{\rho_P c^2} + \sqrt{\frac{A^2}{\rho_P^2 c^4} + \frac{\rho_m^2}{\rho_P^2}}\right]. \tag{65}$$

As we have recalled in Sec. II G, the rest-mass density ρ_m of the SF represents DM and the internal energy u of the SF represents DE [1].

Remark.—In the two-fluid model associated with the logotropic model (see Sec. II H), the DE has an equation of state $P_{\rm de}(\epsilon_{\rm de})$ which is obtained by eliminating ρ_m between Eqs. (64) and (65) and by identifying $P(u)$ with $P_{\rm de}(\epsilon_{\rm de})$. It can be written in inverse form as[16]

$$\epsilon_{\rm de} = \rho_P c^2 e^{P_{\rm de}/A} - P_{\rm de} - 2A$$
$$- \rho_P c^2 \sqrt{e^{2P_{\rm de}/A} - \frac{2A}{\rho_P c^2} e^{P_{\rm de}/A}}. \tag{66}$$

---

[16]This relation can be obtained simply by solving Eq. (65) to get $\rho_m(P)$ and by using Eqs. (46) and (60).

V. THE EVOLUTION OF THE PARAMETERS WITH THE SCALE FACTOR

In our model, strictly speaking, there is no DM and no DE. There is just a single SF [or a single dark fluid (DF)]. This is an example of unified models of DM and DE that are referred to as unified dark matter (UDM) models or "quartessence" models [45]. The logotropic model is therefore fundamentally different from the ΛCDM model in which DM and DE are interpreted as two distinct entities (see Appendices D 1 and D 2).[17] Nevertheless, since the ΛCDM model works remarkably well in describing the large-scale structure of the Universe, it is important to make a connection between the logotropic model and the ΛCDM model. This connection will allow us to determine in which limit the ΛCDM model is valid from the viewpoint of our more general model and to obtain the parameters of the LDF by using the values of the parameters that have been obtained from cosmological observations interpreted in the framework of the ΛCDM model.

A. Early Universe: DM-like regime

In the early Universe ($a \to 0$), the general equations of Sec. III reduce to

$$\rho \sim \frac{Qm}{a^3}, \tag{67}$$

$$\epsilon \sim \rho c^2 \sim \frac{Qmc^2}{a^3}, \tag{68}$$

$$\frac{E_{\rm tot}}{mc^2} \to 1, \tag{69}$$

$$P \sim A \ln\left(\frac{Qm}{\rho_P a^3}\right), \tag{70}$$

$$P \sim A \ln\left(\frac{\epsilon}{\rho_P c^2}\right), \tag{71}$$

$$w \sim \frac{A}{\rho c^2} \ln\left(\frac{\rho}{\rho_P}\right), \tag{72}$$

$$w \sim \frac{Aa^3}{Qmc^2} \ln\left(\frac{Qm}{\rho_P a^3}\right), \tag{73}$$

$$w \sim \frac{A}{\epsilon} \ln\left(\frac{\epsilon}{\rho_P c^2}\right). \tag{74}$$

Since $\epsilon \propto a^{-3}$ and $w \simeq 0$ we see that the LDF behaves at early times similar to DM. If we impose that the LDF matches the ΛCDM model for $a \ll 1$ (see Appendix D 2), we obtain

---

[17]Actually, the ΛCDM model can also be regarded as a UDM model as discussed in Appendix D 3.

$$Qmc^2 = \Omega_{m,0}\epsilon_0. \qquad (75)$$

Therefore, the quantity Qmc^2 which is proportional to the charge of the SF corresponds to the present energy density of DM ($\epsilon_{m,0} = \Omega_{m,0}\epsilon_0$) in the ΛCDM model [see also Eq. (51)].[18] Using the values of Appendix H, we get

$$Qm = 2.66 \times 10^{-24} \text{ g m}^{-3}. \qquad (76)$$

Remark.—In the DM-like era, the energy and the pulsation of the SF are given by $E_{\text{tot}} \sim mc^2$ and $\omega \sim mc^2/\hbar$ like for a free SF. They are constant. For a boson mass $m \sim 10^{-22}$ eV/c^2 (see Appendix E 3), we get $\omega \sim 10^{-7}$ s^{-1}. On the other hand, in the DM-like era, the pseudo-rest-mass density ρ coincides with the true rest-mass density ρ_m (see Sec. IV).

B. Late Universe: DE-like regime

In the late Universe $a \to +\infty$, the general equations of Sec. III reduce to

$$\rho \to \rho_{\text{min}} = \frac{2A}{c^2}, \qquad (77)$$

$$\epsilon \to \epsilon_{\text{min}} = A \ln\left(\frac{\rho_P c^2}{2A}\right), \qquad (78)$$

$$\frac{E_{\text{tot}}}{mc^2} \to 0, \qquad (79)$$

$$P \to P_{\text{min}} = -\epsilon_{\text{min}}, \qquad (80)$$

$$w \to w_{\text{min}} = \frac{P_{\text{min}}}{\epsilon_{\text{min}}} = -1. \qquad (81)$$

Since the energy density ϵ tends to a constant ϵ_{min} and since the equation of state parameter $w \to -1$ we see that the LDF behaves at late times similar to DE. We shall come back to the value of ϵ_{min} in Sec. XIV. We can check that the equation of state parameter w is always strictly larger than -1 so the Universe does not become phantom.[19] It asymptotically tends to a de Sitter–like solution. This is an important difference with our previous logotropic model

[1–4], based on a different equation of state [see Eq. (1)], which displays a phantom behavior at late times (in that case, the scale factor has a super–de Sitter behavior).

Remark.—The asymptotic value ρ_{min} of the pseudo-rest-mass density corresponds to the limit where the rest-mass term $m^2c^2/\hbar^2$ in the KG equation (2) is compensated by the self-interaction term $2dV/d|\varphi|^2$. In that case, $\omega \simeq 0$ according to Eq. (14) and the fast oscillation regime ceases to be valid (see Sec. XIII).

C. Intermediate regime: Stiff matter

Considering the subleading terms in Eqs. (55), (57), and (59) for large values of a, one obtains the following expressions for the pseudo-rest-mass density, energy density, and pressure:

$$\rho = \rho_{\text{min}} + \frac{(Qmc^2)^2}{2Aa^6} + \dots \qquad (82)$$

$$\epsilon = \epsilon_{\text{min}} + \frac{(Qmc^2)^2}{4Aa^6} + \dots \qquad (83)$$

$$P = P_{\text{min}} + \frac{(Qmc^2)^2}{4Aa^6} + \dots \qquad (84)$$

These equations describe the mixture of a cosmological constant ϵ_{min} [first terms in Eqs. (83) and (84)] with a form of "stiff" matter described by the equation of state $P = \epsilon$ [second terms in Eqs. (83) and (84)] in which the speed of sound is equal to the speed of light.[20] Therefore, the logotropic model interpolates between different phases of the Universe. Initially, the Universe behaves as if it were dominated by a pressureless (dust) fluid. Ultimately, the density becomes asymptotically constant implying a de Sitter evolution. There is also an intermediate phase which can be described by a cosmological constant mixed with a stiff matter fluid. The interesting point is that such an evolution is accounted for by a single fluid. This is similar to the Chaplygin gas model [46].

VI. THE VALUE OF THE FUNDAMENTAL CONSTANT OF OUR MODEL

A. An important identity obtained in the present Universe

Applying the general equations (57) and (59) at the present time ($a = 1$) we get

$$\epsilon_0 = \rho_0 c^2 - A \ln\left(\frac{\rho_0}{\rho_P}\right) - 2A \qquad (85)$$

and

---

[18]To simplify the presentation, we ignore the presence of baryons.

[19]This is a general result for a complex SF. It is shown after Eq. (38) that a complex SF in the fast oscillation regime can never have a phantom behavior whatever the form of the self-interaction potential. This is because we have considered a SF with a Lagrangian $L = \frac{1}{2c^2}|\dot{\varphi}|^2 - V_{\text{tot}}(|\varphi|^2)$ involving a *positive* kinetic term. A SF with a negative kinetic term has always a phantom behavior. Therefore, a complex SF has either a normal behavior (if it has a positive kinetic term) or a phantom behavior (if it has a negative kinetic term) but it cannot pass from a normal to a phantom regime.

[20]This stiff matter era is completely different from the one considered in Sec. II E.

$$\rho_0 c^2 = A + \sqrt{A^2 + (Qmc^2)^2}. \tag{86}$$

Substituting Eq. (86) into Eq. (85) we obtain

$$\epsilon_0 = \sqrt{A^2 + (Qmc^2)^2} - A \ln\left[\frac{A + \sqrt{A^2 + (Qmc^2)^2}}{\rho_P c^2}\right] - A. \tag{87}$$

Using Eq. (75), this relation can be rewritten as

$$\epsilon_0 = -A + \sqrt{A^2 + (\Omega_{m,0}\epsilon_0)^2} \\ - A \ln\left[\frac{A + \sqrt{A^2 + (\Omega_{m,0}\epsilon_0)^2}}{\rho_P c^2}\right]. \tag{88}$$

Assuming that A and ρ_P are universal constants, this equation gives a relation between $\Omega_{m,0}$ and ϵ_0. Inversely, we can use Eq. (88) and the measured values of ϵ_0 and $\Omega_{m,0}$ to determine the constants of our model (see Appendix H).

As in our previous papers [1–4], it is convenient to write

$$A = B\epsilon_\Lambda, \tag{89}$$

where B is a dimensionless constant and

$$\epsilon_\Lambda = \rho_\Lambda c^2 = (1 - \Omega_{m,0})\epsilon_0 \tag{90}$$

is the present density of DE. Numerically,

$$\rho_\Lambda = 5.96 \times 10^{-24} \text{ g m}^{-3}. \tag{91}$$

In the ΛCDM model (see Appendix D), ρ_Λ represents the cosmological density which is related to the Einstein cosmological constant Λ by

$$\rho_\Lambda = \frac{\Lambda}{8\pi G} \tag{92}$$

with $\Lambda = 1.00 \times 10^{-35} \text{ s}^{-2}$. For given ρ_Λ, Eq. (89) is just a change of notation. In the following, we shall work with B instead of A. In that case, Eqs. (85) and (86) can be rewritten as

$$\frac{1}{1 - \Omega_{m,0}} = \frac{\rho_0}{\rho_\Lambda} - B \ln\left(\frac{\rho_0 \rho_\Lambda}{\rho_\Lambda \rho_P}\right) - 2B \tag{93}$$

and

$$\frac{\rho_0}{\rho_\Lambda} = B + \sqrt{B^2 + \left(\frac{Qm}{\rho_\Lambda}\right)^2}. \tag{94}$$

Using Eqs. (75) and (90), we also have

$$\frac{\rho_0}{\rho_\Lambda} = B + \sqrt{B^2 + \left(\frac{\Omega_{m,0}}{1 - \Omega_{m,0}}\right)^2}. \tag{95}$$

Substituting Eq. (95) into Eq. (93) we obtain the exact identity

$$\frac{1}{1 - \Omega_{m,0}} = -B + \sqrt{B^2 + \left(\frac{\Omega_{m,0}}{1 - \Omega_{m,0}}\right)^2} \\ - B \ln\left[B + \sqrt{B^2 + \left(\frac{\Omega_{m,0}}{1 - \Omega_{m,0}}\right)^2}\right] \\ + B \ln\left(\frac{\rho_P}{\rho_\Lambda}\right), \tag{96}$$

which is equivalent to Eq. (88). We can also rewrite Eq. (75) as

$$Qmc^2 = \frac{\Omega_{m,0}}{1 - \Omega_{m,0}}\rho_\Lambda c^2. \tag{97}$$

B. The value of B

Equation (96) determines the relation between B and ρ_P from the measured values of $\Omega_{m,0}$ and $\rho_\Lambda = (1 - \Omega_{m,0})\epsilon_0/c^2$. We will find that $B \ll 1$ so we can make the approximation

$$B = \frac{1}{\ln\left(\frac{\rho_P}{\rho_\Lambda}\right) - 1 - \ln\left(\frac{\Omega_{m,0}}{1 - \Omega_{m,0}}\right)}. \tag{98}$$

We will also find that $1 + \ln\left[\Omega_{m,0}/(1 - \Omega_{m,0})\right]$ is much smaller than $\ln\left(\rho_P/\rho_\Lambda\right)$ so we can make the additional approximation

$$B = \frac{1}{\ln\left(\frac{\rho_P}{\rho_\Lambda}\right)}. \tag{99}$$

This is the same result as in our previous papers [1–4]. Equation (99) can be rewritten as

$$\frac{\rho_P}{\rho_\Lambda} = e^{1/B}. \tag{100}$$

Now the crucial remark is to observe that Eq. (100) is analogous to the fundamental identity

$$\frac{\rho_P}{\rho_\Lambda} = 10^{123} \tag{101}$$

expressing the fact that the Planck density

$$\rho_P = \frac{c^5}{\hbar G^2} = 5.16 \times 10^{99} \text{ g/m}^3 \tag{102}$$

and the cosmological density

$$\rho_\Lambda = \frac{\Lambda}{8\pi G} = 5.96 \times 10^{-24} \text{ g m}^{-3} \tag{103}$$

differ by 123 orders of magnitude (this is related to the cosmological constant problem [47,48]). Following our previous works [1–4], this analogy prompts us to identify ρ_P with the Planck density.[21] In that case, B is fully determined by Eq. (99). Its numerical value is

$$B = 3.53 \times 10^{-3}. \tag{104}$$

We note that $B \simeq 1/[123 \ln(10)]$, so that B is essentially the inverse of the famous number 123 (up to a conversion factor from Naperian to decimal logarithm). We note that B has a small but *nonzero* value. This is because B depends on the Planck constant $\hbar$ through the Planck density ρ_P in Eq. (99) and because $\hbar$ has a small but nonzero value. In the semiclassical limit $\hbar \to 0$, we find that $\rho_P \to +\infty$ and $B \to 0$. In that case, we recover the ΛCDM model (see Sec. VII D). The fact that B is nonzero means that quantum effects ($\hbar \neq 0$) play a fundamental role in the logotropic model. Indeed, ρ_P explicitly appears in the logarithmic potential from Eq. (54). Since the effects of B manifest themselves in the late Universe (see below), this implies—surprisingly—that quantum mechanics affects the late acceleration of the Universe. As we shall see in Sec. XIV, quantum mechanics provides (in the framework of our model) a small correction to the Einstein cosmological constant.

C. The value of A

The logarithmic potential from Eq. (54) involves two constants: A and ρ_P. We have seen that ρ_P is the Planck density. On the other hand, in line with our previous works [1–4], we interpret the logotropic constant A as a new fundamental constant of physics which supersedes (in the framework of our model) the Einstein cosmological constant Λ or the Einstein cosmological density $\rho_\Lambda = \Lambda/8\pi G$. Indeed, the logotropic constant A is responsible for the late acceleration of the Universe. According to Eqs. (89) and (99) we have

$$A = \frac{\rho_\Lambda c^2}{\ln(\frac{\rho_P}{\rho_\Lambda})}. \tag{105}$$

Its numerical value is

$$A/c^2 = 2.10 \times 10^{-26} \text{ g m}^{-3}. \tag{106}$$

We note that A/c^2 is equal to the Einstein cosmological density ρ_Λ divided by 123 (up to a logarithmic conversion factor). More precisely, the logotropic constant A is related to the Einstein cosmological constant Λ by

$$A = B\frac{\Lambda c^2}{8\pi G} \tag{107}$$

with $B = 1/\ln(\rho_P/\rho_\Lambda) = 3.53 \times 10^{-3}$. We stress, however, that, in the logotropic model, the DE density is not constant (see Sec. IV).

Remark.—Using Eq. (105), the logotropic equation of state (55) can be rewritten as

$$P = -\frac{\rho_\Lambda c^2}{\ln(\frac{\rho_P}{\rho_\Lambda})} \ln\left(\frac{\rho_P}{\rho}\right). \tag{108}$$

We note that $P = -\rho_\Lambda c^2$ at $\rho = \rho_\Lambda$, i.e., when the pseudo-rest-mass density is equal to the present DE density.

D. Validity of our approximations and a curious result

We can now check the validity of our approximations. Since $B = 3.53 \times 10^{-3} \ll 1$, the approximation leading from Eq. (96) to Eq. (98) is valid. We also observe that $1 + \ln[\Omega_{m,0}/(1 - \Omega_{m,0})] = 0.195$ is much smaller than $\ln(\rho_P/\rho_\Lambda) = 283$ so we can make the additional approximation leading from Eq. (98) to Eq. (99).

As an interesting (and intriguing) remark, we note the following. If we assume that B is *exactly* given by Eq. (99), then, according to Eq. (98), we get

$$1 + \ln\left(\frac{\Omega_{m,0}}{1 - \Omega_{m,0}}\right) = 0. \tag{109}$$

This equation determines the value of $\Omega_{m,0}$ which, in the ΛCDM model, represents the present proportion of DM.[22] We get

$$\Omega_{m,0}^{th} = \frac{1}{1 + e} = 0.269. \tag{110}$$

Remarkably, this value is reasonably close to the measured value $\Omega_{m,0} = 0.3089$. This result was previously obtained in [4] in the framework of the original logotropic model.

Remark.—For the simplicity of the presentation, we have ignored the presence of baryonic matter (in a sense, baryonic matter has been incorporated into DM). If we take into account the presence of baryons as an independent species and redo the preceding analysis, we find that

---

[21]Actually, the density ρ_* that appears in the logotropic equation of state $P = A \ln(\rho/\rho_*)$ [1] could be smaller than the Planck density ρ_P, being equal for example to the characteristic scale $\rho_{GUT} \sim 10^{-3}\rho_P$ of a generic grand unified theory (GUT). However, for definiteness, we shall take $\rho_* = \rho_P$.

[22]In the framework of our model where there is no DM and no DE (just a single DF), $\Omega_{m,0}$ represents the coefficient that appears in the asymptotic behavior $\epsilon/\epsilon_0 \sim \Omega_{m,0}/a^3$ of the energy density when $a \ll 1$ [see Eq. (68) with Eq. (75)]. This coefficient, which is related to the charge Qmc^2 of the SF, is expected to be universal.

Eq. (109) is replaced by $1 + \ln(\Omega_{dm,0}/\Omega_{de,0}) = 0$.[23] This implies that the present ratio between DE and DM is equal to the Euler number

$$\frac{\Omega^{th}_{de,0}}{\Omega^{th}_{dm,0}} = e = 2.71828\ldots \quad (111)$$

If we introduce the present proportion of baryons $\Omega_{b,0}$ and use Eq. (111) together with $\Omega_{dm,0} + \Omega_{de,0} + \Omega_{b,0} = 1$, we find that the present proportions of DM and DE are

$$\Omega^{th}_{dm,0} = \frac{1}{1 + e}(1 - \Omega_{b,0}), \quad (112)$$

$$\Omega^{th}_{de,0} = \frac{e}{1 + e}(1 - \Omega_{b,0}). \quad (113)$$

If we neglect baryonic matter $\Omega_{b,0} = 0$ we obtain the pure numbers $\Omega^{th}_{de,0} = \frac{e}{1+e} = 0.731059\ldots$ and $\Omega^{th}_{dm,0} = \frac{1}{1+e} = 0.268941\ldots$ which give the correct proportions 70% and 25% of DE and DM [4]. If we take baryonic matter into account and use the measured value of $\Omega_{b,0} = 0.0486 \pm 0.0010$, we get $\Omega^{th}_{de,0} = 0.6955 \pm 0.0007$ and $\Omega^{th}_{dm,0} = 0.2559 \pm 0.0003$ which are very close to the observed values $\Omega_{de,0} = 0.6911 \pm 0.0062$ and $\Omega_{dm,0} = 0.2589 \pm 0.0057$ within the error bars.[24] We note that the predicted ratio $\Omega^{th}_{de,0}/\Omega^{th}_{dm,0} = e = 2.71828\ldots$ is independent of $\Omega_{b,0}$ and close to the empirical value $\Omega_{de,0}/\Omega_{dm,0} = 2.66937 \pm 0.08$. Finally, combining the foregoing formulas, we find that the charge $Qmc^2 = \Omega_{dm,0}\epsilon_{tot,0}$ of the SF [see Eq. (75)] can be written as $Qmc^2 = \rho_\Lambda/e$. The postulate from Eq. (109) means that the fundamental constant A is equal to $\rho_\Lambda c^2/\ln(\rho_P/\rho_\Lambda)$ where ρ_Λ is the *present* DE density. This can be viewed as a strong cosmic coincidence [4] giving to our epoch a particular (central) place in the history of the Universe.[25] The same results are obtained with the original logotropic model. These important results are emphasized in a specific paper [49].

---

[23]If ϵ denotes the energy density of DM + DE (without baryons) and ϵ_{tot} the total energy density (including baryons) we have $\epsilon_{dm,0}/\epsilon_0 = \Omega_{dm,0}/(\Omega_{dm,0} + \Omega_{de,0})$ and $\epsilon_{de,0}/\epsilon_0 = \Omega_{de,0}/(\Omega_{dm,0} + \Omega_{de,0})$, where $\Omega_{dm,0} = \epsilon_{dm,0}/\epsilon_{tot,0}$ and $\Omega_{de,0} = \epsilon_{de,0}/\epsilon_{tot,0}$ are the present proportions of DM and DE. Therefore, we just have to replace $\Omega_{m,0}$ by $\Omega_{dm,0}/(\Omega_{dm,0} + \Omega_{de,0})$ and $1 - \Omega_{m,0}$ by $\Omega_{de,0}/(\Omega_{dm,0} + \Omega_{de,0})$ in the foregoing equations to account for the presence of baryons (see a more detailed calculation in [49]).

[24]We see that the agreement with the observations is better if we treat DM and baryons as two different species instead of a single one (i.e., if we incorporate baryons in DM). This is at variance with the ΛCDM model where baryons and DM behave similarly.

[25]Since the logotropic model is able to predict the values of the proportions of DM and DE, it solves the cosmic coincidence problem of the ΛCDM model [50,51]. However, this is at the price of introducing another intriguing coincidence.

E. Validity of the nonrelativistic regime

According to the results of Sec. V, the nonrelativistic regime is valid provided that[26]

$$\rho c^2 \gg \epsilon_\Lambda, \qquad \frac{Qmc^2}{a^3} \gg \epsilon_\Lambda. \quad (114)$$

Using Eqs. (75) and (90), these conditions can be rewritten as

$$\rho \gg \rho_\Lambda, \qquad a \ll a_t = \left(\frac{\Omega_{m,0}}{1 - \Omega_{m,0}}\right)^{1/3}, \quad (115)$$

like for the ΛCDM model (see Appendix D). The scale factor $a_t = 0.765$ determines the transition between the DM era and the DE era. In the nonrelativistic regime, we have $\epsilon \sim \rho c^2$, $E_{tot} \sim mc^2$, $\rho \sim \Omega_{m,0}(\epsilon_0/c^2)/a^3$, and $w \ll 1$. The SF behaves at large (cosmological) scales as pressureless DM. Note, however, that the logotropic pressure manifests itself at small (galactic) scales even in the nonrelativistic regime and can solve the problems of the CDM model such as the core-cusp problem and the missing satellite problem (see Sec. XIV).

VII. DIMENSIONLESS EQUATIONS

A. General equations

It is convenient to write the equations of the problem in terms of dimensionless variables. Introducing $\tilde{\rho} = \rho/\rho_\Lambda$, $\tilde{\epsilon} = \epsilon/\rho_\Lambda c^2$, $\tilde{P} = P/\rho_\Lambda c^2$, and $\tilde{E}_{tot} = E_{tot}/mc^2$, we obtain

$$\tilde{\rho}\sqrt{1 - \frac{2B}{\tilde{\rho}}} = \frac{\Omega_{m,0}}{1 - \Omega_{m,0}}\frac{1}{a^3}, \quad (116)$$

$$\tilde{\epsilon} = \tilde{\rho} - B\ln\tilde{\rho} + 1 - 2B, \quad (117)$$

$$\tilde{E}_{tot} = \sqrt{1 - \frac{2B}{\tilde{\rho}}}, \quad (118)$$

$$\tilde{P} = B\ln\tilde{\rho} - 1, \quad (119)$$

$$\tilde{\epsilon} = e^{1/B}e^{\tilde{P}/B} - \tilde{P} - 2B, \quad (120)$$

$$w = \frac{\tilde{P}}{\tilde{\epsilon}} = \frac{B\ln\tilde{\rho} - 1}{\tilde{\rho} - B\ln\tilde{\rho} + 1 - 2B}. \quad (121)$$

We can easily solve the first equation to express the pseudo-rest-mass density in terms of the scale factor as

---

[26]More generally, the nonrelativistic regime is valid when the rest-mass energy density $\rho_m c^2$ (DM) is much larger than the internal energy u (DE).
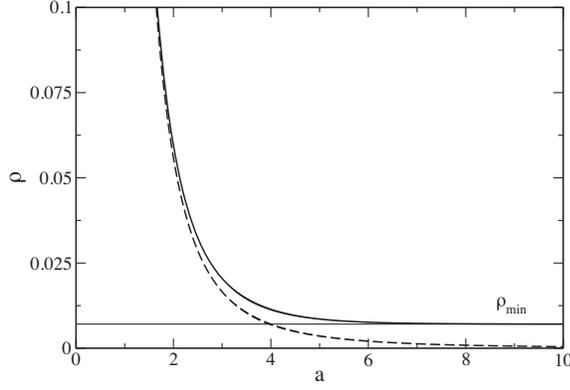
FIG. 1. Pseudo-rest-mass density as a function of the scale factor. Here and in the following figures, the dashed line corresponds to the ΛCDM model ($B = 0$).

$$\tilde{\rho} = B + \sqrt{B^2 + \left(\frac{\Omega_{m,0}}{1 - \Omega_{m,0}}\right)^2 \frac{1}{a^6}}. \qquad (122)$$

We can then inject this relation into the other equations to obtain the evolution of the different dimensionless variables as a function of a. Their evolution is represented in solid lines in Figs. 1–8. The dashed lines in these figures correspond to the ΛCDM model which is recovered from the logotropic model when $B = 0$ (see Sec. VII D).

The pressure vanishes ($\tilde{P} = w = 0$) when

$$\tilde{\rho}_w = e^{1/B} = 8.65 \times 10^{122}, \qquad (123)$$

corresponding to $\rho = \rho_P$. Using Eqs. (116) and (117), this corresponds to a scale factor

$$a_w \simeq \left(\frac{\Omega_{m,0}}{1 - \Omega_{m,0}}\right)^{1/3} e^{-1/(3B)} = 8.02 \times 10^{-42} \qquad (124)$$

and an energy density

$$\tilde{\epsilon}_w \simeq e^{1/B} = 8.65 \times 10^{122}. \qquad (125)$$

The pressure is positive ($P > 0$) when $a < a_w$ and negative ($P < 0$) when $a > a_w$.[27] We note that the equation of state parameter w reaches a maximum value $w_{max} = 1.50 \times 10^{-126}$ at $a_* = 5.75 \times 10^{-42}$.

The pressure is equal to $\tilde{P} = -1$ (i.e., $P = -\rho_\Lambda c^2$) when

$$\tilde{\rho} = 1, \qquad (126)$$

corresponding to $\rho = \rho_\Lambda$. Using Eqs. (116) and (117), this corresponds to a scale factor

---

[27]Since ρ_P has been identified with the Planck density, and since the logotropic model is expected to unify DM and DE but not the early inflation where the density is of the order of the Planck scale, we conclude that the logotropic model is valid only for $\rho \ll \rho_P$. In that regime, the pressure is always negative.
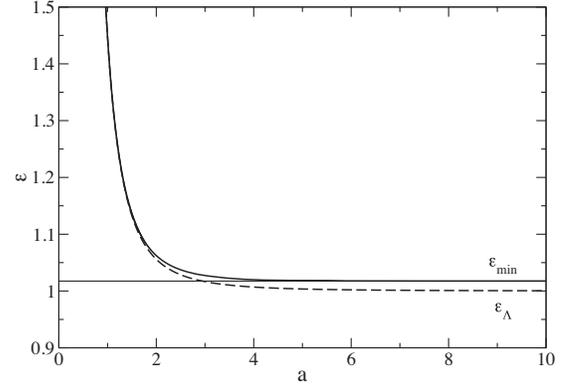
FIG. 2. Energy density as a function of the scale factor.
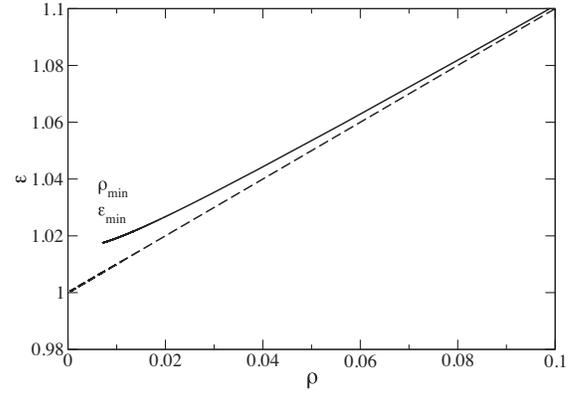
FIG. 3. Relation between the energy density and the pseudo-rest-mass density.

$$a = \left(\frac{\Omega_{m,0}}{1 - \Omega_{m,0}}\right)^{1/3} \frac{1}{(1 - 2B)^{1/6}} = 0.765 \qquad (127)$$

and an energy density

$$\tilde{\epsilon} = 2(1 - B) = 1.99. \qquad (128)$$
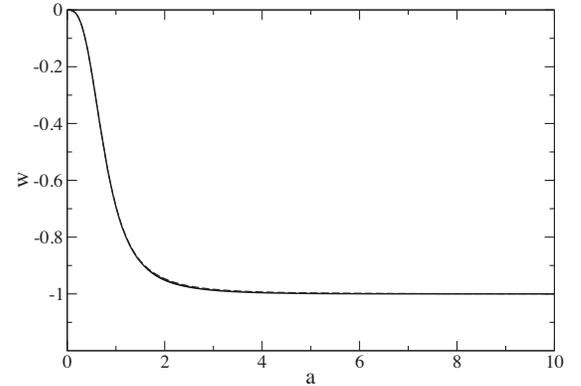
FIG. 4. Equation of state parameter as a function of the scale factor.
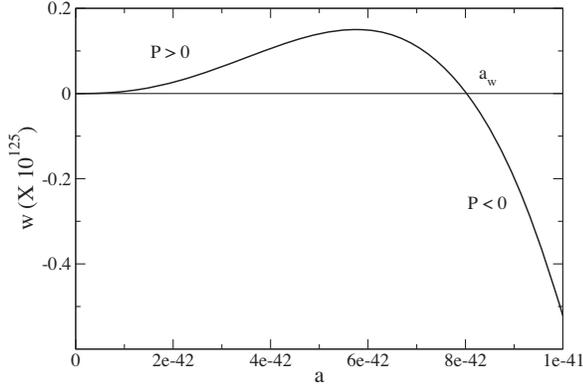
FIG. 5. Enlargement of Fig. 4 at very small values of the scale factor where the pressure passes from positive to negative values.
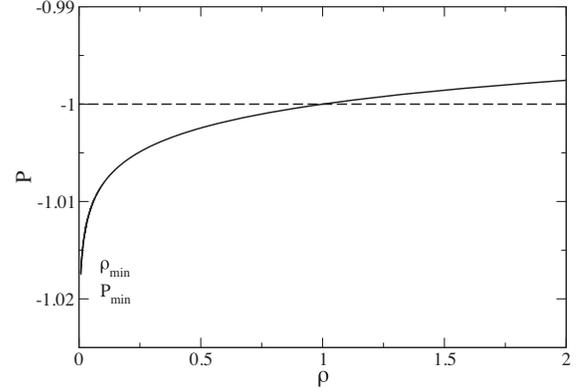
FIG. 7. Pressure as a function of the pseudo-rest-mass density ($\tilde{P} = -1$ for $\tilde{\rho} = 1$).
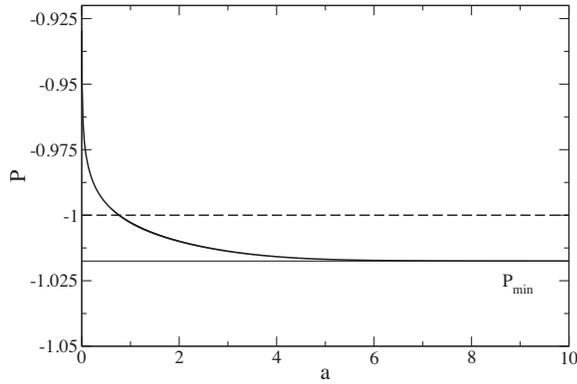
FIG. 6. Pressure as a function of the scale factor ($\tilde{P} = -1$ for $a = 0.765$).
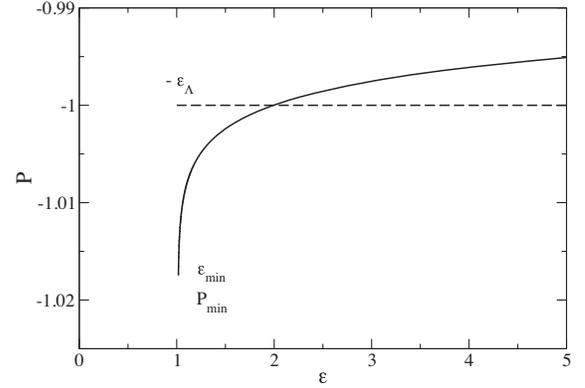
FIG. 8. Pressure as a function of the energy density ($\tilde{P} = -1$ for $\tilde{\epsilon} = 1.99$).

At that point $w = -1/[2(1 - B)] = -0.502$. This corresponds typically to the time of equality between DM and DE in the ΛCDM model (see Appendix D).

B. Early Universe

In the early Universe ($a \to 0$), we get

$$\tilde{\rho} \sim \tilde{\epsilon} \sim \frac{\Omega_{m,0}}{1 - \Omega_{m,0}} \frac{1}{a^3}, \tag{129}$$

$$\tilde{E}_{\text{tot}} \to 1, \tag{130}$$

$$\tilde{P} \simeq B \ln \left(\frac{\Omega_{m,0}}{1 - \Omega_{m,0}} \frac{1}{a^3} \right) - 1, \tag{131}$$

$$\tilde{P} \simeq B \ln \tilde{\epsilon} - 1, \tag{132}$$

$$w \sim \frac{B \ln \tilde{\rho} - 1}{\tilde{\rho}}, \tag{133}$$

$$w \sim \frac{1 - \Omega_{m,0}}{\Omega_{m,0}} a^3 \left[B \ln \left(\frac{\Omega_{m,0}}{1 - \Omega_{m,0}} \frac{1}{a^3} \right) - 1 \right], \tag{134}$$

$$w \sim \frac{B \ln \tilde{\epsilon} - 1}{\tilde{\epsilon}}. \tag{135}$$

C. Late Universe

In the late Universe ($a \to +\infty$), we get

$$\tilde{\rho} \to \tilde{\rho}_{\min} = 2B = 7.065 \times 10^{-3}, \tag{136}$$

$$\tilde{\epsilon} \to \tilde{\epsilon}_{\min} = 1 - B \ln(2B) = 1.02, \tag{137}$$

$$\tilde{E}_{\text{tot}} \to 0, \tag{138}$$

$$\tilde{P} \to \tilde{P}_{\min} = -\tilde{\epsilon}_{\min}, \tag{139}$$

$$w \to w_{\min} = \frac{\tilde{P}_{\min}}{\tilde{\epsilon}_{\min}} = -1. \tag{140}$$

D. Recovery of the ΛCDM model when $B = 0$

When $B = 0$, the general equations of Sec. VII A reduce to

$$\tilde{\rho} = \frac{\Omega_{m,0}}{1 - \Omega_{m,0}} \frac{1}{a^3}, \tag{141}$$

$$\tilde{\epsilon} = \tilde{\rho} + 1, \tag{142}$$

$$\tilde{\epsilon} = \frac{\Omega_{m,0}}{1 - \Omega_{m,0}} \frac{1}{a^3} + 1, \tag{143}$$

$$\tilde{P} = -1, \tag{144}$$

$$\tilde{E}_{\text{tot}} = 1, \tag{145}$$

$$w = -\frac{1}{\tilde{\rho} + 1} = -\frac{1}{\tilde{\epsilon}}, \tag{146}$$

$$w = -\frac{1}{\frac{\Omega_{m,0}}{1 - \Omega_{m,0}} \frac{1}{a^3} + 1}. \tag{147}$$

Therefore, for $B = 0$, we recover the equations of the ΛCDM model (see Appendix D). Since the ΛCDM model works very well at large scales, the logotropic model should also work well provided that B is small enough. We recall that B is not a free parameter of our model that could be tuned in order to fit the data. It is actually determined by the theory (see Sec. VI B). Indeed, if we identify ρ_P with the Planck density, this automatically fixes B through Eq. (99). Therefore, our model is fully predictive. As we have seen in Sec. VI B, the limit $B \to 0$ corresponds to $\rho_P \to +\infty$ or $\hbar \to 0$ (quantum effects negligible). Therefore, the ΛCDM model corresponds to the semiclassical limit $\hbar \to 0$ of the logotropic model. However, because of the fundamentally nonzero value of $\hbar$, the logotropic model with a nonzero value of $B = 3.53 \times 10^{-3}$ should be privileged over the ΛCDM model (corresponding to $B = 0$).

Remark.—It is instructive to establish the connection between the LDF and the ΛCDM model directly from the dimensional equation of state (55). This equation can be rewritten as

$$P = A \ln\left(\frac{\rho}{\rho_\Lambda}\right) - A \ln\left(\frac{\rho_P}{\rho_\Lambda}\right). \tag{148}$$

Taking the limit $A \to 0$ and $\rho_P \to +\infty$ with $A \ln(\rho_P/\rho_\Lambda) = \rho_\Lambda c^2$ fixed [see Eq. (105)], we obtain

$$P = \frac{\rho_\Lambda c^2}{\ln(\frac{\rho_P}{\rho_\Lambda})} \ln\left(\frac{\rho}{\rho_\Lambda}\right) - \rho_\Lambda c^2 \simeq -\rho_\Lambda c^2. \tag{149}$$

This returns the constant equation of state of the ΛCDM model in its UDM interpretation (see Appendix D 3).

VIII. EFFECTIVE DM AND DE

In terms of dimensionless variables, the rest-mass density is given by (see Sec. IV)

$$\tilde{\rho}_m = \tilde{\rho} \sqrt{1 - \frac{2B}{\tilde{\rho}}} \tag{150}$$

and the internal energy $u = \tilde{\epsilon} - \tilde{\rho}_m$ is given by

$$\tilde{u} = \tilde{\rho} - B \ln \tilde{\rho} + 1 - 2B - \tilde{\rho} \sqrt{1 - \frac{2B}{\tilde{\rho}}}. \tag{151}$$

Using Eq. (122), they evolve with the scale factor a as

$$\tilde{\rho}_m = \frac{\Omega_{m,0}}{1 - \Omega_{m,0}} \frac{1}{a^3} \tag{152}$$

and

$$\tilde{u} = 1 - B + \sqrt{B^2 + \left(\frac{\Omega_{m,0}}{1 - \Omega_{m,0}}\right)^2 \frac{1}{a^6}}$$
$$- B \ln\left[B + \sqrt{B^2 + \left(\frac{\Omega_{m,0}}{1 - \Omega_{m,0}}\right)^2 \frac{1}{a^6}}\right] - \frac{\Omega_{m,0}}{1 - \Omega_{m,0}} \frac{1}{a^3}. \tag{153}$$

As indicated previously, the rest-mass density ρ_m can be interpreted as DM and the internal energy density u can be interpreted as DE [1]. The proportions of DM and DE as a function of the scale factor a are plotted in Fig. 9. At early times, the Universe is dominated by DM ($\rho_m c^2 \gg u$) and at late times, the Universe is dominated by DE ($\rho_m c^2 \ll u$). The DE density increases monotonically from $\tilde{u} \sim 3B \ln a \to -\infty$ when $a \to 0$ to $\tilde{u} \to 1 - B \ln(2B)$ when $a \to +\infty$. Since the DE density corresponds to the internal energy density u of the LDF, it can very well be negative as long as the total energy density ϵ is positive. In the regime of interest ($\rho_m \ll \rho_P$) where the logotropic model is valid, the DE density $\epsilon_{de} = u$ is positive.
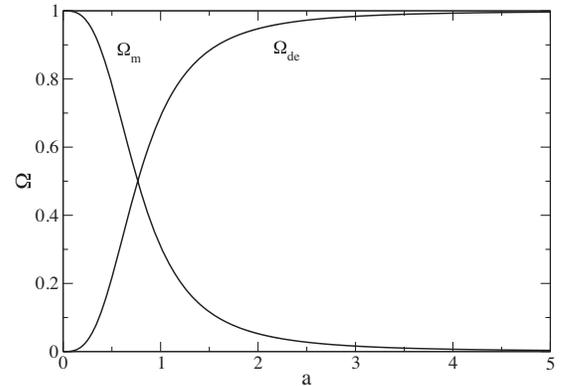
FIG. 9. Proportions of DM (rest mass) and DE (internal energy) as a function of the scale factor ($\Omega_m = \rho_m c^2/\epsilon$ and $\Omega_{de} = u/\epsilon$).

Remark.—For the ΛCDM model ($B = 0$), we find that $\rho = \rho_m \propto a^{-3}$ and $u = \rho_\Lambda c^2$ (see also Appendices D and E).

IX. DECELERATION PARAMETER

In a flat Universe without cosmological constant ($k = \Lambda = 0$), the deceleration parameter $q = -\ddot{a}a/\dot{a}^2$ is related to the equation of state parameter w by (see, e.g., [52])

$$q = \frac{1 + 3w}{2}. \tag{154}$$

Therefore, we can easily deduce the evolution of q from the evolution of w obtained in Sec. VII. The function $q(a)$ is represented in Fig. 10.

The Universe starts accelerating when $q = 0$ corresponding to $w_c = -1/3$. At that point $\tilde{\rho}_c \simeq 2$, $\tilde{\epsilon}_c \simeq 3$, and $a_c \simeq 0.607$ like for the ΛCDM model (the difference is less than 1%).

The present value of the deceleration parameter is

$$q_0 = \frac{1 + 3w_0}{2}, \tag{155}$$

where

$$w_0 = \frac{B \ln \tilde{\rho}_0 - 1}{\tilde{\rho}_0 - B \ln \tilde{\rho}_0 + 1 - 2B} \tag{156}$$

with

$$\tilde{\rho}_0 = B + \sqrt{B^2 + \left(\frac{\Omega_{m,0}}{1 - \Omega_{m,0}}\right)^2}. \tag{157}$$

We get $\tilde{\rho}_0 = 0.4505$, $\tilde{\epsilon}_0 = 1.45$, $\tilde{E}_{tot} = 0.992$, $\tilde{P} = -1.00$, $w_0 = -0.693$, and $q_0 = -0.540$. For the ΛCDM model, we obtain $\tilde{\rho}_0 = 0.447$, $\tilde{\epsilon}_0 = 1.45$, $\tilde{E}_{tot} = 1$, $\tilde{P} = -1$,
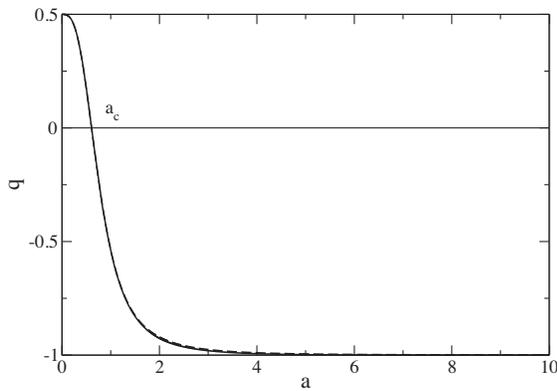
FIG. 10. Deceleration parameter as a function of the scale factor. The value $a_c = 0.607$ corresponds to the moment at which the Universe starts accelerating.

$w_0 = -0.691$, and $q_0 = -0.537$. The values of the two models are very close to each other, differing by less than 1%.

X. SPEED OF SOUND

A. Dimensional variables

The speed of sound c_s is defined by

$$c_s^2 = P'(\epsilon)c^2. \tag{158}$$

Differentiating Eq. (60) with respect to ϵ and using Eq. (55) we obtain

$$\frac{c_s^2}{c^2} = \frac{1}{\frac{\rho c^2}{A} - 1}. \tag{159}$$

Since $\rho \geq \rho_{min} = 2A/c^2$ we find that $c_s^2 \geq 0$ and $c_s < c$. The speed of sound tends to zero ($c_s \to 0$) when $\rho \to +\infty$ and to the speed of light ($c_s \to c$) when $\rho \to \rho_{min}$ (see Fig. 11).[28]

In the early Universe,

$$\frac{c_s^2}{c^2} \sim \frac{A}{\rho c^2}, \tag{160}$$

$$\frac{c_s^2}{c^2} \sim \frac{A}{Qmc^2} a^3, \tag{161}$$

$$\frac{c_s^2}{c^2} \sim \frac{A}{\epsilon}. \tag{162}$$

In the late Universe,

$$c_s \to c. \tag{163}$$

Remark.—The pseudo speed of sound c_s^* defined by $(c_s^*)^2 = P'(\rho)$ is given by

$$(c_s^*)^2 = \frac{A}{\rho}. \tag{164}$$

It coincides with the true speed of sound c_s in the nonrelativistic regime $\rho \gg A/c^2$ (early Universe). On the other hand, in the late Universe, we get $c_s^* = c/\sqrt{2}$ when $\rho = \rho_{min} = 2A/c^2$.

---

[28]We note that the squared speed of sound in the LDF is positive in spite of the fact that its pressure is negative. This is a very important property because, in many cases, fluids with negative pressure obeying a barotropic equation of state suffer from hydrodynamic or tachyonic instabilities at small scales due to an imaginary speed of sound. This does not occur in the present model. In addition, the speed of sound is always less than the speed of light. By contrast, in the original logotropic model [1], the speed of sound diverges as we enter the phantom era, before becoming imaginary.
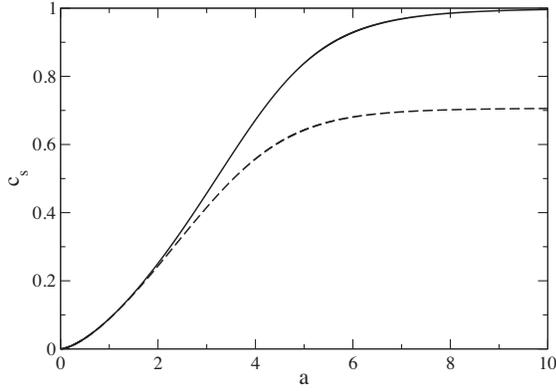
FIG. 11. Speed of sound as a function of the scale factor (the dashed line corresponds to the pseudo speed of sound). We note that $c_s = 0$ in the ΛCDM model.

B. Dimensionless variables

Introducing the dimensionless speed of sound $\tilde{c}_s = c_s/c$ and using the dimensionless variables defined previously, we get

$$\tilde{c}_s^2 = \frac{1}{\frac{\tilde{\rho}}{B} - 1}. \tag{165}$$

In the early Universe,

$$\tilde{c}_s^2 \sim \frac{B}{\tilde{\rho}}, \tag{166}$$

$$\tilde{c}_s^2 \sim B \frac{1 - \Omega_{m,0}}{\Omega_{m,0}} a^3, \tag{167}$$

$$\tilde{c}_s^2 \sim \frac{B}{\tilde{\epsilon}}. \tag{168}$$

In the late Universe,

$$\tilde{c}_s \to 1. \tag{169}$$

The present value of the squared speed of sound is

$$(\tilde{c}_s^2)_0 = \frac{1}{\frac{\tilde{\rho}_0}{B} - 1} = 7.90 \times 10^{-3}, \tag{170}$$

showing that the present Universe is strongly special relativistic [$(c_s)_0 \sim 0.1c$]. The pseudo squared speed of sound is $(\tilde{c}_s^*)^2 = B/\tilde{\rho}$ and its present value is $(\tilde{c}_s^*)_0^2 = B/\tilde{\rho}_0 = 7.84 \times 10^{-3}$. As discussed in Sec. XVI and in Appendix C the present value of the squared speed of sound $c_s^2/c^2 \sim 10^{-2}$ is too large to enable the formation of clusters of galaxies and to account for the observations of the power spectrum. This is a serious problem of the logotropic model.

C. ΛCDM model ($B = 0$)

For $B = 0$, corresponding to $\rho_P \to +\infty$ (no quantum effects), we find that

$$c_s = 0. \tag{171}$$

The speed of sound vanishes in the ΛCDM model since the pressure $P = -\rho_\Lambda c^2$ is constant (see Appendix D 3). The vanishing of the speed of sound in the ΛCDM model (implying the absence of pressure gradient to balance the gravitational attraction in DM halos) is at the origin of the small-scale crisis of the CDM model. The fact that the speed of sound is nonzero in the logotropic model ($B = 3.53 \times 10^{-3}$) while it vanishes in the ΛCDM model ($B = 0$) is an important difference between the two models. Indeed, a nonzero speed of sound may solve the CDM small-scale crisis. However, the fact that the speed of sound increases with the scale factor in the logotropic model (see Fig. 11) poses new problems regarding the formation of structures as discussed in Sec. XVI.

XI. EVOLUTION OF THE SCALE FACTOR

The evolution of the scale factor of the Universe is determined by the Friedmann equation (8) combined with the relation $\epsilon(a)$ between the energy density and the scale factor. This yields an equation of the form

$$H = \frac{\dot{a}}{a} = \left(\frac{8\pi G}{3c^2}\right)^{1/2} \epsilon^{1/2}(a). \tag{172}$$

Introducing the dimensionless energy $\tilde{\epsilon} = \epsilon/\rho_\Lambda c^2$ and the dimensionless time $\tilde{t} = (8\pi G\rho_\Lambda/3)^{1/2}t$, this equation can be rewritten as

$$\frac{\dot{a}}{a} = \tilde{\epsilon}^{1/2}(a). \tag{173}$$

It can be integrated into

$$\tilde{t} = \int_0^a \frac{dx}{x\tilde{\epsilon}^{1/2}(x)} \equiv \tilde{t}(a), \tag{174}$$

which gives $a(\tilde{t})$ in reversed form. In the logotropic model, the relation $\tilde{\epsilon}(a)$ between the dimensionless energy and the scale factor is determined by Eqs. (117) and (122). One can then solve Eq. (174) numerically. The function $a(\tilde{t})$ is plotted in Fig. 12.

In the early Universe $t \to 0$, using Eq. (129), we get

$$a = \left[\frac{3}{2}\left(\frac{8\pi G\rho_\Lambda}{3}\right)^{1/2}\left(\frac{\Omega_{m,0}}{1 - \Omega_{m,0}}\right)^{1/2} t\right]^{2/3}, \tag{175}$$

which can be rewritten as

$$a = \left(\frac{3}{2}\sqrt{\Omega_{m,0}} H_0 t\right)^{2/3}, \tag{176}$$
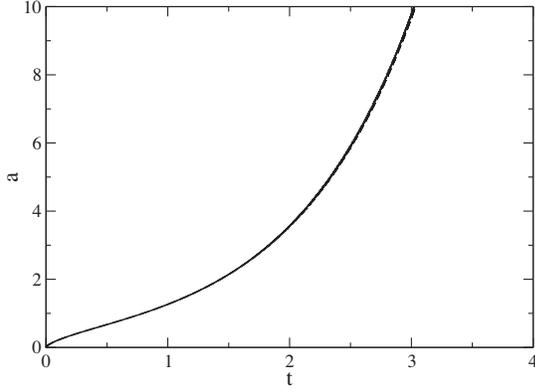
FIG. 12. Scale factor as a function of time. The logotropic model starts to deviate from the ΛCDM model for $a \gtrsim 2$ but the difference between the two models is hardly perceptible on this representation.

where H_0 is the present value of the Hubble constant. This is the usual Einstein–de Sitter solution.

In the late Universe $t \rightarrow +\infty$, using Eq. (137), we get

$$a \propto e^{(\frac{8\pi G\rho_\Lambda}{3})^{1/2}[1-B\,\ln(2B)]^{1/2}t}. \qquad (177)$$

This is the de Sitter solution with a B-modified cosmological constant. As discussed in Secs. VI and XIV A, this modification has a quantum origin.

The age of the Universe in the logotropic model is

$$t_0 = \left(\frac{3}{8\pi G\rho_\Lambda}\right)^{1/2} \int_0^1 \frac{dx}{x\tilde{\epsilon}^{1/2}(x)}. \qquad (178)$$

We obtain $\tilde{t}_0 = 0.795$ giving $t_0 = 13.8$ Gyr like for the ΛCDM model corresponding to $B = 0$ (the difference is less than 1%).

XII. TOTAL POTENTIAL

A. Dimensional variables

In the logotropic model, the total potential of the SF including the rest-mass term and the logarithmic term [see Eqs. (3) and (53)] is

$$V_{\mathrm{tot}}(|\varphi|^2) = \frac{m^2 c^2}{2\hbar^2}|\varphi|^2 - A\,\ln\left(\frac{m^2|\varphi|^2}{\hbar^2\rho_P}\right) - A. \qquad (179)$$

Introducing the pseudo-rest-mass density defined by Eq. (25) it can be rewritten as

$$V_{\mathrm{tot}} = \frac{1}{2}\rho c^2 - A\,\ln\left(\frac{\rho}{\rho_P}\right) - A. \qquad (180)$$

It is represented in Fig. 13. It behaves as $V_{\mathrm{tot}} \sim -A\,\ln\rho$ for $\rho \rightarrow 0$ and as $V_{\mathrm{tot}} \sim (1/2)\rho c^2$ for $\rho \rightarrow +\infty$. It has a minimum at
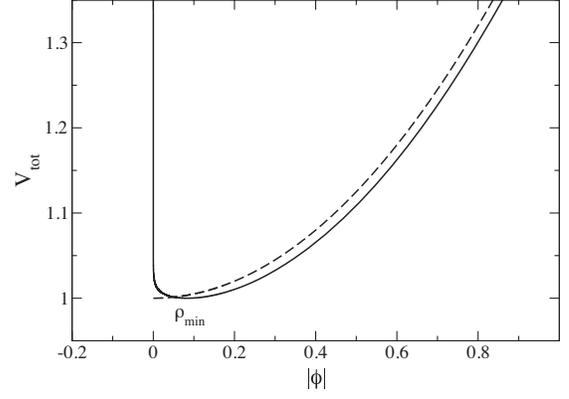
FIG. 13. Total potential of the logotropic SF. The SF descends the potential by rapidly spinning around the vertical axis. Only the exterior branch $\rho \geq \rho_{\mathrm{min}}$ is accessible. The dashed line corresponds to the total potential of the ΛCDM model in its SF representation (see Appendix E).

$$\rho_{\mathrm{min}} = \frac{2A}{c^2}, \qquad V_{\mathrm{min}} = \epsilon_{\mathrm{min}} = A\,\ln\left(\frac{\rho_P c^2}{2A}\right). \qquad (181)$$

We note that ρ_{min} corresponds to the asymptotic value of the pseudo-rest-mass density for $a \rightarrow +\infty$ (see Sec. V B). Since $\rho \geq \rho_{\mathrm{min}}$, only the exterior branch of the potential is accessible. For a complex SF, the potential is symmetric with respect to the origin $|\varphi| = 0$ and, by rotation around the vertical axis, the exterior branch defines a surface similar to the surface of a "bowl" (there is also a central "wall" corresponding to the interior branch). The SF slowly descends the potential on the surface of the bowl by rapidly spinning around the vertical axis. We note that the SF does not reach the origin $|\varphi| = \rho = 0$ because of the presence of the central wall. This is a particularity of the logotropic model. In the SF representation of the ΛCDM model, there is no central wall. In that case, $\rho_{\mathrm{min}} = 0$ and the SF can reach the origin (see Appendix E 2). We also note that the modulus $|\varphi|$ of a complex SF does *not* oscillate, contrary to the case of a real SF. Only its phase θ oscillates. This corresponds to the spintessence phenomenon described in Sec. II C. In this sense, the evolution of a complex SF is very different from the evolution of a real SF.

B. Dimensionless variables

Introducing the dimensionless variables $\tilde{V}_{\mathrm{tot}} = V_{\mathrm{tot}}/\rho_\Lambda c^2$ and $\tilde{\varphi} = (m/\hbar)\varphi/\sqrt{\rho_\Lambda}$ in addition to those defined previously, we can rewrite the total SF potential of the logotropic model under the form

$$\tilde{V}_{\mathrm{tot}} = \frac{1}{2}|\tilde{\varphi}|^2 - B\,\ln|\tilde{\varphi}|^2 - B + 1, \qquad (182)$$

or

$$\tilde{V}_{\mathrm{tot}} = \frac{1}{2}\tilde{\rho} - B\,\ln\tilde{\rho} - B + 1, \qquad (183)$$

where

$$\tilde{\rho} = |\tilde{\varphi}|^2. \qquad (184)$$

C. ΛCDM model ($B = 0$)

For $B = 0$, the foregoing equations reduce to

$$\tilde{V}_{\text{tot}} = \frac{1}{2}|\tilde{\varphi}|^2 + 1 = \frac{1}{2}\tilde{\rho} + 1. \qquad (185)$$

Coming back to the original variables, or taking the limit $A \to 0$ and $\rho_P \to +\infty$ with $A \ln(\rho_P/\rho_\Lambda) \to \rho_\Lambda c^2$ fixed [see Eq. (105)] in Eqs. (179) and (180), we obtain

$$V_{\text{tot}}(|\varphi|^2) = \frac{m^2 c^2}{2\hbar^2}|\varphi|^2 + \rho_\Lambda c^2 = \frac{1}{2}\rho c^2 + \rho_\Lambda c^2. \quad (186)$$

We recover the constant potential $V = \epsilon_\Lambda = \rho_\Lambda c^2$ of the complex SF associated with the ΛCDM model that we call the ΛFDM model (see Appendix E).

XIII. VALIDITY OF THE FAST OSCILLATION REGIME (TF APPROXIMATION) IN COSMOLOGY

The previous results are valid in the fast oscillation regime of the complex SF. We have seen that it corresponds to the TF approximation. Let us determine the domain of validity of this approximation. The fast oscillation regime is valid provided that $\omega \gg H$, where $\omega = \dot{\theta} = \dot{S}_{\text{tot}}/\hbar = -E_{\text{tot}}/\hbar$ is the pulsation of the SF and $H = \dot{a}/a$ is the Hubble constant which is related to the energy density by the Friedmann equation $H^2 = (8\pi G/3c^2)\epsilon$. In terms of the dimensionless variables introduced previously, the fast oscillation regime is valid provided that

$$\frac{\tilde{\epsilon}}{\tilde{E}_{\text{tot}}^2} \ll \sigma, \qquad (187)$$

where

$$\sigma = \frac{3m^2 c^4}{8\pi G\hbar^2 \rho_\Lambda} \qquad (188)$$

is a dimensionless parameter. It can be written as

$$\sigma = \left(\frac{m}{m_\Lambda}\right)^2, \qquad (189)$$

where

$$m_\Lambda = \frac{\hbar}{c^2}\left(\frac{8\pi G\rho_\Lambda}{3}\right)^{1/2} = \frac{\hbar}{c^2}\sqrt{\frac{\Lambda}{3}} = 1.20 \times 10^{-33} \text{ eV}/c^2 \qquad (190)$$

is the cosmon mass.[29] The fast oscillation regime will be valid over a large period of time provided that $\sigma \gg 1$, i.e.,

$$m \gg m_\Lambda. \qquad (191)$$

Therefore, the mass of the SF has to be much larger than the cosmon mass.[30] The mass of the boson required in the FDM model to explain DM halos—one of the smallest particle mass quoted in the literature—is of the order of $m_{22} = 10^{-22}$ eV/c^2 (see Appendix E). For this value, we get $\sigma_{22} = 6.93 \times 10^{21} \gg 1$ implying that the fast oscillation regime is valid over a large period of time. For future comparison, we note that the criterion (191) determining the validity of the fast oscillation regime (or TF approximation) in cosmology can also be written as

$$m \gg \frac{B\sqrt{8\pi G\hbar^2 \rho_\Lambda^3}}{A}, \qquad (192)$$

where we have used Eq. (89).

In the logotropic model, the quantities $\tilde{\epsilon}$ and $\tilde{E}_{\text{tot}}$ are given as a function of the scale factor a by Eqs. (117), (118), and (122). The curve $(\tilde{\epsilon}/\tilde{E}_{\text{tot}}^2)(a)$ is plotted in Fig. 14. It presents a minimum value $(\tilde{\epsilon}/\tilde{E}_{\text{tot}}^2)_{\text{min}} = 1.18$ at $a = 1.71$. The condition $\tilde{\epsilon}/\tilde{E}_{\text{tot}}^2 < \sigma$ can be fulfilled provided that $\sigma \geq \sigma_{\text{min}} = 1.18$, i.e., $m \geq 1.09\, m_\Lambda = 1.30 \times 10^{-33}$ eV/c^2. When this condition is satisfied, we find that the fast oscillation regime is valid for $a_v^{(1)} \ll a \ll a_v^{(2)}$, where $a_v^{(1)}$ and $a_v^{(2)}$ are given by

$$\frac{a_v}{a_t} = f\left(\frac{3m^2 c^4}{8\pi G\hbar^2 \rho_\Lambda}\right) \qquad (193)$$

with

---

[29]This mass scale is often interpreted as the smallest mass of the elementary particles predicted by string theory [53] or as the upper bound on the mass of the graviton [54]. The mass m_Λ also represents the quantum of mass in theories of extended supergravity [55]. The mass scale m_Λ is simply obtained by equating the Compton wavelength of the particle $\lambda_C = \hbar/mc$ with the Hubble radius $R_\Lambda = c/H_0$ (the typical size of the visible Universe) giving $m_\Lambda = \hbar H_0/c^2 \sim \hbar\sqrt{\Lambda}/c^2$ (since $H_0^2 \sim G\rho_\Lambda \sim \Lambda$). The mass m_Λ corresponds to Wesson's [56] minimum mass interpreted as a quantum of DE [Wesson's maximum mass $M_\Lambda = (4/3)\pi(\epsilon_0/c^2)R_\Lambda^3 = c^3/2GH_0 = 9.20 \times 10^{55}$ g is of the order of the mass of the Universe]. These mass scales were also introduced in [4]. Böhmer and Harko [57] proposed to call the elementary particle of DE having the mass m_Λ the "cosmon." Cosmons were originally introduced by Peccei *et al.* [58] to name SFs that could dynamically adjust the cosmological constant to zero (see also [59–61]). The name cosmon was also used in a different context [62] to designate a very light scalar particle (dilaton) of mass $\sim 10^{-3}$ eV/c^2 which could mediate new macroscopic forces in the submillimeter range.

[30]In particular, the validity of our approach requires that the mass of the SF is nonzero.
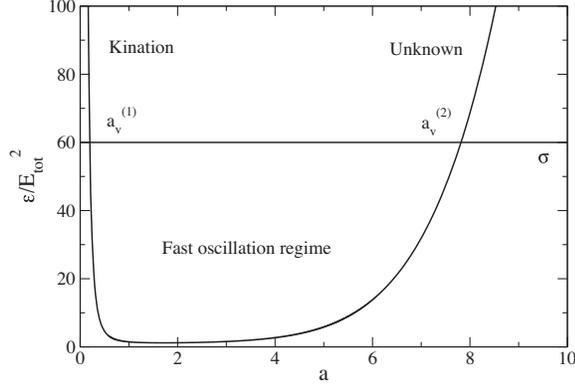
FIG. 14. Graphical construction determining the range of validity of the fast oscillation regime in the logotropic model (we have represented $\tilde{\epsilon}/\tilde{E}_{\rm tot}^2$ versus a).

$$f(\sigma) = \frac{1}{r^{1/3}(1 - 2B/r)^{1/6}} \qquad (194)$$

and

$$\sigma = \frac{r - B \ln r + 1 - 2B}{1 - 2B/r}. \qquad (195)$$

We have introduced the transition scale factor a_t from Eq. (115). Equations (194) and (195) define the two-valued function $f(\sigma)$ in parametric form. When $\sigma \gg 1$, we find that

$$\frac{a_v^{(1)}}{a_t} \sim \frac{1}{\sigma^{1/3}} \qquad (196)$$

and

$$\frac{a_v^{(2)}}{a_t} \sim \frac{\sigma^{1/6}}{(2B)^{1/3}[1 - B \ln(2B)]^{1/6}}. \qquad (197)$$

For a SF of mass $m_{22} = 10^{-22}$ eV/c², corresponding to $\sigma_{22} = 6.93 \times 10^{21}$, we obtain $a_v^{(1)} = 4.01 \times 10^{-8}$ and $a_v^{(2)} = 1.73 \times 10^4$. Therefore, the range of validity of the fast oscillation regime is large. For a larger mass m of the SF, the range of validity of the fast oscillation regime is even larger.

According to the previous discussion, the fast oscillation regime is valid for $m \gg m_\Lambda$ on the period $a_v^{(1)} \ll a \ll a_v^{(2)}$. During this period, we have seen that the SF behaves successively as DM and DE. The transition between the DM-like era and the DE-like era corresponds to a scale factor (see Sec. VI E)[31]

$$a_t = 0.765. \qquad (198)$$

The fast oscillation regime is not valid at very early times (i.e., $a < a_v^{(1)}$). In that case, the SF is in a slow oscillation regime of kination (see Sec. II E). As discussed in [20,28], this gives rise to a stiff matter era. The stiff matter era usually takes place in the very early Universe. Therefore, $a_v^{(1)}$ marks the end of the stiff matter era and the beginning of the DM era.[32] The logotropic SF successively experiences a stiff matter era, a DM era, and a DE era (this is also the case for the ΛFDM model discussed in Appendix E). More surprisingly, the fast oscillation regime ceases to be valid at very late times (i.e., $a > a_v^{(2)}$). This shows that quantum mechanics becomes important in the very late Universe. In that case, we have to come back to the full set of KGF equations, or their hydrodynamic representation [20], and take the terms in $\hbar$ into account (i.e., we have to go beyond the TF approximation). Quantum mechanics will change the results derived on the basis of the fast oscillation (or TF) approximation. Therefore, in the logotropic model, the very late Universe will not remain in a de Sitter stage. It may experience a stiff matter era again, or another (unknown) era, possibly passing from a phase of acceleration to a phase of deceleration. It should return to a de Sitter stage ultimately as it falls in the bottom of the potential. Note, by contrast, that the fast oscillation regime is always valid at late times in the ΛFDM model (see Appendix E).

We can represent the previous results on a dynamical phase diagram (see Fig. 15) where we plot the transition scales $a_v^{(1)}$ and $a_v^{(2)}$ as a function of the mass m of the SF. For $m > 1.09 m_\Lambda$, the logotropic complex SF undergoes four successive eras: a stiff matter era for $a < a_v^{(1)}$, a DM era for $a_v^{(1)} < a < a_t$, a DE era for $a_t < a < a_v^{(2)}$, and another (unknown) era for $a > a_v^{(2)}$.

It is interesting, in parallel, to discuss how the complex SF evolves in the potential $V_{\rm tot}(|\varphi|^2)$ during these different periods. During the stiff matter era ($a < a_v^{(1)}$), corresponding to a slow oscillation regime, the SF rolls down the potential well without oscillating. Then, for $a > a_v^{(1)}$, the SF enters in the fast oscillation regime and descends the potential by oscillating rapidly about the vertical axis as explained in Sec. XII. This covers the DM and DE eras. Finally, for $a > a_v^{(2)}$, the SF stops oscillating rapidly again. Its detailed behavior, which corresponds to an evolution different from an exponential (de Sitter) expansion, is unknown. The evolution of the SF—roll versus oscillations—is represented schematically in Fig. 16.

Remark.—Combining the present results with those of [20,28], we can propose a more general complex SF model based on a potential of the form

---

[31]To define the transition between the DM-like era and the DE-like era, we could have alternatively used the value $a_c = 0.607$ at which the Universe starts accelerating.

[32]If the SF has an additional $|\varphi|^4$ self-interaction (see the Remark below), a radiationlike era may be present between the stiff matter era and the DM era [20,28].
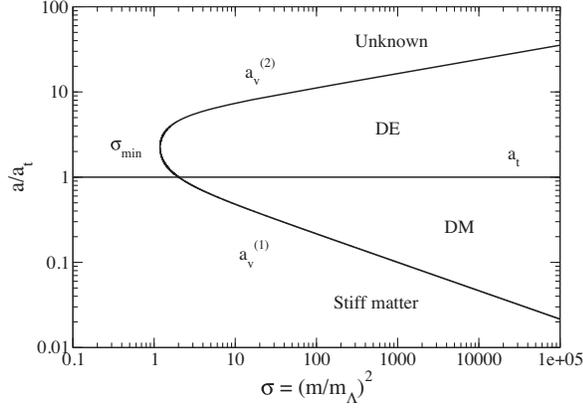
FIG. 15. Dynamical phase diagram of the logotropic model showing the different eras experienced by the SF during the evolution of the Universe as a function of its mass m (this figure also determines the validity of the fast oscillation regime between $a_v^{(1)}$ and $a_v^{(2)}$). We see how the fundamental cosmon mass m_Λ comes into play in the problem.

$$V_{\rm tot}(|\varphi|^2) = \frac{m^2c^2}{2\hbar^2}|\varphi|^2 + \frac{2\pi a_s m}{\hbar^2}|\varphi|^4 - A\ln\left(\frac{m^2|\varphi|^2}{\hbar^2\rho_P}\right) - A.$$

(199)

This potential applies to a self-interacting relativistic Bose-Einstein condensate (BEC) in the framework of the logotropic model. Indeed, it includes a $|\varphi|^4$ self-interaction potential, proportional to the scattering length a_s of the bosons, in addition to the logarithmic potential. When $a_s > 0$ (repulsive self-interaction), the $|\varphi|^4$ potential produces a radiationlike era in the fast oscillation regime preceding the DM era (see [20,28] for details). Therefore, a complex SF evolving in the potential defined by Eq. (199) experiences successively a stiff matter era, a (dark)
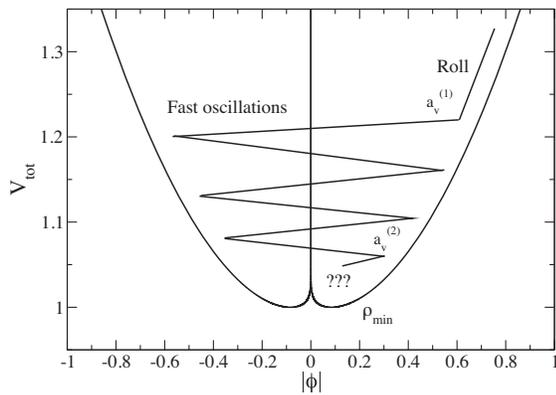
FIG. 16. Schematic evolution of the logotropic complex SF in the total potential $V_{\rm tot}(|\varphi|^2)$ (the scales are not respected). For $a < a_v^{(1)}$, it rolls down the potential well without oscillating (stiff matter era); for $a_v^{(1)} < a < a_v^{(2)}$, it oscillates rapidly about the vertical axis (DM and DE eras); for $a > a_v^{(2)}$, it stops oscillating rapidly (its evolution remains to be characterized in detail).

radiationlike era, a DM era, and a DE era (the case of an attractive self-interaction is more complicated [20]). For $A \to 0$ and $\rho_P \to +\infty$ with $A\ln(\rho_P/\rho_\Lambda) = \rho_\Lambda c^2$ fixed [see Eq. (105)], the DE era is equivalent to a cosmological constant (see Appendix E) and the potential from Eq. (199) reduces to

$$V_{\rm tot}(|\varphi|^2) = \frac{m^2c^2}{2\hbar^2}|\varphi|^2 + \frac{2\pi a_s m}{\hbar^2}|\varphi|^4 + \epsilon_\Lambda.$$

(200)

It applies to a self-interacting relativistic self-interacting BEC in the presence of a cosmological constant.

XIV. ANALOGIES AND DIFFERENCES BETWEEN THE LOGOTROPIC MODEL AND THE ΛCDM MODEL

In this section, we compare the predictions of the logotropic and ΛCDM models.

A. Minimum energy density

Since the ΛCDM model corresponds to $B = 0$ and since the predicted value of $B = 3.53 \times 10^{-3}$ is relatively small, we expect that the logotropic model will not differ substantially from the ΛCDM model regarding the description of the large-scale structure of the Universe. This is a prerequisite to any viable cosmological model since the ΛCDM model works well at large scales. Actually, the two models are almost indistinguishable for what concerns the evolution of the cosmological background up to the present epoch, and they will only slightly differ in the far future. The two models both tend to a constant energy density, ultimately leading to a de Sitter era, but the values of this minimum energy density slightly differ.

In the ΛCDM model, the energy density tends, for $a \to +\infty$, to the Einstein cosmological density

$$\epsilon_{\min}^{\Lambda\rm CDM} = \rho_\Lambda c^2,$$

(201)

which is the constant density of DE. In the logotropic model, the energy density tends to the value

$$\epsilon_{\min}^{\rm LDF} = \rho_\Lambda c^2[1 - B\ln(2B)].$$

(202)

Their ratio is

$$\frac{\epsilon_{\min}^{\rm LDF}}{\epsilon_{\min}^{\Lambda\rm CDM}} = 1 - B\ln(2B) = 1.02.$$

(203)

They differ by 2%.[33] The difference, which is due to the nonzero value of B, may be interpreted as a quantum

---

[33]Such a difference may be accessible to the precision of modern cosmology. It would be interesting to carefully compare the logotropic model with the observations to see if it can relieve some tensions experienced by the ΛCDM model or, on the contrary, if it increases them.

correction to the Einstein cosmological constant (since B depends on ρ_P) in a theory of quantum gravity. It is interesting to find a logarithmic correction. Similar logarithmic corrections due to quantum effects arise in particle physics and in the context of black hole thermodynamics.

Remark.—We note that the present results substantially differ from those obtained in the framework of the original logotropic model developed in [1–4]. In these former works, we found that the logotropic model is indistinguishable from the ΛCDM model up to the present epoch but, at later times, the energy density in the logotropic model increases logarithmically with the scale factor (implying a phantom era), while in the ΛCDM model the energy density always decreases and tends to a constant. This leads to a super–de Sitter behavior instead of a standard de Sitter behavior. It was shown in [1–4] that the two models would substantially differ in about 25 Gyr when the logotropic Universe becomes phantom. The present logotropic model does not display a phantom behavior. It rather evolves toward a de Sitter era, like the ΛCDM model, but with a quantum-modified cosmological constant. This may be an advantage of the new logotropic model over the original one because phantom models are known to lead to pathologies and singularities. By contrast, a model that tends to a de Sitter era is well behaved and respects the cosmic censorship. On the other hand, in the original logotropic model [1–4], the speed of sound becomes larger than the speed of light as we approach the phantom regime, then becomes imaginary. We do not have such anomalies in the present model since the speed of sound is always real and smaller than the speed of light ($0 \leq c_s \leq c$). As discussed in Sec. X, it increases from 0 to c as the Universe expands. In comparison, the speed of sound is always equal to zero in the ΛCDM model.

B. Logotropic DM halos

As discussed in our previous papers [1–4] (see also Appendix F), the main interest of the logotropic model with respect to the ΛCDM model becomes manifest when this model is applied to DM halos. When treating DM halos, one can use Newtonian gravity. Furthermore, in this section, we shall make the Thomas-Fermi approximation which amounts to neglecting the quantum potential.[34] In that case, the equilibrium state of a logotropic DM halo results from the balance between the gravitational attraction and the repulsion due to the pressure force. It is described by the classical equation of hydrostatic equilibrium

$$\nabla P + \rho \nabla \Phi = \mathbf{0} \qquad (204)$$

coupled to the Poisson equation

$$\Delta \Phi = 4\pi G\rho. \qquad (205)$$

These equations can be combined into a single differential equation

$$-\nabla \cdot \left(\frac{\nabla P}{\rho}\right) = 4\pi G\rho, \qquad (206)$$

which determines, together with the equation of state (55), the density profile of a logotropic DM halo.

In the framework of the ΛCDM model (see Appendix D), the pressure is zero ($P = 0$) or constant ($P = -\epsilon_\Lambda$) so there is no pressure gradient to balance the gravitational attraction. This leads to cuspy density profiles. This also leads to the formation of structures at all scales since the Jeans length vanishes owing to the fact that the speed of sound is zero: $\lambda_J/2\pi = c_s/\sqrt{4\pi G\rho} = 0$. These two predictions of the ΛCDM model are in contradiction with the observations which reveal that DM halos have a core instead of a cusp (core-cusp problem) and that there is no DM halo below a certain scale of order $M \sim 10^8\ M_\odot$ and $R \sim 1$ kpc (missing satellite problem). The fact that the pressure, or pressure gradient, vanishes in the ΛCDM model is the basic reason of the so-called CDM small-scale crisis.

In the framework of the logotropic model, the equation of state is given by Eq. (55) where ρ can be assimilated, in the nonrelativistic regime, to the mass density. Since the pressure is nonzero (and nonconstant), the pressure gradient can balance the gravitational attraction leading to cores instead of cusps.[35] The structure of the logotropic DM halos is studied in detail in Sec. 5 of Ref. [1] (see also Appendix F). Their density profile can be obtained by numerically solving the Lane-Emden equation of index $n = -1$. It presents a core for $r \to 0$ and decreases as $\rho \sim (A/8\pi G)^{1/2} r^{-1}$ for $r \to +\infty$. In addition, the Jeans length in the logotropic model is nonvanishing and can account for the absence of structures below a certain scale as discussed in Sec. 6 of Ref. [1] (see also Sec. XVI). These results remain valid in the present logotropic model because, in the nonrelativistic regime, the equation of state (55) coincides with the equation of state studied in our former works [1–4].

A remarkable result of the logotropic model is to predict that all the DM halos (of any size) have the same surface density $\Sigma_0 = \rho_0 r_h$, where ρ_0 is the central density and r_h is the halo radius at which the central density is divided by 4. Furthermore, the logotropic model predicts that this universal surface density is given by

---

[34]The domain of validity of the TF approximation at the scale of DM halos is discussed in Sec. XV.

[35]We introduced the logotropic model in [1] by looking for the equation of state that is the closest to a constant in order to have cored density profiles at small (galactic) scales while producing the smallest deviation from the ΛCDM model at large (cosmological) scales (see Appendix A).

$$\Sigma_0^{\text{th}} = \left(\frac{A}{4\pi G}\right)^{1/2} \xi_h = 133 \; M_\odot/\text{pc}^2, \qquad (207)$$

where A is the fundamental constant of Eq. (106) and $\xi_h = 5.8458\ldots$ is the dimensionless halo radius obtained by solving the Lane-Emden equation of index $n = -1$ numerically (see Ref. [1] and Appendix F). It turns out that the theoretical value (207) is in very good agreement with the value $\Sigma_0^{\text{obs}} = \rho_0 r_h = 141^{+83}_{-52} \; M_\odot/\text{pc}^2$ obtained from the observations [17]. This is remarkable because there is no free (or adjustable) parameter in our model. As discussed in Sec. VI, the value of the logotropic constant A is determined by cosmological considerations (large scales) while the result from Eq. (207) applies to DM halos (small scales). This suggests that there is a connection between the acceleration of the Universe and the universality of the surface density of DM halos. They are both due to the logotropic constant A. Indeed, the logarithmic potential from Eq. (53) or the logotropic equation of state from Eq. (55) accounts both for the acceleration of the Universe and for the universality of the surface density of DM halos.

Remark.—We can write the universal surface density of DM halos given by Eq. (207) in terms of the Einstein cosmological constant Λ. Using $A = B\rho_\Lambda c^2$ and $\rho_\Lambda = \Lambda/(8\pi G)$, we get[36]

$$\Sigma_0^{\text{th}} = \left(\frac{B}{32}\right)^{1/2} \frac{\xi_h}{\pi} \frac{c\sqrt{\Lambda}}{G} = 0.01955 \frac{c\sqrt{\Lambda}}{G}, \quad (209)$$

where we have used the numerical value of B from Eq. (104). Recalling that B is given by Eq. (99) with $\rho_P/\rho_\Lambda = 8\pi c^5/\hbar G\Lambda$, we also have

$$\Sigma_0^{\text{th}} = 0.329 \frac{\frac{c\sqrt{\Lambda}}{G}}{\sqrt{\ln\left(\frac{8\pi c^5}{\hbar G\Lambda}\right)}}. \qquad (210)$$

These identities express the universal surface density of DM halos in terms of the fundamental constants of physics G, c, Λ, and $\hbar$. We stress that the prefactors are also determined by our model. We note that the identities from Eqs. (208)–(210), which can be checked by a direct numerical application, are interesting in themselves even in the case where the logotropic model would turn out to be wrong. Furthermore, as observed in [4], the surface density of DM halos is of the same order of magnitude as the surface density of the electron. As a result, the identities

---

[36]Recalling that ρ_Λ represents the present density of DE, it may be more relevant to express Σ_0^{th} in terms of the present value of the Hubble constant H_0. Using $\Lambda = 3(1 - \Omega_{\text{m},0})H_0^2$ obtained from Eqs. (8), (90), and (92), we get

$$\Sigma_0^{\text{th}} = 0.02815 \frac{H_0 c}{G}. \qquad (208)$$

from Eqs. (208)–(210) allow us to express the mass of the electron in terms of the cosmological constant (or the Hubble constant) and the other fundamental constants of physics as [4]

$$m_e \sim \left(\frac{\Lambda \hbar^4}{G^2 c^2}\right)^{1/6} \quad \text{or} \quad m_e \sim \left(\frac{H_0 \hbar^2}{Gc}\right)^{1/3}. \qquad (211)$$

This returns the Eddington-Weinberg relation [35,63] which provides a curious connection between atomic physics (microphysics) and cosmology (macrophysics) [49].

XV. LOGOTROPIC WAVE EQUATIONS

The logotropic model developed in this paper is based on a complex SF theory relying on the KG equation taking into account quantum effects ($\hbar \neq 0$). In the previous sections, we have neglected quantum effects by making the TF approximation ($\hbar \to 0$). In this section, we present more general equations that are valid beyond this approximation.

A. Logotropic KG equation

For a spatially inhomogeneous complex SF, the Klein-Gordon-Einstein (KGE) equations read (see, e.g., [30])

$$\Box\varphi + \frac{m^2 c^2}{\hbar^2}\varphi + 2\frac{dV}{d|\varphi|^2}\varphi = 0, \qquad (212)$$

$$R_{\mu\nu} - \frac{1}{2}g_{\mu\nu}R = \frac{8\pi G}{c^4}T_{\mu\nu}, \qquad (213)$$

where $\Box$ is the d'Alembertian operator, $R_{\mu\nu}$ is the Ricci tensor, R is the Ricci scalar, and

$$T_{\mu\nu} = \frac{1}{2}(\partial_\mu\varphi^*\partial_\nu\varphi + \partial_\nu\varphi^*\partial_\mu\varphi)$$
$$- g_{\mu\nu}\left[\frac{1}{2}g^{\rho\sigma}\partial_\rho\varphi^*\partial_\sigma\varphi - V_{\text{tot}}(|\varphi|^2)\right] \qquad (214)$$

is the energy-momentum tensor of the SF. For the logarithmic potential (53), the wave equation (212) becomes

$$\Box\varphi + \frac{m^2 c^2}{\hbar^2}\varphi - \frac{2A}{|\varphi|^2}\varphi = 0. \qquad (215)$$

This is the logotropic KG equation [1]. This equation involves a nonlinear term, measured by the logotropic constant A, which is responsible for the late acceleration of the Universe. In Sec. VI we have interpreted A as a fundamental constant of physics superseding the Einstein cosmological constant. Therefore, instead of introducing a cosmological constant Λ in the geometric part of the equations of general relativity, i.e., on the left-hand side of Eq. (213), as Einstein did, we introduce a new fundamental constant A directly in the wave equation (215). This is a

radically different point of view. We have seen in Sec. XIV B that this term accounts not only for the present acceleration of the Universe but also for the universal surface density of the DM halos. We cannot obtain this last result with the ΛCDM model. Therefore, our approach is substantially different from the ΛCDM model.

Remark.—If we include a $|\varphi|^4$ self-interaction potential in addition to the logarithmic potential in the complex SF potential [see Eq. (199)], we obtain the generalized KG equation

$$\Box\varphi + \frac{m^2 c^2}{\hbar^2}\varphi + \frac{8\pi a_s m}{\hbar^2}|\varphi|^2\varphi - \frac{2A}{|\varphi|^2}\varphi = 0. \quad (216)$$

B. Logotropic GP equation

In the nonrelativistic limit $c \to +\infty$, using the Klein transformation,

$$\varphi(\mathbf{r}, t) = \frac{\hbar}{m}e^{-imc^2 t/\hbar}\psi(\mathbf{r}, t), \quad (217)$$

the KGE equations (212) and (213) reduce to Gross-Pitaevskii-Poisson (GPP) equations[37] (see, e.g., [30])

$$i\hbar\frac{\partial\psi}{\partial t} = -\frac{\hbar^2}{2m}\Delta\psi + m\Phi\psi + m\frac{dV}{d|\psi|^2}\psi, \quad (218)$$

$$\Delta\Phi = 4\pi G|\psi|^2, \quad (219)$$

where ψ is the wave function such that $\rho = |\psi|^2$ represents the mass density. For the logarithmic potential (54), the nonrelativistic wave equation (218) becomes

$$i\hbar\frac{\partial\psi}{\partial t} = -\frac{\hbar^2}{2m}\Delta\psi + m\Phi\psi - \frac{Am}{|\psi|^2}\psi. \quad (220)$$

This is the logotropic GP equation [1]. For $A = 0$ we recover the Schrödinger-Poisson equations which correspond to the FDM model (see Appendix E 3).

Remark.—If we include a $|\psi|^4$ self-interaction potential in addition to the logarithmic potential in the complex SF potential [see Eq. (199)], we obtain the generalized GP equation

$$i\hbar\frac{\partial\psi}{\partial t} = -\frac{\hbar^2}{2m}\Delta\psi + m\Phi\psi + \frac{4\pi a_s \hbar^2}{m^2}|\psi|^2\psi - \frac{Am}{|\psi|^2}\psi. \quad (221)$$

C. Madelung transformation

Writing the wave function as

$$\psi(\mathbf{r}, t) = \sqrt{\rho(\mathbf{r}, t)}e^{iS(\mathbf{r}, t)/\hbar}, \quad (222)$$

where $S(\mathbf{r}, t)$ is the action, and making the Madelung [64] transformation

$$\mathbf{u} = \frac{\nabla S}{m}, \quad (223)$$

where $\mathbf{u}(\mathbf{r}, t)$ is the velocity field, the GPP equations (218)–(220) can be written under the form of hydrodynamic equations

$$\frac{\partial\rho}{\partial t} + \nabla\cdot(\rho\mathbf{u}) = 0, \quad (224)$$

$$\frac{\partial\mathbf{u}}{\partial t} + (\mathbf{u}\cdot\nabla)\mathbf{u} = -\frac{1}{m}\nabla Q_B - \frac{1}{\rho}\nabla P - \nabla\Phi, \quad (225)$$

$$\Delta\Phi = 4\pi G\rho, \quad (226)$$

where

$$Q_B = -\frac{\hbar^2}{2m}\frac{\Delta\sqrt{\rho}}{\sqrt{\rho}} = -\frac{\hbar^2}{4m}\left[\frac{\Delta\rho}{\rho} - \frac{1}{2}\frac{(\nabla\rho)^2}{\rho^2}\right] \quad (227)$$

is the Bohm quantum potential taking into account the Heisenberg uncertainty principle and $P(\rho)$ is the pressure determined by Eq. (36). For the logarithmic potential (54), we obtain the logotropic equation of state (55).

Remark.—If we include a $|\varphi|^4$ self-interaction potential in addition to the logarithmic potential in the complex SF potential [see Eq. (199)], we need to account for an additional pressure term

$$P = \frac{2\pi a_s \hbar^2}{m^3}\rho^2 \quad (228)$$

in the quantum Euler equation (225).

D. Condition of quantum hydrostatic equilibrium

The condition of quantum hydrostatic equilibrium is expressed by the equation

$$\frac{\rho}{m}\nabla Q_B + \nabla P + \rho\nabla\Phi = \mathbf{0} \quad (229)$$

coupled to the Poisson equation

$$\Delta\Phi = 4\pi G\rho. \quad (230)$$

These equations describe the balance between the repulsion due to the quantum potential, the repulsion due to the logotropic pressure, and the gravitational attraction.

In the TF approximation where the quantum potential can be neglected, we recover the classical condition of hydrostatic equilibrium (204). This leads to classical logotropic DM halos such as those studied in Sec. 5 of [1] and in Appendix F. However, in the general case ($Q_B \neq 0$), Eq. (229) implies that logotropic DM halos have, like in the FDM model (see Appendix E 3), a quantum core (soliton) in which the pressure is provided by the Heisenberg uncertainty principle. This quantum core is surrounded by a logotropic envelope where the density decreases as r^{-1}.

E. Generalized Lane-Emden equation

Combining Eqs. (229) and (230), and using Eq. (227), we obtain the fundamental differential equation of quantum hydrostatic equilibrium

$$\frac{\hbar^2}{2m^2} \Delta \left(\frac{\Delta \sqrt{\rho}}{\sqrt{\rho}} \right) - \nabla \cdot \left(\frac{\nabla P}{\rho} \right) = 4\pi G \rho. \qquad (231)$$

This equation determines the density profile of BECDM halos described by the GPP equations.[38] For the logotropic equation of state (55), it becomes

$$\frac{\hbar^2}{2m^2} \Delta \left(\frac{\Delta \sqrt{\rho}}{\sqrt{\rho}} \right) + A \Delta \left(\frac{1}{\rho} \right) = 4\pi G \rho. \qquad (232)$$

If we define

$$\theta = \frac{\rho_0}{\rho}, \qquad \xi = \left(\frac{4\pi G \rho_0^2}{A} \right)^{1/2} r, \qquad (233)$$

where ρ_0 is the central density, we find that Eq. (232) takes the form of a generalized Lane-Emden equation

$$\chi \Delta \left(\frac{\Delta \theta^{-1/2}}{\theta^{-1/2}} \right) + \Delta \theta = \frac{1}{\theta} \qquad (234)$$

with a quantum coefficient

$$\chi = \frac{2\pi G \hbar^2 \rho_0^3}{m^2 A^2}. \qquad (235)$$

In the TF approximation $\chi \ll 1$, Eq. (234) reduces to the usual Lane-Emden equation of index $n = -1$ [see Ref. [1] and Eq. (F3)].

F. Validity of the TF approximation for DM halos

The TF approximation for DM halos is valid when $\chi \ll 1$, i.e., when

$$m \gg m_0 \equiv \frac{\sqrt{2\pi G \hbar^2 \rho_0^3}}{A}. \qquad (236)$$

If we consider an ultracompact DM halo of typical density $\rho_0 \sim 10^8 \, M_\odot/\text{kpc}^3$ (Fornax), we find that $m_0 = 3.57 \times 10^{-22} \, \text{eV}/c^2$. Remarkably, this mass scale is precisely of the same order of magnitude as the mass $m \sim 10^{-22} \, \text{eV}/c^2$ of the ultralight boson that occurs in the FDM model (see Appendix E).[39] The mass m of the SF determines the importance of the quantum core (soliton) relative to the logotropic envelope in a DM halo. When $m \ll m_0$, the DM halo is dominated by the quantum core, like in the FDM model, and the logotropic envelope is negligible. Inversely, in the TF approximation $m \gg m_0$, there is no quantum core. In that case, the DM halo is purely logotropic and the mass of the SF disappears from the equations (see Sec. XIV B and Appendix F). When $m \sim m_0$, we have to take into account both the presence of the quantum core (soliton) and the logotropic envelope. This is the case in particular for the ultralight boson of mass $m \sim 10^{-22} \, \text{eV}/c^2$ that occurs in the FDM model.

Remark.—Using the fact that $\rho_0 = k\rho_\Lambda$ with $k \sim 10^6$ and $A = B\rho_\Lambda c^2$, we find that

$$m_0 = \frac{\sqrt{3} k^{3/2}}{2B} m_\Lambda, \qquad (237)$$

where $m_\Lambda = 1.20 \times 10^{-33} \, \text{eV}/c^2$ is the cosmon mass [see Eq. (190)]. We get $m_0 \sim 3 \times 10^{11} m_\Lambda$. Therefore, the mass scale m_0 is equal to the cosmon mass multiplied by a large prefactor.

G. Interpretation of the logotropic term

There are two manners to interpret the logotropic term in Eqs. (215) and (220). Naively, we could interpret this term as a property of the SF measuring, for example, the strength of its self-interaction. However, since A is a fundamental constant of physics rather than being a property of the SF like its mass m or its scattering length a_s, it is more relevant to interpret this term as an *intrinsic* term, independent of the SF, that is always present in the wave equation. In many situations, this term is negligible and we recover the standard KG and Schrödinger equations. However, when considering galactic or cosmological scales, this term

---

[38]More precisely, Eq. (231) determines the ground state of a self-gravitating BEC. This solution describes ultracompact DM halos—dwarf spheroidals (dSphs) like Fornax—or the quantum core (soliton) of large DM halos. In large DM halos, the soliton is surrounded by an extended envelope which arises from the quantum interferences of excited states [65]. On a coarse-grained scale, this envelope has a structure similar to the NFW profile (see Appendix E 3).

[39]We note that the criterion $m \gg m_0 = 3.57 \times 10^{-22} \, \text{eV}/c^2$ determining the validity of the TF approximation at the scale of DM halos differs by 11 orders of magnitude from the criterion $m \gg m_\Lambda = 1.20 \times 10^{-33} \, \text{eV}/c^2$ determining the validity of the TF approximation at the cosmological level (see Sec. XIII).

becomes important and is responsible for the accelerating expansion of the Universe (DE) and for the universal surface density of the DM halos.[40] It can therefore account for the effects of DM and DE in a unified manner. We suggest therefore that Eqs. (215) and (220) could be fundamental equations of physics superseding the standard KG and Schrödinger equations. We note that these wave equations are nonlinear. In this point of view, the standard KG and Schrödinger equations appear as *approximations* of the more general nonlinear wave equations (215) and (220).

H. Analogies and differences between the logotropic model and the ΛFDM model

The ΛFDM model (see Appendix E) is based on a complex SF with a constant potential $V(|\varphi|^2) = \epsilon_\Lambda$ equal to the cosmological density. In that case, the relativistic wave equation (212) reduces to the standard KG equation (E12) and the nonrelativistic wave equation (218) reduces to the standard Schrödinger equation (E13) like in the FDM model. Therefore, the constant SF potential $V(|\varphi|^2) = \epsilon_\Lambda$ does not explicitly appear in the fundamental wave equations of quantum mechanics since only the derivative of V matters. However, the constant potential $V(|\varphi|^2) = \epsilon_\Lambda$ appears in the energy density and in the pressure of the SF [see Eqs. (4) and (5)]. In the fast oscillation regime, a homogeneous complex SF with a constant potential $V(|\varphi|^2) = \epsilon_\Lambda$ behaves as a gas with a constant pressure (see Appendix E 1)

$$P = -\epsilon_\Lambda. \qquad (238)$$

As a result, it is equivalent to the ΛCDM model and can therefore account for the accelerating expansion of the Universe and to the clustering of DM.[41] If we apply this model to DM halos and ignore quantum effects (TF approximation), we recover the small-scale problems of the CDM model. Indeed, since the pressure is uniform [see Eq. (238)],

there is no pressure gradient to balance the gravitational attraction. This leads to cuspy density profiles. However, if we take quantum effects into account (see Appendix E 3) the quantum potential can stabilize the system against gravitational collapse and produce a core instead of a cusp. At the level of DM halos, a complex SF with a constant potential is equivalent to the FDM model which can possibly solve the small-scale crisis of CDM.

There remains, however, an important problem with this model. Indeed, the FDM model, unlike the logotropic model, does not account for the universal surface density of DM halos. In the FDM model, the core mass-radius relation scales as $M \sim \hbar^2/(Gm^2R)$ (see Appendix E 3) and, consequently, the surface density $\Sigma \sim M/R^2$ of DM halos scales with the radius as

$$\Sigma \propto \frac{\hbar^2}{Gm^2R^3}. \qquad (239)$$

Therefore, the surface density of FDM halos decreases as the size of the DM halos increases instead of being constant. Correspondingly, the mass of the FDM halos decreases as their radius increases. This is in sharp contrast with the observations of DM halos which reveal that their mass increases with their radius as $M \propto R^2$ in agreement with a constant surface density ($\Sigma \sim 1$) [17].

The problems of the FDM model were mentioned by the author at several occasions (see, e.g., Appendix F of Ref. [23], the Introduction of Ref. [24], and Appendix L of [25]) and they have been recently emphasized by Burkert [26] and Deng *et al.* [27]. These are serious drawbacks of the FDM model.[42] It has been advocated that these problems could be solved by taking into account the effect of an isothermal halo and distinguishing between the quantum core radius R_c and the isothermal core radius r_0 (see Ref. [25] and Appendix F 7 for more details). Alternatively, we note that the logotropic model based on the nonlinear Schrödinger equation (220) does not suffer from the problems of the FDM model based on the usual Schrödinger equation (E13) since it leads, in the TF approximation, to a constant surface density $\Sigma \sim 1$ and a $M \propto R^2$ mass-radius relation in agreement with the observations (see Sec. XIV B), unlike the FDM model.[43]

Finally, we expect that the logotropic GPP equations (219) and (220), similar to the Schrödinger-Poisson equations (E13) and (E15) of the FDM model, undergo a process of violent relaxation and gravitational cooling (see Appendix E 3). This should lead, in the general case, to DM

---

[40]We note that the logotropic term $A/(|\psi|^2c^2) \sim \rho_\Lambda/\rho$ becomes important at very low densities, typically when ρ becomes comparable to the cosmological density $\rho_\Lambda = 5.96 \times 10^{-24}\,\mathrm{g\,m^{-3}}$ which is the absolute minimum density in the Universe. At higher densities, the logotropic term is negligible because the value of $A/c^2 \sim \rho_\Lambda$ is extremely small. This forces us to properly define what we call "vacuum." For example, a density ρ_{lab} may look small at the laboratory scale although it is much larger than ρ_Λ. Therefore, we should not take $\rho_{\mathrm{lab}} = 0$ in Eqs. (215) and (220) because that would make the logotropic term $A/(\rho_{\mathrm{lab}}c^2)$ diverge while in reality this term is negligible. If we interpret ρ_Λ as typically representing the smallest possible value of the density in the Universe [in line with Eq. (78)], then the logotropic term is always less than unity.

[41]A complex SF with a constant potential $V(|\varphi|^2) = \epsilon_\Lambda$, corresponding to the ΛFDM model, provides a simple unification of DM and DE. By contrast, a complex SF with a vanishing potential $V(|\varphi|^2) = 0$, corresponding to the FDM model, has a vanishing pressure ($P = 0$) in the fast oscillation regime and behaves only as DM.

[42]The fermionic DM model and the BECDM model with a repulsive self-interaction experience the same problems (see Appendix L of [25]).

[43]This remark suggests that DM halos should be in the TF regime so that they are dominated by the logotropic profile, not by the solitonic profile. According to the criterion from Eq. (236), this implies that $m \gg m_0$ with $m_0 \sim 10^{-22}$ eV/c².

halos possessing a quantum core (soliton) + an inner logotropic envelope whose density decreases as r^{-1} (yielding a universal surface density) + an outer envelope with a density profile decreasing as r^{-3} (consistent with the NFW profile). In the TF regime valid when $m \gg m_0$, the quantum core should be replaced by a classical logotropic core. The resulting structure made of a logotropic core + a NFW halo turns out to be in agreement with the observed structure of DM halos.

XVI. JEANS INSTABILITY IN A LOGOTROPIC UNIVERSE

In this section, we study the Jeans instability of a spatially homogeneous self-gravitating logotropic gas in the expanding Universe. We use a nonrelativistic approach[44] and make the TF approximation which amounts to neglecting quantum effects.[45] This approximate treatment will be sufficient to point out important problems encountered by the logotropic model regarding the formation of the large-scale structures of the Universe.

A. The Jeans scales

We first study how the Jeans length λ_J and the Jeans mass M_J of the logotropic gas depend on the density of the Universe ρ. In the nonrelativistic regime (DM-like era) the density evolves with time as [67]

$$\frac{\rho}{\text{g/m}^3} = 2.25 \times 10^{-24} a^{-3}, \qquad (240)$$

where a is the scale factor. The beginning of the nonrelativistic regime, which can be identified with the epoch of matter-radiation equality (i.e., the transition between the radiation era and the DM era), occurs at $a_{\text{eq}} = 2.95 \times 10^{-4}$ (corresponding to a redshift $z_{\text{eq}} = 1/a_{\text{eq}} - 1 = 3390$). At that moment, the density of the Universe is $\rho_{\text{eq}} = 8.77 \times 10^{-14}$ g/m^3. The present density of the Universe is $\rho_0 = 2.25 \times 10^{-24}$ g/m^3.

In the nonrelativistic + TF approximation, the Jeans wave number k_J is given by [68]

$$k_J = \left(\frac{4\pi G \rho}{c_s^2} \right)^{1/2}, \qquad (241)$$

where $c_s^2 = P'(\rho)$ is the squared speed of sound. The Jeans length is $\lambda_J = 2\pi/k_J$ and the comoving Jeans length is $\lambda_J^c = \lambda_J/a$. The Jeans radius and the Jeans mass are defined by

$$R_J = \frac{\lambda_J}{2}, \qquad M_J = \frac{4}{3} \pi \rho R_J^3. \qquad (242)$$

They represent the minimum radius and the minimum mass of a fluctuation that can collapse at a given epoch. They are therefore expected to provide an order of magnitude of the minimum size and minimum mass of DM halos.

For the logotropic equation of state

$$P = A \ln \left(\frac{\rho}{\rho_P} \right), \qquad (243)$$

the squared speed of sound reads

$$c_s^2 = P'(\rho) = \frac{A}{\rho}. \qquad (244)$$

The speed of sound increases as the density decreases. The Jeans length and the Jeans mass are given by

$$\lambda_J = 2\pi \left(\frac{A}{4\pi G} \right)^{1/2} \frac{1}{\rho}, \qquad (245)$$

$$M_J = \frac{4}{3} \pi^4 \left(\frac{A}{4\pi G} \right)^{3/2} \frac{1}{\rho^2}. \qquad (246)$$

They can be written as

$$\frac{\lambda_J}{\text{pc}} = 9.67 \times 10^{-15} \frac{\text{g/m}^3}{\rho}, \qquad (247)$$

$$\frac{M_J}{M_\odot} = 6.99 \times 10^{-27} \left(\frac{\text{g/m}^3}{\rho} \right)^2. \qquad (248)$$

Using Eq. (240), we find that during the expansion of the Universe the Jeans length increases as a^3 and the Jeans mass increases as a^6 (the comoving Jeans length increases as a^2). Eliminating the density between Eqs. (245) and (246), we obtain

$$M_J = \frac{\pi^2}{3} \left(\frac{A}{4\pi G} \right)^{1/2} \lambda_J^2. \qquad (249)$$

This relation is similar to the mass-radius relation $M_h(r_h)$ of logotropic DM halos (see Appendix F).

At the epoch of matter-radiation equality, we find $\lambda_J = 0.110$ pc and $M_J = 0.910\ M_\odot$ (the comoving Jeans length is $\lambda_J^c = \lambda_J/a = 374$ pc).[46] In the case of CDM where $c_s = 0$, the Jeans length and the Jeans mass vanish.

---

[44]In principle, the nonrelativistic approximation is valid for $a \ll a_t = 0.765$ (see Sec. VI E). Since our discussion is essentially qualitative, we shall extrapolate our nonrelativistic results up to the present Universe ($a = 1$).

[45]The validity of the TF approximation for the Jeans problem is discussed in Sec. XVI E. A more general study going beyond the TF approximation will be reported in a forthcoming paper [66].

[46]The Jeans mass computed at the epoch of matter-radiation equality where structures start to form gives a lower bound on the mass of the DM halos observed today. Indeed, the Jeans instability leads to clumps of mass M_J and size λ_J. These clumps can merge to form bigger structures but, in general, their mass cannot decrease.

Therefore, structures can form at all scales. This is in contradiction with the observations which reveal that DM halos exist only above a minimum size $R \sim 1$ kpc and above a minimum mass $M \sim 10^8 \, M_\odot$ corresponding to typical dSphs. In the framework of the logotropic model, DM halos can form only above $\lambda_J = 0.110$ pc and $M_J = 0.910 \, M_\odot$. The logotropic model implies the existence of a "minimum halo" but the size and mass of this minimum halo are much too small to solve the missing satellite problem. We shall come back to this problem in Sec. XVI D.

At the present epoch, we find $\lambda_J = 4.30 \times 10^3$ Mpc and $M_J = 1.38 \times 10^{21} \, M_\odot$. These values are of the order of the size and mass of the Universe (see below). Therefore, the Jeans instability is inhibited in the present Universe even at very large scales, i.e., at the scale of the clusters of galaxies. We shall come back to this problem in Sec. XVI F.

Remark.—We can rewrite the Jeans length (245) and the Jeans mass (246) as

$$\lambda_J = 2\pi \left[\frac{2B(1 - \Omega_{m,0})}{3\Omega_{m,0}^2} \right]^{1/2} R_\Lambda a^3, \qquad (250)$$

$$M_J = \pi^3 \left[\frac{2B(1 - \Omega_{m,0})}{3\Omega_{m,0}^2} \right]^{3/2} \Omega_{m,0} M_\Lambda a^6, \qquad (251)$$

where $R_\Lambda = c/H_0 = 4.44 \times 10^3$ Mpc is the size of the visible Universe and $M_\Lambda = (4/3)\pi(\epsilon_0/c^2)R_\Lambda^3 = c^3/2GH_0 = 4.62 \times 10^{22} \, M_\odot$ is its mass. To obtain Eqs. (250) and (251), we have used $\rho = \Omega_{m,0}(\epsilon_0/c^2)a^{-3}$, $H_0^2 = (8\pi G/3c^2)\epsilon_0$ and Eqs. (89) and (90). We see more clearly on these expressions that the present values of the Jeans length and Jeans mass are of the order of the size and mass of the Universe. This is due to the fact that the speed of sound approaches the speed of light ($c_s \sim c$) when $\rho \to \rho_\Lambda$. As a result, the Jeans length $\lambda_J \sim c_s/\sqrt{G\rho_0}$ with $H_0^2 = 8\pi G\rho_0/3$ becomes comparable to the Hubble length $\lambda_H = c/H$ (horizon) and this prevents the formation of structures (see below).[47]

B. Theory of perturbations in the linear regime

In the nonrelativistic + TF approximation, the equation determining the evolution of the density contrast $\delta_k = \delta\rho_k/\rho$ in the linear regime of structure formation is given by [69]

$$\frac{d^2\delta_k}{da^2} + \frac{3}{2a}\frac{d\delta_k}{da} + \frac{3}{2a^2}\left(\frac{c_s^2 k^2}{4\pi G\rho a^2} - 1\right)\delta_k = 0, \qquad (252)$$

where $c_s^2 = P'(\rho)$ is the squared speed of sound from Eq. (244). For the logotropic equation of state, the comoving Jeans wave number is

---

[47]For the same reason, structure formation is impossible during the radiation era where $c_s = c/\sqrt{3}$.

$$k_J^c = \left(\frac{4\pi G\rho a^2}{c_s^2}\right)^{1/2} = \left(\frac{4\pi G\rho^2 a^2}{A}\right)^{1/2}. \qquad (253)$$

Recalling that $\rho \propto a^{-3}$ it can be written as $k_J^c = \kappa_J/a^2$ where $\kappa_J = (4\pi G\rho^2 a^6/A)^{1/2}$ is a constant independent of time (it is equal to the present Jeans wave number). In terms of this parameter, Eq. (252) can be rewritten as

$$\frac{d^2\delta_k}{da^2} + \frac{3}{2a}\frac{d\delta_k}{da} + \frac{3}{2a^2}\left(\frac{k^2 a^4}{\kappa_J^2} - 1\right)\delta_k = 0. \qquad (254)$$

The CDM model is recovered by taking $\kappa_J \to +\infty$ in Eq. (254) yielding

$$\frac{d^2\delta_{\rm CDM}}{da^2} + \frac{3}{2a}\frac{d\delta_{\rm CDM}}{da} - \frac{3}{2a^2}\delta_{\rm CDM} = 0. \qquad (255)$$

The growing solution is $\delta_{\rm CDM} \propto a$ (there is also a decaying solution proportional to $a^{-3/2}$). It is usually considered that $\delta_i \sim 10^{-5}$ at the initial time $a_i \sim 10^{-4}$ of matter-radiation equality [70]. Therefore, the growing evolution of the density contrast in the CDM model can be written as

$$\delta_{\rm CDM}(a) = \frac{\delta_i}{a_i}a. \qquad (256)$$

We will take this CDM result as a reference and compare it with the prediction of the logotropic model. We note that Eq. (254) for the density contrast of the logotropic gas reduces to Eq. (255) when $k \to 0$ and when $a \to 0$ because the logotropic term $k^2 a^4/\kappa_J^2$ becomes negligible in these two limits. Therefore, the logotropic gas is expected to behave similar to CDM at large scales and at early times as specified below.

C. Evolution of the density contrast

In this section, we study the evolution of the density contrast $\delta_k(a)$ in the linear regime of structure formation. It turns out that Eq. (254) can be solved analytically [69]. The growing solution is given by

$$\delta_k(a) = \frac{\mathcal{A}(k)}{a^{1/4}} J_{\frac{5}{8}}\left(\frac{\sqrt{6}}{4}\frac{k}{\kappa_J}a^2\right), \qquad (257)$$

where $J_{5/8}(x)$ is the Bessel function of order 5/8 [there is also a decaying solution proportional to $J_{-5/8}(x)$]. The amplitude $\mathcal{A}(k)$ is determined by requiring that the asymptotic behavior of Eq. (257) for $a \to 0$ exactly matches the solution (256) of the CDM model. This gives

$$\mathcal{A}(k) = \Gamma\left(\frac{13}{8}\right)\frac{8^{5/8}}{6^{5/16}}\left(\frac{\kappa_J}{k}\right)^{5/8}\frac{\delta_i}{a_i}. \qquad (258)$$

Equations (257) and (258) determine the evolution of the density contrast $\delta_k(a)$ in the logotropic gas. We can identify two regimes:

(i) Early times/large wavelengths: We first consider the case $ka^2/\kappa_J \ll 1$. For a given wave number k, this corresponds to a scale factor $a \ll (\kappa_J/k)^{1/2}$. Alternatively, for a given scale factor a, this corresponds to a wavelength $\lambda \gg \lambda_J^c(a)$. Since the wavelength of the perturbation is larger that the comoving Jeans length, the density contrast $\delta_k(a)$ increases. Using the asymptotic expansion of the Bessel function for large arguments, we find that

$$\delta_k(a) \sim \frac{\delta_i}{a_i} a, \tag{259}$$

independent of k. This solution is valid for $a \ll (\kappa_J/k)^{1/2}$. In that case, the perturbation grows like in the CDM model [see Eq. (256)].

(ii) Late times/small wavelengths: We now consider the case $ka^2/\kappa_J \gg 1$. For a given wave number k, this corresponds to a scale factor $a \gg (\kappa_J/k)^{1/2}$. Alternatively, for a given scale factor a, this corresponds to a wavelength $\lambda \ll \lambda_J^c(a)$. Since the wavelength of the perturbation is smaller that the comoving Jeans length, the density contrast $\delta_k(a)$ displays damped oscillations similar to acoustic oscillations (with Hubble damping). Using the asymptotic expansion of the Bessel function for small arguments, we find that

$$\delta_k(a) \sim \Gamma\left(\frac{13}{8}\right) \frac{8^{9/8}}{6^{9/16}} \frac{1}{\sqrt{\pi}} \frac{\delta_i}{a_i} \frac{1}{a^{5/4}} \left(\frac{\kappa_J}{k}\right)^{9/8}$$
$$\times \cos\left(\frac{\sqrt{6}}{4} \frac{k}{\kappa_J} a^2 - \frac{9\pi}{16}\right). \tag{260}$$

This solution is valid for $a \gg (\kappa_J/k)^{1/2}$. We see that the amplitude of the oscillations decreases like $a^{-5/4}$ as the Universe expands.

In conclusion, when $a \ll (\kappa_J/k)^{1/2}$ or $\lambda \gg \lambda_J^c(a)$, the perturbation grows linearly with the scale factor like in the CDM model; when $a \gg (\kappa_J/k)^{1/2}$ or $\lambda \ll \lambda_J^c(a)$, the perturbation oscillates with a decreasing amplitude scaling as $a^{-5/4}$.

A typical example of evolution of the density contrast is represented in Fig. 17. We assume that the matter era starts at $a_i = 10^{-4}$ and we study the evolution of the density contrast up to the present time ($a_0 = 1$). We consider a perturbation with a wavelength $\lambda > \lambda_J^c(a_i)$. This perturbation first starts to grow like in the CDM model. However, at late times, the perturbation decays and undergoes damped oscillations. This behavior can be understood as follows. Initially, for small a, the LDF behaves as pressureless CDM and all relevant scales are gravitationally unstable [$\lambda > \lambda_J^c(a)$]. Therefore, the LDF exhibits growing modes and clusters like ordinary matter. Thus, the density contrast increases as $\delta \propto a$. However, as the Universe expands, the
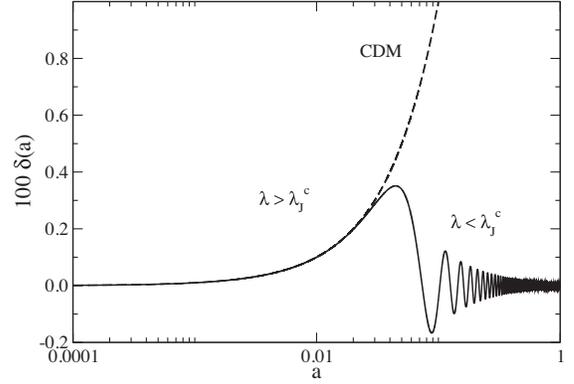
FIG. 17. Evolution of the density contrast $\delta_k(a)$ in the logotropic model for $k/\kappa_J = 1000$ (semilog plot). The comoving Jeans length $\lambda_J^c(a)$ increases as the Universe expands. As a result, the perturbation grows at early times like in the CDM model [$\lambda > \lambda_J^c(a)$] and undergoes damped oscillations at late times [$\lambda < \lambda_J^c(a)$].

comoving Jeans length increases significantly until there are no relevant gravitationally unstable scales anymore ($\lambda < \lambda_J^c(a)$). The perturbation $\delta_k(a)$ stops growing and begins to oscillate and decrease to zero when we enter the DE era, becoming a smooth component of the Universe.[48] Therefore, because of the increase of the comoving Jeans length with a (which is due to the increase of the speed of sound), the formation of structures is blocked as the Universe expands.

The transition between the growing regime and the oscillating regime occurs when $k \sim k_J^c(a) = \kappa_J/a^2$, i.e., when $a = a_*(k)$ with

$$a_*(k) = \left(\frac{\kappa_J}{k}\right)^{1/2}. \tag{261}$$

Therefore, the typical value of the maximum density contrast achieved by a perturbation of wavelength k is $(\delta_k)_{\max} \sim \delta_k[a_*(k)]$, i.e.,

$$(\delta_k)_{\max} = \Gamma\left(\frac{13}{8}\right) \frac{8^{5/8}}{6^{5/16}} \frac{\delta_i}{a_i} J_{\frac{5}{8}}\left(\frac{\sqrt{6}}{4}\right) \left(\frac{\kappa_J}{k}\right)^{1/2}. \tag{262}$$

Since $(\delta_k)_{\max} \sim a_*(k) \sim (\kappa_J/k)^{1/2}$ and $\kappa_J \sim 1/R_\Lambda$, we see that a perturbation with a wavelength λ smaller than the horizon R_Λ cannot achieve a large density contrast during its evolution. Therefore, it cannot trigger the nonlinear regime leading to the formation of the large-scale structures of the Universe that we observe today. This illustrates the blocking effect of the logotropic gas.

---

[48]Similarly, it is well known that the density perturbation in a universe dominated by the cosmological constant is zero (i.e., $\delta_{cc} = 0$).
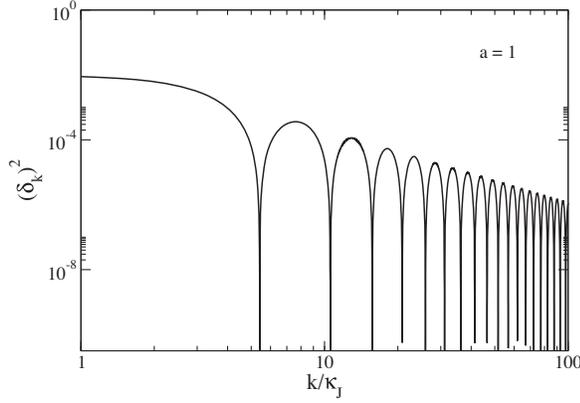
FIG. 18. Squared density contrast $(\delta_k)^2$ at the present time ($a = 1$) as a function of the wave number k of the perturbation. The matter power spectrum has the same structure, displaying oscillations at large k.

In Fig. 18, we plot the squared density contrast $(\delta_k)^2$ at the present epoch ($a = 1$) as a function of the wave number k of the perturbation. For $k \to 0$, it tends to $(\delta_i/a_i)^2$. For $k \to +\infty$, it decreases as $(k/\kappa_J)^{-9/4}$ by oscillating. This function gives an idea of the behavior of the matter power spectrum in the logotropic model that is discussed in Sec. XVI F.

D. Comparison between the logotropic model and the FDM model

In the previous sections we have made the TF approximation in the logotropic model which amounts to neglecting quantum effects. For comparison, it is interesting to consider the opposite limit where we take quantum effects into account but neglect the logotropic pressure. In that case we are led back to the FDM model (see Appendix E). The Jeans instability of the FDM model has been studied in detail in our previous papers [29,67–69,71,72]. We recall below the main results of these studies.

In the FDM model, the quantum Jeans wave number is given by [68]

$$k_J = \left(\frac{16\pi G\rho m^2}{\hbar^2} \right)^{1/4}. \tag{263}$$

During the expansion of the Universe, the Jeans length increases as $\lambda_J \propto a^{3/4}$ and the Jeans mass decreases as $M_J \propto a^{-3/4}$ (the comoving Jeans length decreases as $\lambda_J^c \propto a^{-1/4}$). As a result, the Jeans mass-radius relation $M_J(\lambda_J) = \pi^4\hbar^2/(6Gm^2\lambda_J)$ decreases, similar to the core mass-radius relation $M_c(R_c)$ of FDM halos [see Eq. (E17) and [72]]. Let us consider a boson mass $m = 2.92 \times 10^{-22}$ eV/c^2 representative of the FDM model [72]. At the epoch of matter-radiation equality, we find $\lambda_J = 124$ pc and $M_J = 1.31 \times 10^9 \, M_\odot$ (the comoving Jeans length is $\lambda_J^c = \lambda_J/a = 0.420$ Mpc). At the present epoch, we find $\lambda_J = 55.3$ kpc and $M_J = 2.94 \times 10^6 \, M_\odot$.

In the nonrelativistic regime of the FDM model, the equation determining the evolution of the density contrast in the linear regime of structure formation is given by [69]

$$\frac{d^2\delta_k}{da^2} + \frac{3}{2a}\frac{d\delta_k}{da} + \frac{3}{2a^2}\left(\frac{\hbar^2 k^4}{16\pi G\rho m^2 a^4} - 1 \right)\delta_k = 0. \tag{264}$$

This equation, which is based on the Schrödinger-Poisson equations, takes quantum effects into account. It has been studied in detail in [29,69]. It is found (see Fig. 4 of [29]) that $\delta_k(a)$ first oscillates for small a (quantum regime) then grows like in the CDM model for large a (classical regime).

This behavior can be understood as follows. Initially, for small a, most scales are stable [$\lambda < \lambda_J^c(a)$] and the perturbation oscillates. However, as the Universe expands, the comoving Jeans length decreases significantly and the relevant scales become gravitationally unstable [$\lambda > \lambda_J^c(a)$]. In that case, FDM behaves as pressureless CDM.[49] It exhibits growing modes and clusters like ordinary matter. Thus, the density contrast increases as $\delta \propto a$. Therefore, because of the decrease of the comoving Jeans length with a, the formation of structures is facilitated as the Universe expands.

These results are reversed as compared to those obtained in the logotropic model. Indeed, as the Universe expands, the Jeans mass M_J and the comoving Jeans length λ_J^c decrease in the FDM model while they increase in the logotropic model.[50] As a result, in the FDM model, the density contrast initially oscillates, then grows like CDM while, in the logotropic model, it first grows like CDM, then undergoes damped oscillations. On the other hand, the value of the Jeans mass $M_J = 1.31 \times 10^9 \, M_\odot$ at the epoch of matter-radiation equality computed in the framework of the FDM model is much larger than the Jeans mass $M_J = 0.910 \, M_\odot$ computed in the framework of the logotropic model. The Jeans mass $M_J = 1.31 \times 10^9 \, M_\odot$ is of the order of the mass of the smallest DM halos (dSphs) observed at present. Therefore, the FDM model is consistent with the observations and can solve the missing satellite problem (unlike the classical logotropic model). The main drawback of the FDM model is that (i) it does not account for the universal surface density of DM halos and (ii) it does not account for the present acceleration of the Universe (without adding an additional DE component like a cosmological constant). By contrast, the logotropic model can account for these two features simultaneously.

These results suggest that, regarding the formation of the large-scale structures of the Universe (Jeans problem), it is important to take into account quantum effects in the

---

[49]This is true at large (cosmological) scales. At the scale of DM halos, the quantum pressure is able to stabilize the system against gravitational collapse and solve the core-cusp problem and the missing satellite problem [68].

[50]The Jeans length λ_J increases in the two models. Consequently, the Jeans mass-radius relation $M_J(\lambda_J)$ decreases in the FDM model and increases in the logotropic model.

logotropic model, i.e., to go beyond the TF approximation. The general expression of the Jeans wave number of a complex SF (including quantum effects and self-interaction) is given by [68]

$$k_J^2 = \frac{2m^2}{\hbar^2}\left(-c_s^2 + \sqrt{c_s^4 + \frac{4\pi G\rho\hbar^2}{m^2}}\right). \qquad (265)$$

On the other hand, the general equation determining the evolution of the density contrast of a nonrelativistic complex SF in the linear regime of structure formation is given by [69]

$$\frac{d^2\delta_k}{da^2} + \frac{3}{2a}\frac{d\delta_k}{da} + \frac{3}{2a^2}\left(\frac{c_s^2 k^2}{4\pi G\rho a^2} + \frac{\hbar^2 k^4}{16\pi G\rho m^2 a^4} - 1\right)\delta_k = 0. \qquad (266)$$

This equation, which is based on the GPP equations, takes quantum effects into account in addition to a nonzero speed of sound like in Eq. (244) for the logotropic gas. This equation will be studied in a specific paper [66] for the logotropic equation of state[51] but we can already mention its main properties. At early times, we can neglect the logotropic pressure and we recover the results of the FDM model. Quantum effects prevent the formation of structure below a minimum mass ($\lesssim 1.31 \times 10^9 \, M_\odot$) and solve the missing satellite problem as we have just seen. At late times, we can neglect the quantum potential and we recover the results of the logotropic model in the TF approximation (see Sec. XVI C). In conclusion, the perturbation $\delta_k(a)$ first oscillates like in the FDM model, then grows like in the CDM model, and finally undergoes damped oscillations like in the classical logotropic model [66].

E. Validity of the TF approximation in the Jeans instability analysis

Considering the order of magnitude of the quantum and logotropic terms in Eq. (265) [using Eq. (244)] or comparing Eqs. (241) and (263), we find that the TF approximation is valid when

$$c_s^2 \gg \left(\frac{G\rho\hbar^2}{m^2}\right)^{1/2} \quad \text{i.e.,} \quad \rho \ll \rho_t \sim \left(\frac{m^2 A^2}{G\hbar^2}\right)^{1/3}. \qquad (267)$$

For a boson mass $m \sim 10^{-22}$ eV/c^2 we obtain $\rho_t = 5.34 \times 10^{-18}$ g/m^3 (corresponding to $a_t = 7.50 \times 10^{-3}$ and $z_t = 132$). Quantum effects are important when $\rho \gg \rho_t$ while they can be neglected (TF approximation) when $\rho \ll \rho_t$. In particular, we must take into account quantum effects at the beginning of the epoch of structure formation corresponding to $\rho_{\rm eq} = 8.77 \times 10^{-14}$ g/m^3. Quantum

effects could be neglected at this epoch (TF approximation) provided that

$$m \gg m_t = \frac{\sqrt{G\hbar^2 \rho_{\rm eq}^3}}{A}. \qquad (268)$$

We find $m_t = 2.10 \times 10^{-16}$ eV/c^2.[52] Since $m \ll m_t$ in general (see Appendix E), the TF approximation is not valid at the epoch of matter-radiation equality. On the contrary, the quantum pressure is more important than the logotropic pressure. At early times, the system is equivalent to the FDM model and the results of Sec. XVI D apply. Therefore, the *quantum* logotropic model can solve the missing satellite problem.

Remark.—At the present epoch, the TF approximation is valid if

$$m \gg m_0' = \frac{\sqrt{G\hbar^2 \rho_0^3}}{A}, \qquad (269)$$

where ρ_0 denotes here the present density of the Universe (not the central density of DM halos). We find $m_0' = 2.73 \times 10^{-32}$ eV/c^2, which is of the order of the cosmon mass m_Λ. Since $m \gg m_\Lambda$ in general (see Appendix E), the TF approximation is always valid at the present epoch.

F. The problem of the oscillations in the matter power spectrum

In the logotropic model, the speed of sound increases as the density of the Universe decreases. At early time, the speed of sound is small and the LDF clusters identically to CDM. In this regime, the Jeans length is small so that most fluctuations are gravitationally unstable and grow. As one approaches the present time, when the LDF starts behaving like DE, the speed of sound increases. Correspondingly, the Jeans scale becomes large. This prevents gravitational collapse and clustering from happening, even at large scales. Fluctuations with wavelength below the comoving Jeans scale λ_J^c are pressure supported (the pressure effectively opposes gravity) and oscillate rather than grow.

---

[51]It has been studied in [29] for a quadratic equation of state corresponding to self-interacting BECs.

[52]We note that the criterion $m \gg m_t = 2.10 \times 10^{-16}$ eV/c^2 determining the validity of the TF approximation for the Jeans problem at the epoch of matter-radiation equality differs by 6 orders of magnitude from the criterion $m \gg m_0 = 3.57 \times 10^{-22}$ eV/c^2 determining the validity of the TF approximation at the scale of ultracompact DM halos (see Sec. XV F) and by 17 orders of magnitude from the criterion $m \gg m_\Lambda = 1.20 \times 10^{-33}$ eV/c^2 determining the validity of the TF approximation at the cosmological level (see Sec. XIII). In particular, for a particle mass $m \sim 10^{-22}$ eV/c^2, the TF approximation is not valid for the Jeans problem at the epoch of matter-radiation equality, while it is valid at the cosmological level to describe the evolution of the background and marginally valid at the scale of ultracompact DM halos to determine their structure.

Therefore, the large speed of sound produces oscillations in the matter power spectrum (see Fig. 18 for a schematic view).

These oscillations in the matter power spectrum are not seen in observed data. To be a successful model for UDM, the LDF should mimic the inhomogeneous Universe as in the ΛCDM model. For this, it is necessary that the LDF clusters similar to CDM at all observable scales. Accordingly, the agreement with the observations will be obtained provided that B is small enough since, for $B = 0$, the logotropic model becomes equivalent to the ΛCDM model which has $c_s = 0$. Developing this argument, Ferreira and Avelino [5] showed that B must be smaller than $B_{max} \sim 6 \times 10^{-7}$. Unfortunately, this upper bound is smaller than our theoretical prediction $B = 3.53 \times 10^{-3}$. This is an important problem of the logotropic model.[53]

These problems were first encountered in the context of the GCG model [73–77],[54] which is based on an equation of state of the form

$$P = -\frac{A}{(\epsilon/c^2)^\alpha} \qquad (270)$$

with $A > 0$ and $0 \leq \alpha \leq 1$, and they actually arise in any UDM model. In particular, Sandvik et al. [75] ruled out a broad class of UDM models by showing that they produce oscillations (or exponential blowups) of the DM power spectrum that are inconsistent with the observations. For the GCG model, they showed that 99.999% of the parameter space is excluded. In order to obtain the mass power spectra that we observe today, one needs $|\alpha| < 10^{-5}$ rendering the GCG indistinguishable from the standard ΛCDM model corresponding to $\alpha = 0$ (see Appendix D 3). Similar conclusions were reached by Carturan and Finelli [76] and Amendola et al. [77] who studied the effect of the GCG on density perturbations and on CMB anisotropies and found that the GCG strongly increases the amount of integrated Sachs-Wolfe effect.

More generally, these results apply to any UDM model where P is a unique function of ϵ. Such models are ruled out if the speed of sound is large, i.e., if the function $P(\epsilon)$

departs substantially from a constant over the range where pressure is important. Quantitatively, we must have $|d \ln P/d \ln \epsilon| < 10^{-5}$ (see footnote 53) leaving essentially only the standard ΛCDM model.[55] In other words, a viable UDM model must have negligible pressure gradient, i.e., the pressure must be essentially spatially constant like a Λ term.[56]

In conclusion, UDM or quartessence models can often correctly explain the evolution of the homogeneous background (zeroth order cosmology) but they fail at explaining the growth of linear perturbations (first order cosmology) because they produce unphysical features in the matter power spectrum in the form of huge oscillations or exponential blowups which are not seen in the observed matter power spectrum. If a solution to these problems cannot be provided, this would appear as evidence for an independent origin of DM and DE (i.e., they are two distinct substances) and the demise of UDM models [75].

G. Possible solutions to the problems of the logotropic model

Some solutions to the problems mentioned above have been proposed in the context of the GCG. Since the LDF experiences the same problems as the GCG, these solutions could also be invoked for the LDF. We review these different solutions below.

1. Two-fluid models

In the beginning of the matter era the GCG agglomerates in the same way as CDM. Later, it behaves as DE and becomes a smooth component of the total matter existing in the Universe. It does not cluster anymore and produces decaying oscillations (or exponential blowup) in the matter power spectrum. As we have seen, this is a problem of any UDM model.[57] Therefore, the GCG model needs additional CDM in order to explain the dynamics of the clusters of galaxies since a fraction of the total DM must remain clustered until today. Consequently, a more realistic model is a two-fluid model where, besides the GCG, normal fluid must be present. Therefore, some authors [73,74,76,77] (see also [78–82]) have proposed that GCG describes only DE and that it must be mixed with CDM. In this viewpoint, the GCG simply plays the role of DE like in quintessence models. This "Chaplygin quintessence" scenario would

---

[53]This constraint can be understood as follows. The matter power spectrum of the logotropic model displays oscillations when $\lambda < \lambda_J^c(a)$ or, equivalently, when $k > k_J^c(a)$. Since these oscillations are not observed, we need $\lambda_J^c(a = 1) < R$ where $R \sim$ 15 Mpc is the typical size of the clusters of galaxies. The present value of the Jeans length must be smaller than the size of the clusters of galaxies $R \sim 15$ Mpc so that the linear growth of cosmic structures on comoving scales larger than R is not significantly affected with respect to the standard ΛCDM result. From Eq. (250), we have $\lambda_J^c(a = 1) \sim 10\sqrt{B}R_\Lambda$. Therefore, we need $100B < (R/R_\Lambda)^2 \sim 10^{-5}$, i.e., $B < 10^{-7}$. We note that the constraint $\lambda_J^c(a = 1) < R$ is satisfied in the FDM model with $m = 2.92 \times 10^{-22}$ eV/c^2 since $\lambda_J^c(a = 1) = 55.3$ kpc.

[54]Figure 17 can be compared to Fig. 2 of [74] and to Fig. 2 of [76]. Figure 18 can be compared to Fig. 1 of [75].

[55]This criterion is not valid for a linear equation of state. The corresponding criterion is given in Appendix C.

[56]However, in that case, we face the core-cusp problem and the missing satellite problem (see Sec. XIV).

[57]Quintessence models have no such problems. Although they have high speeds of sound, this does not prevent DM from clustering since it is a separate component. Quintessence models would fail if they were tightly coupled to DM and this is effectively what happens with UDM models since DM and DE are one and the same substance.

solve the above mentioned problems but the original interest of the GCG as a UDM (quartessence) model has been lost.[58]

2. Baryons

Some authors [76,77,83] proposed to include baryons in analyses of UDM scenarios. Indeed, while pressure effects prevent the Chaplygin gas from collapsing, the baryon fluctuations can still keep growing since this is an independent component with a low speed of sound. Therefore, baryons keep on clustering at all times after decoupling, even after the end of the Jeans instability for the GCG component. Amendola *et al.* [77] showed that the inclusion of baryons affects the total linear matter power spectrum, smoothing out the oscillations of the GCG component and improving the agreement with observations. As a result, the inclusion of baryons in the analysis leads to less stringent bounds on the GCG parameter α. However, this parameter remains tightly constrained by cosmological observations. Therefore, including baryons in UDM models may not be sufficient to save the model.

3. Nonlinear effects

The importance of nonlinear effects in UDM models was first mentioned in [76,77]. In the context of the Chaplygin gas, Bilic *et al.* [84] proposed to take nonlinear effects into account in the growth of inhomogeneities by generalizing the Zeldovich approximation and the spherical model so as to include sonic horizon effects. They showed that if the initial perturbation is above a certain threshold then the perturbation always grows like in the ΛCDM model [in contrast to linear theory where the speed of sound eventually stops $\delta(a)$ from growing irrespective of the initial value of the perturbation]. If the initial perturbation is below the critical threshold, the perturbation does not grow even in the nonlinear regime. Therefore, a fraction of the Chaplygin gas condensates (i.e., collapses in gravitationally bound structures) and never reaches a stage where its properties change from DM to DE. Unfortunately, the detailed calculations of Bilic *et al.* [84] show that the collapse fraction (the fraction of Chaplygin gas that goes into condensate) is not sufficient to solve the problems reported above. Nonlinear condensate, while present, is insufficient to

save the Chaplygin gas model.[59] The importance of nonlinear effects was also pointed out by Avelino *et al.* [87] using simple considerations. They argued that nonlinear effects severely complicate the analysis and render linear results invalid even on large cosmological scales. However, in the case of the Chaplygin gas, similar to Bilic *et al.* [84], they argued that nonlinear effects are too small to significantly affect the linear results. In a more recent work, Avelino *et al.* [88] relaxed earlier simplifying assumptions and showed that, if clustering is strong enough, the linear theory results no longer hold and the backreaction of the small-scale structures on the large-scale evolution of the Universe render the Chaplygin gas model virtually indistinguishable from the ΛCDM model for all possible values of the GCG parameter α. They concluded that the GCG may be consistent with observational constraints over a wide region of parameter space, provided there is a high level of nonlinear clustering of the UDM component on small scales. A detailed analysis of nonlinear effects would nevertheless require solving the full Einstein field equations for the evolution of realistic cosmological fluctuations, which is a formidable task. (Note: Recently, we came across the very interesting paper of Abdullah *et al.* [89] who argue that a cosmological scenario based on the Chaplygin gas may not be ruled out from the viewpoint of structure formation as usually claimed. Indeed, a nonlinear analysis may predict collapse rather than a reexpansion of small-scale perturbations so that nonlinear clustering may occur in the Chaplygin gas. This is because pressure forces in UDM fluids decrease with increasing density so that systems that are stable against self-gravitating collapse in the linear regime may become unstable in the nonlinear regime. As a result, the problem of acoustic oscillations in the linear power spectrum of UDM models may not be as serious as usually assumed provided the hierarchical structure formation process is adequately taken into account. These arguments also apply to the logotropic model.)

4. Nonadiabatic perturbations

A possible solution to the problem of oscillations would be to allow for nonadiabatic perturbations in the Jeans stability analysis to make the effective speed of sound vanish, even in the nonperturbative regime.[60] Indeed, the isentropic perfect fluid approximation might break down at

---

[58]We have seen in Sec. II H that a single-fluid model like the Chaplygin gas or the LDF can be viewed as a two-fluid model made of effective DM and DE (the effective equation of state of DE in the Chaplygin gas model and in the original logotropic model has been determined in Appendix D 3 of [21]). The single-fluid model and the two-fluid model are equivalent at the level of the homogeneous background but they differ from each other for what concerns the formation of structures. The two-fluid model does not present the problems of the single-fluid model reported above.

[59]In later works, Bilic *et al.* [85,86] repeated their study for a tachyon condensate model (a k-essence model corresponding to the string-inspired tachyon Lagrangian that extends the Born-Infeld Lagrangian of the original Chaplygin gas model) in full general relativity and obtained, this time, gravitational condensates in significant quantities. This is because this model reduces the Jeans length by several orders of magnitude.

[60]In the adiabatic case, the effective speed of sound and the adiabatic speed of sound are equal. However, this may not be true anymore if entropy perturbations are present [90].

sufficiently large densities or small scales. Reis *et al.* [91,92] have shown that if nonadiabatic perturbations are allowed, the quartessence GCG models may be compatible with observations. Indeed, entropy perturbations eliminate instabilities and oscillations in the mass power spectrum of these models.

5. Braneworld models

Another possible solution, proposed by Bilic *et al.* [84], would be to exploit the braneworld connection of the Lagrangian associated with the Chaplygin gas. In brane-world models [93], the Einstein equations are modified, e.g., by dark radiation. Similar changes are also brought about by the radion mode [94] which yields a scalar-tensor gravity.

6. Higher order derivatives

The GCG can be obtained from a field theory based on a k-essence Lagrangian. For the original Chaplygin gas ($\alpha = 1$), this yields the Born-Infeld Lagrangian for *d*-brane in a ($d + 1$, 1) spacetime [95]. Creminelli *et al.* [96] have shown that, for a k-essence Lagrangian, one can add a specific higher derivative operator in the original action that does not change the background evolution for the field or its energy density and pressure. But for the perturbations, this extra higher derivative operator leads to a vanishing speed of sound ($c_s^2 = 0$). In such a scenario, the pressure perturbation vanishes and the k-essence clusters at all scales like the nonrelativistic matter. These are called "clustering quintessence" models. Given the fact that GCG as a UDM model fails because of the large speed of sound through the fluid during the DE domination, Kumar and Sen [97] proposed to apply this idea to the "clustering GCG" model and explored its consequences. In that case, they showed that the matter power spectrum for the parameter values of $0 \leq \alpha \leq 0.043$ are well behaved without any unphysical features (note that the original Chaplygin gas $\alpha = 1$ is still ruled out). Therefore, by properly modifying the k-essence Lagrangian, we can ensure that the GCG clusters at all scales similar to the CDM model, leaving, at the same time, the background evolution of the Universe unaltered (i.e., the GCG behaves like CDM in the early time and like DE in the late time). This added clustering property makes the GCG a suitable candidate for UDM models. Thus, the study of Kumar and Sen [97] renewed interest in the GCG as a viable option for UDM models. It would be interesting to redo their analysis in the framework of the logotropic model in order to obtain an enlarged range of allowed values for the parameter B and see if the theoretical value $B = 3.53 \times 10^{-3}$ is included in that range.

7. Scale dependence

Another way to try to avoid these problems could be by introducing some sort of scale dependence into the equations. For example, Padmanabhan and Choudhury [98] discussed a model based on a tachyonic SF that exhibits different equations of state at different scales. The field behaves like pressureless DM on small scales and like smoothly distributed DE on large scales.

The solutions introduced in the context of the GCG model could be applied to the logotropic model as well. It must be recognized that none of them brings an undisputable answer. Therefore, the problems essentially remain. In spite of these difficulties, we think that the GCG and logotropic models deserve further investigation. It is possible that these models are incomplete rather than being ruled out. On the other hand, a thorough investigation of the nonlinear regime of the growth of inhomogeneities through extensive numerical simulations is needed for a definite conclusion concerning the compatibility of the GCG and logotropic cosmologies with the observable large-scale structure of the Universe.

Remark.—When applied to DM halos, the logotropic equation of state cannot be valid everywhere because it yields halos with an infinite mass (see Appendix F). Indeed, only the core of DM halos is expected to be logotropic (its density decays as r^{-1}). In practice, the logotropic core is surrounded by an envelope where the density decreases more rapidly as r^{-2} or r^{-3} (see Appendix F). This suggests that the logotropic equation of state is valid only at large scales in an "average" sense, which allows us to correctly describe the evolution of the cosmological background. However, it may cease to be valid everywhere at small scales when considering the more complicated problem of structure formation. In particular, one has to be careful when treating strongly inhomogeneous structures such as DM halos in the nonlinear regime. A full numerical solution of the nonlinear problem (accounting for relativistic and quantum effects) may lead to a matter power spectrum different from the one obtained in the linear regime where it is assumed that the logotropic equation of state holds everywhere.

XVII. CONCLUSION

In this paper, we have proposed a unification of DM and DE based on a complex SF described by the KGE equations (212) and (213) with a potential of the form

$$V_{\text{tot}}(|\varphi|^2) = \frac{m^2 c^2}{2\hbar^2}|\varphi|^2 - A \ln\left(\frac{m^2|\varphi|^2}{\hbar^2 \rho_P}\right) - A, \quad (271)$$

which is the sum of a rest-mass term and a logarithmic term. This model is associated with a logotropic equation of state

$$P = A \ln\left(\frac{\rho}{\rho_P}\right), \quad (272)$$

where $\rho = (m^2/\hbar^2)|\varphi|^2$ is the pseudo-rest-mass density.

The logotropic model is able to account for the present accelerating expansion of the Universe while solving at the same time the small-scale crisis of the ΛCDM model. Indeed, at cosmological scales, the logotropic model is almost indistinguishable from the ΛCDM model up to the present time and even far in the future. By contrast, at galactic scales, it leads to DM halos presenting a central core instead of a cusp. Furthermore, it predicts their universal surface density $\Sigma_0^{\text{th}} = 133\ M_\odot/\text{pc}^2$ (in agreement with the observations giving $\Sigma_0^{\text{obs}} = 141^{+83}_{-52}\ M_\odot/\text{pc}^2$) without adjustable parameter.

The new logotropic model introduced in the present paper is different from the original one [1–4] which is characterized by the equation of state (B5) where ρ_m represents the true rest-mass density. The interest of the new logotropic model is that (i) it is based on a complex SF theory; (ii) it avoids the pathologies of the original logotropic model such as a phantom behavior violating the dominant-energy condition, and leading to a little rip and a superluminal or imaginary speed of sound; (iii) it asymptotically approaches a well-behaved de Sitter era at late times.

At the cosmological level, and for the evolution of the homogeneous background, we have shown that the TF approximation is equivalent to the fast oscillation regime where the complex SF rapidly spins. In this spintessence regime, the SF is described by the logotropic equation of state (272). It behaves as DM in the early Universe ($a \ll a_t = 0.765$) and as DE in the late universe ($a \gg a_t = 0.765$). At the cosmological level, the TF approximation is valid for a large period of time provided that $m \gg m_\Lambda$, where $m_\Lambda = 1.20 \times 10^{-33}$ eV/c^2 is the cosmon mass. For a boson mass $m \sim 10^{-22}$ eV/c^2, the TF approximation is valid from $a_v^{(1)} = 4.01 \times 10^{-8}$ to $a_v^{(2)} = 1.73 \times 10^4$. In the very early Universe ($a < a_v^{(1)} = 4.01 \times 10^{-8}$), the fast oscillation regime is not valid anymore and the SF experiences a kination regime where it behaves as stiff matter. Therefore, the homogeneous SF successively experiences a stiff matter era, a DM-like era, and a DE-like era. The logotropic model has an intrinsically quantum nature (even in the TF regime) because the equation of state (272) involves ρ_P, and it returns the ΛCDM model in the semiclassical limit $\hbar \to 0$.

At the level of DM halos, the logotropic model differs from the ΛCDM model because it generates a pressure which is either of quantum origin (as in the FDM model) or due to the logarithmic potential. Following a process of violent relaxation [99] and gravitational cooling [100], the logotropic DM halos acquire a "core-halo" structure with a quantum or logotropic core surrounded by a classical NFW (or quasi-isothermal) atmosphere resulting from quantum interferences of excited states [65]. The pressure effects can solve the core-cusp problem of the ΛCDM model. In the TF approximation, the core is purely logotropic. The logotropic equation of state implies a constant surface density

$\Sigma_0^{\text{th}} = 5.85\,(A/4\pi G)^{1/2} = 133\ M_\odot/\text{pc}^2$ which is in agreement with the observations. Therefore, the logotropic model avoids the problems of the FDM model reported by the author [23–25] and by [26,27]. At the level of DM halos, the TF approximation is valid provided that $m \gg m_0 = 3.57 \times 10^{-22}$ eV/c^2. For a boson mass $m \sim 10^{-22}$ eV/c^2 we are just at the limit of validity of the TF approximation so we have to take into account a quantum core + a logotropic inner halo + a NFW (or isothermal) outer halo.

We have also discussed the formation of structures (Jeans problem) within the logotropic model. In that case, there are two difficulties: (i) If we naively make the TF approximation, we find that the Jeans mass $M_J = 0.910\ M_\odot$ at the epoch of matter-radiation equality is much too small to solve the missing satellite problem. However, the TF approximation is valid at this period only if $m \gg m_t = 2.10 \times 10^{-16}$ eV/c^2. For a boson mass $m \sim 10^{-22}$ eV/c^2, we are in the opposite limit where quantum effects are more important than the logotropic pressure. In that case, the logotropic model reduces to the FDM model. Quantum effects yield a much larger Jeans mass $M_J = 1.31 \times 10^9\ M_\odot$ that is able to solve the missing satellite problem. At later times ($a \gg 7.50 \times 10^{-3}$) the TF approximation becomes valid and we can use the classical logotropic model. (ii) In the logotropic model, the density contrast $\delta(a)$ first grows like in the ΛCDM model (after the FDM era mentioned above) then undergoes decaying oscillations (see Fig. 17). This is because the squared speed of sound increases as the density decreases. As a result, the comoving Jeans length becomes very large and prevents the formation of structures. This gives rise to oscillations in the matter power spectrum. These features (large Jeans length and oscillations) are in severe disagreement with the observations. The Chaplygin gas model, and more generally most UDM models, share the same problems [75]. We have reviewed several possible solutions proposed in the literature but none of these solutions has gained complete acceptance so far. This remains an important weakness of the logotropic and Chaplygin gas models. The recent paper of Abdullah *et al.* [89] suggests, however, that these problems may not be as insurmountable as previously thought provided that an adequate nonlinear analysis of structure formation is developed.

We note that the criteria (191), (236), and (268) determining the validity of the TF approximation at the cosmological level, at the level of ultracompact DM halos, and for the Jeans problem at the epoch of matter-radiation equality involve different densities (ρ_Λ, ρ_0, and ρ_{eq}) yielding different critical particle masses $m_\Lambda = 1.20 \times 10^{-33}$ eV/c^2, $m_0 = 3.57 \times 10^{-22}$ eV/c^2, and $m_t = 2.10 \times 10^{-16}$ eV/c^2. As a result, for a boson mass $m \sim 10^{-22}$ eV/c^2, the TF approximation is valid during a long period of time for what concerns the evolution of the homogeneous background (quantum terms can be neglected), while it is marginally valid

to describe ultracompact DM halos (both quantum and logotropic terms have to be taken into account), and not valid at all to describe the formation of structures at the beginning of the matter era (logotropic terms can be neglected).

We have argued that the logarithmic term in Eq. (271) is a fundamental term that is always present in the KG equation. It is not a particular attribute of the SF (such as its mass or self-interaction constant) but rather an intrinsic property of spacetime. In other words, the ordinary (linear) KG equation is an approximation of the more fundamental wave equation (215). This equation involves a new fundamental constant of physics A superseding the Einstein cosmological constant Λ. This term accounts simultaneously for the accelerating expansion of the Universe and for the universal surface density of DM halos. The logarithmic potential manifests itself only at extremely low densities and this is why the ordinary (linear) KG and Schrödinger equations are so successful at the laboratory scale where $\rho \gg \rho_\Lambda$. However, the logarithmic potential becomes important at astrophysical and cosmological scales and leads to a logotropic dark fluid which unifies DM and DE. If the logarithmic term in Eq. (271) is replaced by a constant $V = \rho_\Lambda c^2$ mimicking a cosmological constant, we obtain the ΛFDM model which is associated with a constant equation of state $P = -\rho_\Lambda c^2$ (see Appendix E).[61] In the TF approximation, it reduces to the ΛCDM model (see Appendix D).[62] The ΛFDM model accounts for the accelerating expansion of the Universe and solves the core-cusp problem and the missing satellite problem as a consequence of quantum effects (Heisenberg's uncertainty principle). However, it does not account for the universal surface density of DM halos, contrary to the logotropic model. This is an important advantage of the logotropic model.

As discussed above, the KG equation with the potential from Eq. (271) describes a *noninteracting* SF. Indeed, we have argued that the logarithmic term in Eq. (271) is a fundamental term which is rooted in the KG equation. We can now consider more general models, where the bosons have a self-interaction, by including additional terms in the SF potential.

At the end of Secs. XIII, XV A, and XV B we have briefly considered the case of a relativistic BEC with a repulsive $|\varphi|^4$ self-interaction [see Eqs. (199), (216), and (221)]. At a cosmological level, the $|\varphi|^4$ self-interaction is responsible, in the fast oscillation (or TF) regime, for an additional radiationlike era occurring before the matterlike era. Therefore, the homogeneous SF successively

experiences a stiff matter era, a radiationlike era, a DM-like era, and a DE-like era. On the other hand, logotropic DM halos with a repulsive $|\varphi|^4$ self-interaction possess an additional hydrodynamic core stabilized by the self-interaction (see, e.g., [25,68]) in addition to the quantum core (soliton) due to the Heisenberg uncertainty principle, the logotropic core due to the logarithmic potential, and the NFW halo resulting from quantum interferences of excited states.

More generally, we can consider a relativistic BEC with a potential of the form

$$V_{\text{tot}}(|\varphi|^2) = \frac{m^2 c^2}{2\hbar^2}|\varphi|^2 + \frac{2\pi a_s m}{\hbar^2}|\varphi|^4 + \frac{32\pi^4 a_s^2}{9c^2\hbar^2}|\varphi|^6$$
$$+ \frac{mk_B T}{\hbar^2}|\varphi|^2\left[\ln\left(\frac{m^2|\varphi|^2}{\hbar^2\rho_*}\right) - 1\right]$$
$$- A\,\ln\left(\frac{m^2|\varphi|^2}{\hbar^2\rho_P}\right) - A. \qquad (273)$$

This potential includes a $|\varphi|^2$ rest-mass term, a $|\varphi|^4$ self-interaction which can be repulsive ($a_s > 0$) or attractive ($a_s < 0$), a repulsive $|\varphi|^6$ self-interaction of relativistic origin that can stabilize the system when $a_s < 0$, a $|\varphi|^2 \ln |\varphi|^2$ self-interaction which arises from effective or real thermal effects, and the intrinsic logarithmic $\ln |\varphi|^2$ self-interaction discussed above.[63] A power-law potential (see Appendix C of [22])

$$V(|\varphi|^2) = \frac{K}{\gamma - 1}\left(\frac{m}{\hbar}\right)^{2\gamma}|\varphi|^{2\gamma} \qquad (274)$$

is associated with a polytropic equation of state

$$P = K\rho^\gamma. \qquad (275)$$

In particular, for the $|\varphi|^4$ and $|\varphi|^6$ self-interaction, we have

$$V(|\varphi|^2) = \frac{2\pi a_s m}{\hbar^2}|\varphi|^4 \Rightarrow P = \frac{2\pi a_s \hbar^2}{m^3}\rho^2, \qquad (276)$$

$$V(|\varphi|^2) = \frac{32\pi^4 a_s^2}{9c^2\hbar^2}|\varphi|^6 \Rightarrow P = \frac{64\pi^4 a_s^2\hbar^4}{9m^6 c^2}\rho^3. \qquad (277)$$

On the other hand, the $|\varphi|^2 \ln |\varphi|^2$ self-interaction is associated with an isothermal equation of state

$$P = \rho\frac{k_B T}{m}. \qquad (278)$$

When $T > 0$, it can take into account the finite temperature of DM halos. The KG equation associated with the potential (273) is [see Eq. (212)]

---

[61]This is the limit of the logotropic model when $A \to 0$ and $\rho_P \to +\infty$ with $A\ln(\rho_P/\rho_\Lambda) \to \rho_\Lambda c^2$ fixed (see Secs. VII D and XII C).

[62]For $V = 0$ we get the FDM model which reduces to the CDM model in the TF approximation.

[63]Instead of the logarithmic term we can consider a constant term $V_0 = \epsilon_\Lambda$ mimicking a cosmological constant like in Appendix E. It is associated with a constant equation of state $P = -\epsilon_\Lambda$.

$$\Box\varphi + \frac{m^2 c^2}{\hbar^2}\varphi + \frac{8\pi a_s m}{\hbar^2}|\varphi|^2\varphi + \frac{64\pi^4 a_s^2}{3c^2\hbar^2}|\varphi|^4\varphi$$
$$+ \frac{2mk_B T}{\hbar^2}\ln\left(\frac{m^2|\varphi|^2}{\rho_*\hbar^2}\right)\varphi - \frac{2A}{|\varphi|^2}\varphi = 0, \qquad (279)$$

and the corresponding GP equation, valid in the non-relativistic regime, is [see Eq. (218)]

$$i\hbar\frac{\partial\psi}{\partial t} = -\frac{\hbar^2}{2m}\Delta\psi + m\Phi\psi + \frac{4\pi a_s\hbar^2}{m^2}|\psi|^2\psi$$
$$+ \frac{32\pi^4 a_s^2\hbar^4}{3m^5 c^2}|\psi|^4\psi + k_B T \ln\left(\frac{|\psi|^2}{\rho_*}\right)\psi - \frac{Am}{|\psi|^2}\psi. \qquad (280)$$

At the cosmological level, the rest-mass term is responsible for a DM-like era ($\epsilon \sim a^{-3}$), the repulsive $|\varphi|^4$ self-interaction is responsible for a radiationlike era ($\epsilon \sim a^{-4}$), the $|\varphi|^6$ self-interaction is responsible for a new primordial era ($\epsilon \sim a^{-9/2}$), the $|\varphi|^2 \ln|\varphi|^2$ self-interaction is responsible for a DM-like era with logarithmic corrections, and the logarithmic $\ln|\varphi|^2$ self-interaction is responsible for a DE-like era. At the level of DM halos, the rest-mass term produces a quantum core (soliton) and a NFW envelope, the $|\varphi|^4$ and $|\varphi|^6$ potentials produce a hydrodynamic core, the $|\varphi|^2 \ln|\varphi|^2$ potential produces an isothermal envelope (when $T > 0$), and the logarithmic $\ln|\varphi|^2$ self-interaction produces a logotropic envelope. The $|\varphi|^4$ self-interaction has been studied in [20,28,68,101], the $|\varphi|^6$ self-interaction has been studied in [102], the $|\varphi|^{2\gamma}$ self-interaction has been studied in [22], the $|\varphi|^2 \ln|\varphi|^2$ self-interaction has been studied in [22,25], and the $\ln|\varphi|^2$ self-interaction has been studied in the present paper.

APPENDIX A: MOTIVATION OF THE LOGOTROPIC MODEL

In this appendix, we recall the arguments that led us to introduce the logotropic model in Ref. [1]. In short, we assumed that DM and DE are the manifestation of a single DF and we tried to construct a UDM model with a nonconstant pressure that is as close as possible to the standard ΛCDM model.[64]

Let us consider a DF described by the polytropic equation of state

$$P = K\rho^\gamma, \qquad (A1)$$

where K is the polytropic constant and $\gamma = 1 + 1/n$ is the polytropic index. Up to a slight change of notations, this corresponds to the equation of state of the GCG.

---
[64]As discussed in Appendix B, we can introduce different types of logotropic models. The following arguments apply to all of them.

As shown in Appendix D 3, the ΛCDM model (interpreted as a UDM model) is equivalent to a single DF with a constant pressure

$$P = -\rho_\Lambda c^2, \qquad (A2)$$

where ρ_Λ is the cosmological density. Equation (A2) can be viewed as a particular polytropic equation of state with index $\gamma = 0$ and negative polytropic constant $K = -\rho_\Lambda c^2$. In this sense, the ΛCDM model is the simplest UDM model that one can imagine. Since the ΛCDM model works well at large scales, a viable model must necessarily be close to the ΛCDM model. However, it should not coincide with it, otherwise it would not be able to solve the CDM small-scale crisis such as the core-cusp problem and the missing satellite problem. Therefore, we need a model with a nonzero pressure gradient which can balance the gravitational attraction in DM halos and avoid singularities. In addition, a successful model should account for the constant surface density of DM halos $\Sigma_0^{\rm obs} = 141^{+83}_{-52}\ M_\odot/{\rm pc}^2$, something that the ΛCDM model does not do. Following [1], we look for the simplest extension of the standard ΛCDM model viewed as a UDM model.

A first possibility would be to consider the polytropic equation of state (A1) with an index γ very close to zero (but nonzero). Such a model can be as successful as the ΛCDM model at large scales. However, it seems hard to explain theoretically why a polytropic index like, e.g., $\gamma = -0.0123$ should be selected by nature. Furthermore, if we let $\gamma \to 0$ with K fixed we recover the ΛCDM model, so we have not gained anything (in particular the small-scale crisis remains).

Alternatively, in [1] we considered the limit $\gamma \to 0$ and $K \to \infty$ in such a way that $A = K\gamma$ is finite. Interestingly, this leads to a model close to, but different from, the ΛCDM model. This is how we justified the logotropic model in [1]. We recall below how the logotropic equation of state can be obtained from the polytropic equation of state in that limit [1,103].

To that purpose we consider a nonrelativistic DM halo described by the condition of hydrostatic equilibrium

$$\nabla P + \rho\nabla\Phi = \mathbf{0}. \qquad (A3)$$

For the polytropic equation of state (A1), this condition can be written as

$$K\gamma\rho^{\gamma-1}\nabla\rho + \rho\nabla\Phi = \mathbf{0}. \qquad (A4)$$

Taking the limit $\gamma \to 0$ and $K \to \infty$ with $A = K\gamma$ finite, we obtain

$$\frac{A}{\rho}\nabla\rho + \rho\nabla\Phi = \mathbf{0}. \qquad (A5)$$

Comparing this equation with Eq. (204), we see that the pressure involved in this expression corresponds to the logotropic equation of state[65]

$$P = A \ln\left(\frac{\rho}{\rho_*}\right), \tag{A9}$$

where ρ_* is a constant of integration. It is interesting to note that the logotropic equation of state, when coupled to gravity, yields the Lane-Emden equation of index $n = -1$ (see Appendix F). Therefore, a logotrope is closely related to a polytrope of index $\gamma = 0$ (or $n = -1$).[66] In this sense, the logotropic model may be viewed as the simplest extension of the ΛCDM model (corresponding to $\gamma = 0$) in the framework of UDM models [1].

Remark.—As explained above, the ΛCDM model is equivalent to a fluid with a pressure that is independent of the density. On the other hand, the logotropic equation of state depends on the density very weakly (logarithmically). This is the argument that led us to introduce the logotropic model [1]. Interestingly, by developing this model, we found that the constants ρ_* and A that appear in the logotropic equation of state (A9) can be determined by theoretical considerations and by observations (namely the measured values of $\Omega_{m,0}$ and H_0). As a result, there is no

---

[65]We can obtain the logotropic equation of state (A9) directly from Eq. (A1) by writing

$$P = K e^{\gamma \ln \rho} \tag{A6}$$

and expanding the right-hand side for $\gamma \to 0$, yielding

$$P = K(1 + \gamma \ln \rho + \ldots). \tag{A7}$$

In the limit $\gamma \to 0$ and $K \to \infty$ with $A = K\gamma$ finite, we get

$$P = A \ln \rho + K. \tag{A8}$$

The drawback with this calculation is that it yields an infinite constant ($K \to +\infty$) in addition to the logotropic equation of state so that the procedure is not well justified mathematically. By contrast, the calculation based on Eq. (A4) avoids dealing explicitly with infinite constants since they disappear in the gradients.

[66]Note that the logotropic model differs from a pure polytrope of index $\gamma = 0$ (or $n = -1$) and fixed K which has a constant pressure $P = K$. For this constant pressure model, equivalent to the ΛCDM model, the condition of hydrostatic equilibrium (A4) has no solution (there is no equilibrium state) since there is no pressure gradient. As a result, in the framework of the polytropic equation of state [104,105], the Lane-Emden equation of index $n = -1$ is ill-defined [the scale radius r_0 defined by Eq. (A7) of [105] vanishes]. Therefore, the limit $\gamma \to 0$ and $K \to \infty$ with $A = K\gamma$ finite leading to the logotropic equation of state is very peculiar. The logotropic model allows us to give a physical meaning to the Lane-Emden equation of index $n = -1$ which is excluded by the usual polytropic model. In this sense, the logotropic equation of state naturally completes the class of polytropic equations of state.

adjustable parameter in our model. Furthermore, this model can account for the observed value of the surface density of DM halos $\Sigma_0^{obs} = 141_{-52}^{+83} \; M_\odot/\text{pc}^2$ predicted to be equal to $\Sigma_0^{th} = 0.01955 c\sqrt{\Lambda}/G = 133 \; M_\odot/\text{pc}^2$ and for the present ratio $\Omega_{de,0}^{obs}/\Omega_{dm,0}^{obs} = 2.669$ of DE and DM predicted to be equal to $\Omega_{de,0}^{th}/\Omega_{dm,0}^{th} = e = 2.71828\ldots$. Following our paper [1], some authors [6–8] have introduced a simple extension of the logotropic model by considering an equation of state of the form

$$P = A\left(\frac{\rho}{\rho_*}\right)^{-n} \ln\left(\frac{\rho}{\rho_*}\right), \tag{A10}$$

where n is a free parameter. This equation of state is similar to the Anton-Schmidt [106] equation of state for crystalline solids in the Debye approximation [107]. In that case, the index n can be written as $n = -1/6 - \gamma_G$ where γ_G is the so-called Grüneisen [108] parameter. The original logotropic model is recovered for $n = 0$. However, since n is a free parameter the generalized logotropic model (A10) introduces some indetermination (or freedom) in the analysis, while the original logotropic model [1] is completely predictive. By comparing the results of the generalized logotropic model (A10) with cosmological observations, the authors of [6–8] found that $B \simeq 3.54 \times 10^{-3}$ and $n = -0.147_{-0.107}^{+0.113}$. This confirms the robustness of the value of the fundamental constant $B = 3.53 \times 10^{-3}$ introduced in [1,2]. On the other hand, up to the error bars, the value of n is close to $n = 0$, corresponding to the logotropic model (see also [3]). This suggests that the logotropic model tends to be selected among more general families of models containing additional parameters $\{n\}$.

APPENDIX B: LOGOTROPIC MODELS OF TYPE I, II, AND III

As explained in [21] we can introduce three types of barotropic equations of state with the same functional form depending on whether the pressure P is expressed in terms of the energy density ϵ (model I), the rest-mass density $\rho_m = nm$ (model II), or the pseudo-rest-mass density ρ (model III). These models are equivalent in the nonrelativistic limit but they differ from each other in the relativistic regime. A detailed discussion of these models and their interrelations is given in [21] (see also [1,20,109,110]). In this appendix, we briefly discuss these models in the framework of the logotropic equation of state.

Barotropic models of type I correspond to an equation of state of the form $P = P(\epsilon)$, where ϵ is the energy density. The logotropic model of type I is therefore

$$P = A \ln\left(\frac{\epsilon}{\rho_P c^2}\right). \tag{B1}$$

The energy conservation equation (6) combined with the logotropic equation of state (B1) yields

$$\ln a = -\frac{1}{3} \int_{\epsilon_0}^{\epsilon} \frac{d\epsilon'}{\epsilon' + A \ln\left(\frac{\epsilon'}{\rho_P c^2}\right)}, \qquad (B2)$$

where ϵ_0 denotes the present energy density of the Universe (when $a = 1$). This equation determines the evolution of the energy density $\epsilon(a)$ as a function of the scale factor. When $a \to 0$, we get $\epsilon \propto a^{-3}$ similar to DM. When $a \to +\infty$ we get $\epsilon \to \epsilon_{\min}$ similar to DE where $\epsilon_{\min}$ is the solution of the equation $\epsilon_{\min} + A \ln (\epsilon_{\min}/\rho_P c^2) = 0$. This leads to an exponential (de Sitter) expansion like in the ΛCDM model. If we identify $\epsilon_{\min}$ with the DE density $\rho_\Lambda c^2$ in the ΛCDM model (which coincides with the asymptotic value of ϵ), we get

$$A = \frac{\rho_\Lambda c^2}{\ln\left(\frac{\rho_P}{\rho_\Lambda}\right)}. \qquad (B3)$$

This returns the relation obtained in the logotropic model of type II [1] and in the logotropic model of type III [see Eq. (105)]. This strengthens the validity of this relation [66]. If we set $x = \epsilon'/\epsilon_0$, $A = B\rho_\Lambda c^2$, and $B = 1/\ln(\rho_P/\rho_\Lambda)$ with $\rho_\Lambda = \Omega_{\mathrm{de},0}\epsilon_0/c^2$, we can rewrite Eq. (B2) as

$$\ln a = -\frac{1}{3} \int_1^{\epsilon/\epsilon_0} \frac{dx}{x + B\Omega_{\mathrm{de},0}(\ln x - \ln \Omega_{\mathrm{de},0} - \frac{1}{B})}. \qquad (B4)$$

The function $(\epsilon/\epsilon_0)(a)$ is plotted in Fig. 19. We have taken $\Omega_{\mathrm{de},0} = 0.6911$ and $B = 3.53 \times 10^{-3}$. The logotropic model of type I behaves similar to the ΛCDM model. This model will be studied in more detail in a future work [66].

Barotropic models of type II correspond to an equation of state of the form $P = P(\rho_m)$, where $\rho_m = nm$ is the rest-mass density (n is the particle number density). The logotropic model of type II is therefore
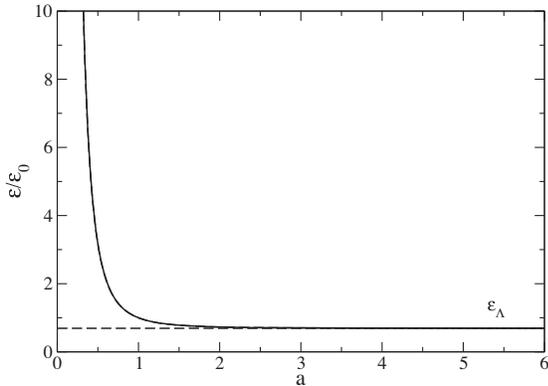
FIG. 19. Normalized energy density ϵ/ϵ_0 as a function of the scale factor a for the logotropic model of type I. It is compared with the ΛCDM model. The two curves are indistinguishable on the figure.

$$P = A \ln\left(\frac{\rho_m}{\rho_P}\right). \qquad (B5)$$

This is the original logotropic model introduced in [1].

Barotropic models of type III correspond to an equation of state of the form $P = P(\rho)$, where ρ is the pseudo-rest-mass density associated with a complex SF (see Sec. II). The logotropic model of type III is therefore

$$P = A \ln\left(\frac{\rho}{\rho_P}\right). \qquad (B6)$$

This is the logotropic model studied in the present paper. It could be called the logotropic complex SF model and referred to as the logotropic CSF model.

In the nonrelativistic limit, we have $\rho \sim \rho_m$ and $\epsilon \sim \rho c^2$, so the three models become equivalent. They correspond to an equation of state of the form $P = P(\rho)$, where ρ is the mass density. The nonrelativistic logotropic equation of state is

$$P = A \ln\left(\frac{\rho}{\rho_P}\right). \qquad (B7)$$

The structure of logotropic DM halos described by the equation of state (B7) has been studied in [1] (see also Appendix F).

APPENDIX C: DM WITH A LINEAR EQUATION OF STATE

In the CDM model it is assumed that DM is pressureless ($P = 0$). In this appendix, we consider the possibility that CDM is described by a linear equation of state $P = \alpha\epsilon$ with $\alpha \geq 0$, yielding a constant (nonzero) speed of sound $c_s = \sqrt{\alpha}c$. We determine the condition that α must satisfy in order to be consistent with the observations of the matter power spectrum.

In the nonrelativistic regime where $\epsilon \sim \rho c^2$, we can rewrite the equation of state as $P = \alpha\rho c^2$. This linear equation of state can be interpreted as an isothermal equation of state of the form $P = \rho k_B T_{\mathrm{eff}}/m$ with $\alpha = k_B T_{\mathrm{eff}}/mc^2$. Here, T_{eff} is a temperature which may be identified with the effective temperature of DM halos. For a typical DM halo of mass $M_h = 10^{11} M_\odot$ (medium spiral), one has $(k_B T_{\mathrm{eff}}/m)^{1/2} = 108$ km/s [25]. This gives $\alpha \sim 10^{-7}$.

According to Eqs. (241) and (242), the Jeans length and the Jeans mass are given by

$$\lambda_J = 2\pi \left(\frac{\alpha c^2}{4\pi G}\right)^{1/2} \frac{1}{\rho^{1/2}}, \qquad (C1)$$

$$M_J = \frac{4}{3}\pi^4 \left(\frac{\alpha c^2}{4\pi G}\right)^{3/2} \frac{1}{\rho^{1/2}}. \qquad (C2)$$

Using Eq. (240), we find that during the expansion of the Universe the Jeans length and the Jeans mass both increase as $a^{3/2}$ (the comoving Jeans length increases as $a^{1/2}$). Eliminating the density between Eqs. (C1) and (C2), we obtain

$$M_J = \frac{\pi^2}{6} \frac{\alpha c^2}{G} \lambda_J. \tag{C3}$$

This relation is similar to the mass-radius relation $M = 2k_B T R / G m$ of an isothermal self-gravitating system confined within a box [111]. Repeating the calculations made at the end of Sec. XVI A we can rewrite the Jeans length and the Jeans mass as

$$\lambda_J = 2\pi \left(\frac{2\alpha}{3\Omega_{m,0}} \right)^{1/2} R_\Lambda a^{3/2}, \tag{C4}$$

$$M_J = \pi^3 \left(\frac{2\alpha}{3\Omega_{m,0}} \right)^{3/2} \Omega_{m,0} M_\Lambda a^{3/2}, \tag{C5}$$

where $R_\Lambda = 4.44 \times 10^3$ Mpc and $M_\Lambda = 4.62 \times 10^{22} \, M_\odot$ represent the typical radius and mass of the visible Universe today. As we have seen in footnote 53, observational constraints from the matter power spectrum require that $\lambda_J(a = 1) < R$ with $R \sim 15$ Mpc. Since $\lambda_J(a = 1) \sim 10\sqrt{\alpha} R_\Lambda$, we need $100\alpha < (R/R_\Lambda)^2 \sim 10^{-5}$. This imposes $\alpha < 10^{-7}$ in agreement with the findings of [112]. Interestingly, the value $\alpha \sim 10^{-7}$ obtained above from the effective temperature of DM halos satisfies this constraint marginally.

APPENDIX D: ΛCDM MODEL

In this appendix, we discuss different equivalent manners to justify the ΛCDM model.

1. DM + Λ

The usual manner to introduce the ΛCDM model in cosmology is to assume that the Universe is filled with DM (in addition to baryonic matter and radiation that we do not consider here for brevity) and that the Einstein cosmological constant Λ has a nonzero value. DM is introduced to explain the formation of the large-scale structures of the Universe and the flat rotation curves of the galaxies (see Appendix D 4). A positive cosmological constant is introduced to explain the present acceleration of the Universe.

DM is usually treated as a pressureless fluid with an equation of state

$$P_m = 0. \tag{D1}$$

Solving the energy conservation equation (6) with the equation of state (D1), we obtain

$$\epsilon_m = \frac{\epsilon_{m,0}}{a^3}, \tag{D2}$$

where $\epsilon_{m,0}$ is a constant of integration which can be identified with the present energy density of DM.

On the other hand, considering the Friedmann equation (7), we see that the cosmological constant Λ is equivalent to a constant energy density

$$\epsilon_\Lambda = \rho_\Lambda c^2 = \frac{\Lambda c^2}{8\pi G}. \tag{D3}$$

Substituting Eq. (D2) into the Friedmann equation (7), we get

$$H^2 = \frac{8\pi G \epsilon_{m,0}}{3c^2 a^3} + \frac{\Lambda}{3}, \tag{D4}$$

where we have assumed $k = 0$. Equation (D4) is equivalent to Eq. (8) with a total energy density

$$\epsilon = \frac{\epsilon_{m,0}}{a^3} + \epsilon_\Lambda. \tag{D5}$$

2. DM + DE

A second manner to introduce the ΛCDM model is to assume that the Universe is filled with DM and DE interpreted as two noninteracting fluids [in that case we take $\Lambda = 0$ in Eq. (7)]. DM is treated as a pressureless fluid with the equation of state (D1). Its energy density evolves with the scale factor according to Eq. (D2). DE is treated as a fluid with a negative pressure determined by the linear equation of state

$$P_{de} = -\epsilon_{de}. \tag{D6}$$

Solving the energy conservation equation (6) with the equation of state (D6), we obtain

$$\epsilon_{de} = \epsilon_\Lambda, \tag{D7}$$

where ϵ_Λ is a constant of integration that is identified with the cosmological density.

The total energy density of the Universe is the sum of DM and DE: $\epsilon = \epsilon_m + \epsilon_{de}$. Summing Eqs. (D2) and (D7), we get

$$\epsilon = \frac{\epsilon_{m,0}}{a^3} + \epsilon_\Lambda, \tag{D8}$$

which is equivalent to Eq. (D5). Introducing the present energy density of the Universe $\epsilon_0 = 3c^2 H_0^2/8\pi G$ (where H_0 is the present value of the Hubble constant) and the present fraction of DM and DE given by $\Omega_{m,0} = \epsilon_{m,0}/\epsilon_0$ and $\Omega_{de,0} = \epsilon_\Lambda/\epsilon_0 = 1 - \Omega_{m,0}$, we obtain

$$\frac{\epsilon}{\epsilon_0} = \frac{\Omega_{m,0}}{a^3} + 1 - \Omega_{m,0}. \tag{D9}$$

The ΛCDM model involves two unknown parameters ϵ_0 and $\Omega_{m,0}$ that must be determined by the observations. When $a \to 0$, the Universe is dominated by DM and we have

$$\epsilon \sim \frac{\Omega_{m,0}\epsilon_0}{a^3}, \tag{D10}$$

leading to a decelerated expansion (Einstein–de Sitter era). When $a \to +\infty$, the Universe is dominated by DE and we have

$$\epsilon \to \epsilon_\Lambda = (1 - \Omega_{m,0})\epsilon_0. \tag{D11}$$

The energy density tends to a constant, leading to an exponential expansion (de Sitter era).

Remark.—Introducing the dimensionless variables of Sec. VII, we can rewrite Eq. (D9) as

$$\tilde{\epsilon} = \frac{\Omega_{m,0}}{1 - \Omega_{m,0}} \frac{1}{a^3} + 1. \tag{D12}$$

The equality between DM and DE in the ΛCDM model corresponds to a scale factor

$$a_t = \left(\frac{\Omega_{m,0}}{1 - \Omega_{m,0}}\right)^{1/3} = 0.765, \tag{D13}$$

an energy density $\tilde{\epsilon}_t = 2$, and a value of the equation of state parameter $w_t = -1/2$.

3. DF

A third manner to introduce the ΛCDM model is to assume that the Universe is filled with a single DF [in that case, we take $\Lambda = 0$ in Eq. (7)] with a constant equation of state

$$P = -\epsilon_\Lambda, \tag{D14}$$

where ϵ_Λ is identified with the cosmological density. We stress that this constant equation of state is different from the linear equation of state (D6). Solving the energy conservation equation (6) with the equation of state (D14), we obtain

$$\epsilon = \frac{\epsilon_{m,0}}{a^3} + \epsilon_\Lambda, \tag{D15}$$

where $\epsilon_{m,0}$ is a constant of integration. This equation is equivalent to Eq. (D5) or (D8). The equation of state parameter is

$$w = \frac{P}{\epsilon} = \frac{-\epsilon_\Lambda}{\frac{\epsilon_{m,0}}{a^3} + \epsilon_\Lambda}. \tag{D16}$$

The squared speed of sound $c_s^2 = P'(\epsilon)c^2$ is equal to zero. This single DF model, based on the equation of state (D14), provides the simplest unification of DM and DE that one can imagine and it coincides with the usual ΛCDM model from Appendices D 1 and D 2.[67] In this connection, the first term in Eq. (D15) plays the role of DM and the second term plays the role of DE. As shown in [1] at a general level, the effective DM term corresponds to the rest-mass energy $\rho_m c^2$ of the DF and the effective DE term corresponds to its internal energy u [for the ΛCDM model, Eq. (D15) can be obtained from Eqs. (46) and (47) with the equation of state (D14) yielding $u = \epsilon_\Lambda$].

Remark.—The relation (D15) between the energy density and the scale factor can be rewritten as

$$\epsilon = \rho_\Lambda c^2 \left[\left(\frac{a_t}{a}\right)^3 + 1\right], \tag{D18}$$

where a_t is the transition scale factor defined by Eq. (D13). Solving the Friedmann equation (8) with the energy density given by Eq. (D18), we find that the temporal evolution of the scale factor is given by

$$\frac{a}{a_t} = \sinh^{2/3}\left(\sqrt{6\pi G\rho_\Lambda}\, t\right). \tag{D19}$$

4. CDM halos

Classical (nonquantum) numerical simulations of CDM lead to DM halos with a universal density profile that is well fitted by the function

$$\rho(r) \propto \frac{1}{\frac{r}{r_s}\left(1 + \frac{r}{r_s}\right)^2}, \tag{D20}$$

where r_s is a scale radius that varies from halo to halo. This is the so-called NFW profile [115]. Such halos result from a process of violent collisionless relaxation. The density decreases as r^{-3} for $r \to +\infty$ and diverges as r^{-1} for

---

[67]It is shown in Refs. [75,113] that the constant pressure model (D14) is equivalent to the ΛCDM not only for the evolution of the background but to all orders in perturbation theory, even in the nonlinear clustering regime (contrary to the initial claim of [114]). If we consider the affine equation of state $P = \alpha\epsilon - \epsilon_\Lambda$, which yields a constant squared speed of sound $c_s^2 = \alpha c^2$, we obtain [52]

$$\epsilon = \frac{\epsilon_{m,0}}{a^{3(1+\alpha)}} + \epsilon_\Lambda. \tag{D17}$$

This is equivalent to a two-fluid model $P_m = \alpha\varepsilon_m$ (DM) and $P_{de} = -\varepsilon_{de}$ (DE).

$r \to 0$. The divergence of the density at the center is related to the fact that classical CDM halos are pressureless $(P = 0)$ so there is no pressure gradient to balance the gravitational attraction. This divergence is not consistent with the observations that reveal that DM halos possess a core, not a cusp. Observed DM halos are better fitted by the function

$$\rho(r) = \frac{\rho_0}{(1 + \frac{r}{r_h})(1 + \frac{r^2}{r_h^2})}, \quad \text{(D21)}$$

where ρ_0 is the central density and r_h is the halo radius defined as the distance at which the central density ρ_0 is divided by 4. This is the so-called Burkert profile [116]. The density decreases as r^{-3} for $r \to +\infty$, similar to the NFW profile, but displays a flat core for $r \to 0$ instead of a cusp. It is important to recall, however, that the Burkert profile is purely empirical and has no fundamental justification.

5. SF

The previous models are purely classical (nonquantum) since $\hbar$ does not explicitly appear in the equations. However, it is possible to introduce SF models that reproduce, in certain limits, the ΛCDM model. These models are more general than the ΛCDM model since a SF, being governed by the KG equation, has a quantum origin.

Let us first consider a spatially homogeneous real SF evolving according to the KG equation[68]

$$\ddot{\varphi} + 3H\dot{\varphi} + \frac{dV}{d\varphi} = 0 \quad \text{(D22)}$$

coupled to the Friedmann equation (8). The SF tends to run down the potential toward lower energies and is submitted to a Hubble friction. The density and the pressure of the SF are given by

$$\epsilon = \frac{1}{2}\dot{\varphi}^2 + V(\varphi), \quad \text{(D23)}$$

$$P = \frac{1}{2}\dot{\varphi}^2 - V(\varphi). \quad \text{(D24)}$$

We can easily check that these equations imply the energy conservation equation (6) [21]. For a general equation of state $P(\epsilon)$, using standard techniques [117–120], we can obtain the SF potential as follows [121]. From Eqs. (D23) and (D24), we get

$$\dot{\varphi}^2 = (w + 1)\epsilon, \quad \text{(D25)}$$

where we have defined $w = P/\epsilon$. Using $\dot{\varphi} = (d\varphi/da)Ha$ and the Friedmann equation (8), we find that the relation between the SF and the scale factor is given by[69]

$$\frac{d\varphi}{da} = \left(\frac{3c^4}{8\pi G}\right)^{1/2}\frac{\sqrt{1+w}}{a}. \quad \text{(D26)}$$

On the other hand, according to Eqs. (D23) and (D24), the potential of the SF is given by

$$V = \frac{1}{2}(1 - w)\epsilon. \quad \text{(D27)}$$

Therefore, the potential of the SF is determined in parametric form by the equations

$$\varphi(a) = \left(\frac{3c^4}{8\pi G}\right)^{1/2}\int \sqrt{1 + w(a)}\frac{da}{a}, \quad \text{(D28)}$$

$$V(a) = \frac{1}{2}[1 - w(a)]\epsilon(a). \quad \text{(D29)}$$

For the constant equation of state (D14) corresponding to the ΛCDM model in its UDM interpretation, Eq. (D28) with Eq. (D16) is readily integrated, leading to the hyperbolic potential [121,122]

$$V(\psi) = \frac{1}{2}\rho_\Lambda c^2(\cosh^2\psi + 1), \quad \text{(D30)}$$

where

$$\psi = -\left(\frac{8\pi G}{3c^4}\right)^{1/2}\frac{3}{2}\varphi. \quad \text{(D31)}$$

The SF is related to the scale factor by

$$(a/a_t)^{-3/2} = \sinh\psi, \quad \text{(D32)}$$

where a_t is the transition scale factor defined by Eq. (D13) and $\psi \geq 0$. We note that this solution is exact in the sense that it does not rely on any approximation. However, it corresponds to a very particular initial condition of the KGF equations [122]. We also note that the SF does not oscillate. According to Eqs. (D19) and (D32) it gently descends the potential.[70]

---

[68]Here $V(\varphi)$ denotes the *total* potential of the SF including the rest-mass term. In addition, the time variable stands here for *ct*.

[69]We assume a nonphantom universe $w > -1$.
[70]We can also associate with the ΛCDM model a tachyonic SF with a potential (see [121,122] for details)

$$V(\psi) = \frac{\rho_\Lambda c^2}{\cos\psi}, \quad \text{(D33)}$$

where $\psi = -\sqrt{6\pi G\rho_\Lambda/c^2}\varphi$. The SF is related to the scale factor by $(a/a_t)^{-3/2} = \tan\psi$ with $0 \leq \psi \leq \pi/2$.

The ΛCDM model can also be obtained from a real SF model with a potential

$$V(\varphi) = \frac{m^2 c^2}{2\hbar^2} \varphi^2 + \epsilon_\Lambda. \tag{D34}$$

In the fast oscillation regime, the SF experiences slowly damped oscillations and behaves as DM. When it reaches the bottom of the potential, the energy density becomes constant ($\epsilon = \epsilon_\Lambda$) and the SF behaves as DE (cosmological constant).

We can finally consider a complex SF with a potential

$$V_{\text{tot}}(|\varphi|^2) = \frac{m^2 c^2}{2\hbar^2} |\varphi|^2 + \epsilon_\Lambda. \tag{D35}$$

This model, referred to as the ΛFDM model, is considered in detail in Appendix E. Here, we just note that, in the fast oscillation regime where quantum effects can be neglected (TF approximation), the SF undergoes a process of spintessence (it slowly descends the potential by rapidly spinning about the vertical axis) and behaves like the ΛCDM model.

We note that the shifted quadratic potentials from Eqs. (D34) and (D35) are very different from the hyperbolic potential from Eq. (D30). In addition, the SF oscillates or spins rapidly in the potentials from Eqs. (D34) and (D35) while it just descends the potential from Eq. (D30) without oscillating. These remarks show that several SF models can behave just like the ΛCDM model while being fundamentally different from each others.

Remark.—If we expand Eq. (D30) for $\varphi \to 0$ we find that

$$V(\varphi) = \rho_\Lambda c^2 + \frac{9 m_\Lambda^2 c^2}{8\hbar^2} \varphi^2 + \dots \tag{D36}$$

We see that the minimum of the potential is equal to the cosmological density $V_0 = \rho_\Lambda c^2$ and that the mass of the SF is $m = (3/2) m_\Lambda$, where $m_\Lambda = 1.20 \times 10^{-33}$ eV/c^2 is the cosmon mass [see Eq. (190)]. Our approach provides therefore a physical interpretation to the cosmon mass as being the mass of the SF responsible for the DE in the late Universe. To the best of our knowledge, this interpretation has not been given before. In comparison, the mass of the SF in the ΛFDM model (D35) is of order $m \sim 10^{-22}$ eV/c^2 (see Appendix E).

APPENDIX E: ΛFDM MODEL

In this appendix, we consider a complex SF model with a constant potential $V = \epsilon_\Lambda$ equal to the cosmological density. This model generalizes the relativistic FDM model described by the KGE equations (212) and (213) with $V = 0$. In the fast oscillation regime or in the TF approximation (where quantum effects can be neglected), it coincides with the ΛCDM model. On the other hand, when quantum effects are taken into account but relativistic

effects are neglected (as in the case of DM halos), it coincides with the nonrelativistic FDM model [123] described by the GPP equations (218) and (219) with $V = 0$ reducing to the Schrödinger-Poisson equations. We shall call it the ΛFDM model.

1. Potential of the ΛFDM model

We assume that DM and DE are described by a single complex SF with a constant potential

$$V = \epsilon_\Lambda, \tag{E1}$$

where ϵ_Λ is the cosmological density. In the fast oscillation regime, using Eq. (36), we find that the pressure is given by

$$P = -\epsilon_\Lambda. \tag{E2}$$

Therefore, the pressure is constant as in the ΛCDM model [see Eq. (D14)]. On the other hand, the equations governing the evolution of the homogeneous background in the fast oscillation regime [Eqs. (32)–(40)] are

$$\rho = \frac{Qm}{a^3}, \tag{E3}$$

$$\epsilon = \rho c^2 + \epsilon_\Lambda, \tag{E4}$$

$$E_{\text{tot}} = mc^2, \tag{E5}$$

$$w = \frac{P}{\epsilon} = -\frac{\epsilon_\Lambda}{\rho c^2 + \epsilon_\Lambda}, \tag{E6}$$

$$c_s = 0. \tag{E7}$$

They return the equations of the ΛCDM model (see Appendix D). In particular, combining Eqs. (E3) and (E4), we obtain

$$\epsilon = \frac{Qmc^2}{a^3} + \epsilon_\Lambda, \tag{E8}$$

which is equivalent to Eq. (D15) with the identification $Qmc^2 = \epsilon_{\text{m},0}$. The constant Qmc^2 (charge of the SF) is equal to the present energy density $\epsilon_{\text{m},0} = \Omega_{\text{m},0} \epsilon_0$ of DM. This result is valid for an arbitrary potential V (see Sec. II G). However, for a constant potential, the pseudo-rest-mass density ρ coincides with the rest-mass density ρ_m [see Eq. (45)] and plays the role of DM ($\rho = \rho_m$). On the other hand, the internal energy is constant ($u = \epsilon_\Lambda$) and plays the role of DE [see Eq. (48)].

The total potential of the SF including the rest-mass term is

$$V_{\text{tot}}(|\varphi|^2) = \frac{m^2 c^2}{2\hbar^2} |\varphi|^2 + \epsilon_\Lambda. \tag{E9}$$

This is a shifted quadratic potential. Using Eq. (25), it can be written as

$$V_{\text{tot}} = \frac{1}{2}\rho c^2 + \epsilon_\Lambda. \qquad \text{(E10)}$$

The total potential of the SF is represented by a dashed line in Fig. 13. In the fast oscillation regime, the SF descends the potential on the surface of the bowl up to the origin $|\varphi| = 0$ by rapidly spinning around the vertical axis (see Sec. XII A).

Remark.—The ordinary FDM model corresponds to a complex SF with a vanishing potential $V = 0$. In the fast oscillation regime, it just describes pressureless DM ($P = 0$). Therefore, it does not provide a unification of DM and DE. DE has to be introduced in a different manner, either by introducing another species (like quintessence) or through a nonvanishing cosmological constant Λ. The ordinary FDM model ($V = 0$) + a cosmological constant is the complex SF generalization of the ΛCDM model of Appendix D 1. We shall call it the ΛFDM model. The FDM model with a constant potential $V = \epsilon_\Lambda$ provides a simple unification of DM and DE. This is the complex SF generalization of the ΛCDM model viewed as a DF or a UDM model (see Appendix D 3). We shall also call it the ΛFDM model.

2. Validity of the fast oscillation regime

Introducing the dimensionless variables of Secs. VII and XIII, and using Eq. (D12), we find that the fast oscillation regime $\omega \gg H$ of the ΛFDM model (where it is equivalent to the ΛCDM model) is valid for $\tilde{\epsilon} \ll \sigma$, where σ is defined by Eqs. (188) and (189). This criterion first requires that $\sigma \gg 1$, i.e., $m \gg m_\Lambda = 1.20 \times 10^{-33}$ eV/c². Therefore, the mass of the SF must be much larger than the cosmon mass. When this condition is fulfilled, the fast oscillation regime is valid for $a \gg a_v$ (see Fig. 20) with
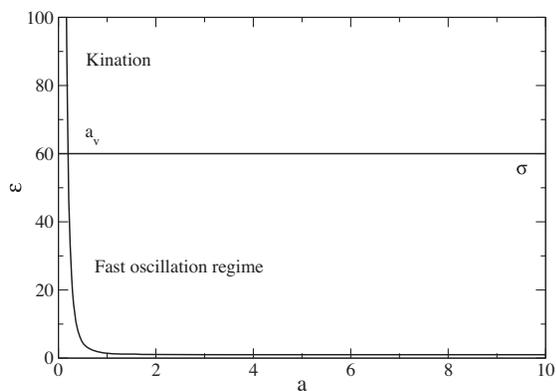
FIG. 20. Graphical construction determining the range of validity of the fast oscillation regime in the ΛFDM model (we have represented $\tilde{\epsilon}$ versus a).
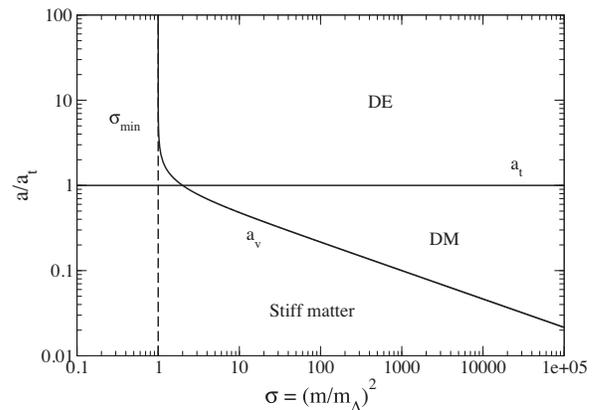
FIG. 21. Dynamical phase diagram of the ΛFDM model showing the different eras experienced by the SF during the evolution of the Universe as a function of its mass m (this figure also determines the validity of the fast oscillation regime above a_v). We see how the fundamental cosmon mass m_Λ comes into play in the problem.

$$\frac{a_v}{a_t} = \left(\frac{1}{\sigma - 1}\right)^{1/3}, \qquad \text{(E11)}$$

where a_t is the transition scale factor from Eq. (D13). The fast oscillation regime is not valid for $a < a_v$. In that case, the SF is in a slow oscillation regime of kination. This gives rise to a stiff matter era as discussed in [20,28] and in Sec. XIII.

In the ΛFDM model the SF undergoes three successive eras: a stiff matter era for $a < a_v$, a DM era for $a_v < a \ll a_t$, and a DE era for $a \gg a_t$ (we recall that $a_t = 0.765$ corresponds to the transition between the DM and DE eras). These results are represented on the dynamical phase diagram of Fig. 21, where we have plotted the transition scale a_v as a function of the mass m of the SF. If the SF has a $|\varphi|^4$ self-interaction, an additional radiationlike era occurs between the stiff matter era and the DM era (see the Remark at the end of Sec. XIII).

In Fig. 22 we have represented the motion of the SF in the potential $V_{\text{tot}}(|\varphi|^2)$ during these different periods. During the stiff matter era ($a < a_v$), corresponding to a slow oscillation regime, the SF rolls down the potential well without oscillating. Then, for $a > a_v$, the SF enters in the fast oscillation regime and descends the potential by oscillating rapidly about the vertical axis until it falls at the bottom of the well $(V_{\text{tot}})_{\text{min}} = \epsilon_\Lambda$ and achieves a constant energy density ϵ_Λ. This evolution successively describes the DM and DE eras.

3. FDM halos

Since the potential $V(|\varphi|^2) = \epsilon_\Lambda$ of the ΛFDM model is constant, it disappears from the wave equations. As a result, the relativistic wave equation (212) reduces to the standard KG equation
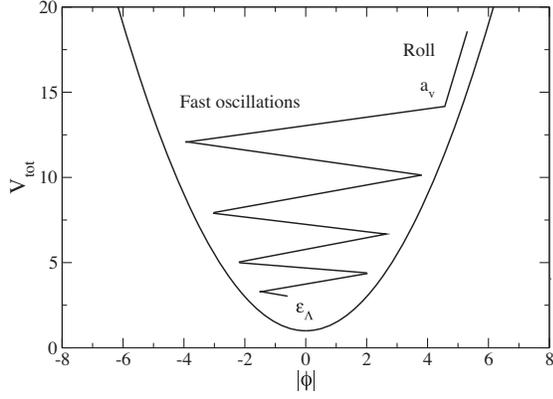
FIG. 22. Schematic evolution of the SF in the total potential $V_{\text{tot}}(|\varphi|^2)$ showing roll versus oscillations (the scales are not respected). For $a < a_v$, the SF rolls down the potential well without oscillating (stiff matter era); for $a > a_v$, it oscillates rapidly (DM and DE eras).

$$\Box\varphi + \frac{m^2 c^2}{\hbar^2}\varphi = 0, \qquad (E12)$$

and the nonrelativistic (GP) wave equation (218) reduces to the standard Schrödinger equation

$$i\hbar\frac{\partial\psi}{\partial t} = -\frac{\hbar^2}{2m}\Delta\psi + m\Phi\psi. \qquad (E13)$$

We thus recover the wave equations of the standard FDM model corresponding to $V = 0$.[71]

When considering DM halos, we can make the nonrelativistic approximation. FDM halos are therefore described by the Schrödinger-Poisson equations. The Schrödinger-Poisson equations are known to undergo a process of gravitational cooling and violent relaxation [65,100]. This leads to FDM halos with a core-halo structure involving a quantum core (soliton) surrounded by an atmosphere of scalar radiation whose coarse-grained structure is consistent with the NFW density profile of CDM halos at large distances. This quantum core-halo structure is observed in numerical simulations of FDM halos [124–132].

The quantum core (soliton) corresponds to the ground state of the Schrödinger-Poisson equations. In the Madelung hydrodynamical representation of the Schrödinger-Poisson equations (see Sec. XV C), it is determined by the condition of quantum hydrostatic equilibrium

$$\frac{\rho}{m}\nabla Q_B + \rho\nabla\Phi = \mathbf{0} \qquad (E14)$$

coupled to the Poisson equation

$$\Delta\Phi = 4\pi G\rho. \qquad (E15)$$

The solitonic core results from the balance between the gravitational attraction and the quantum potential, taking into account the Heisenberg uncertainty principle. Its density profile can be determined by solving numerically the differential equation

$$\frac{\hbar^2}{2m^2}\Delta\left(\frac{\Delta\sqrt{\rho}}{\sqrt{\rho}}\right) = 4\pi G\rho, \qquad (E16)$$

obtained by combining Eqs. (E14) and (E15), as done in [133,134]. The exact core mass-radius relation is given by [133,134]

$$M = 9.95\frac{\hbar^2}{Gm^2 R_{99}}, \qquad (E17)$$

where R_{99} is the radius enclosing 99% of the mass. This mass-radius relation is consistent with the characteristics of the smallest—ultracompact—DM halos observed in the Universe (dSphs like Fornax with $M \sim 10^8\ M_\odot$ and $R \sim 1$ kpc) provided that the boson mass is of the order of[72]

$$m \sim 10^{-22}\ \text{eV}/c^2. \qquad (E18)$$

The exact density profile of the soliton is well approximated by the Gaussian [68]

$$\rho = \rho_0 e^{-r^2/R^2} \qquad (E19)$$

with $M = 5.57\rho_0 R^3$ and $R_{99} = 2.38R$. It can also be fitted by the function [124,125]

$$\rho = \frac{\rho_0}{[1 + (r/R)^2]^8} \qquad (E20)$$

with $M = 0.318\rho_0 R^3$ and $R_{99} = 1.151R$ (see Fig. 2 of [25] for a comparison between these two profiles and the exact one). We note that the density presents a core, not a cusp, when $r \to 0$. Quantum terms are important at "small" scales, implying that the soliton has a size comparable to the de Broglie length ($\lambda_{\text{dB}} \sim 1$ kpc).[73] Quantum mechanics stabilizes the system against gravitational collapse and solves the core-cusp problem.

---

[71]If the SF has a $|\varphi|^4$ self-interaction, it is described by the KGE or GPP equations (216) and (221) with $A = 0$.

[72]Ultracompact DM halos (like dSphs) are assumed to correspond to a pure soliton without atmosphere, or a tiny one. This is the ground state of the Schrödinger-Poisson equations. Large DM halos (like the medium spiral) have a solitonic core surrounded by an extended envelope. The core mass–halo mass relation $M_c(M_h)$ has been obtained in different manners in Refs. [25,105,125,128,132,135–137].

[73]The mass-radius relation of the soliton scales as $M \sim \hbar^2/Gm^2 R$. Introducing a typical velocity scale through the virial relation $v^2 \sim GM/R$, we obtain $R \sim \hbar/mv = \lambda_{\text{dB}}$. Since $v \sim \sqrt{\alpha}c \sim 10^{-3}c$ (see Appendix C), the de Broglie length is larger than the Compton length $\lambda_C = \hbar/mc$ by about 3 orders of magnitude.

The halo of scalar radiation results from the quantum interferences of excited states [65]. It is made of uncondensed bosons with an out-of-equilibrium DF. On the coarse-grained scale the density of the halo is consistent with the NFW density profile of CDM halos [see Eq. (D20)] which decrease as r^{-3} at large distances. It is also consistent with an isothermal profile with an effective temperature T_{eff} as predicted by the statistical theory of violent collisionless relaxation developed by Lynden-Bell [99]. Effective thermal effects are important at "large" scales (≥ 1 kpc). An approximately isothermal halo can account for the flat rotation curves of the galaxies which have a constant circular velocity [e.g., $v_\infty = (2k_B T_{\text{eff}}/m)^{1/2} \sim 153$ km/s for the medium spiral]. On the fine-grained scale, the halo has a granular structure [124,125]. It is made of "quasiparticles" [138] of the size of the solitonic core $\lambda_{\text{dB}} \sim \hbar/mv \sim 1$ kpc (de Broglie wavelength) and with an effective mass $m_{\text{eff}} \sim \rho\lambda_{\text{dB}}^3 \sim 10^7 \, M_\odot \gg m$. These quasiparticles can induce a secular collisional evolution of the halo as discussed in [138–141].

In conclusion, in the FDM model, the quantum core (soliton) is able to solve the core-cusp problem and the approximately isothermal halo accounts for the flat rotation curves of the galaxies. This core-halo structure is in qualitative agreement with the observations. However, as discussed in Sec. XV H, the FDM model cannot account for the universality of the surface density of DM halos $\Sigma_0^{\text{obs}} = 141^{+83}_{-52} \, M_\odot/\text{pc}^2$. This suggests that the constant potential from Eq. (E1) should be replaced by a more general potential such as the logarithmic potential of Eq. (53) leading to the logotropic model, which can account for the universality and the value of Σ_0^{obs}.

APPENDIX F: THE STRUCTURE OF LOGOTROPIC DM HALOS

In this appendix, we describe in detail the structure of logotropic DM halos. We use a nonrelativistic approach that is appropriate to DM halos. This appendix complements the discussion given in Sec. 5 of Ref. [1] and in Sec. XIV B of the present paper.

1. Density profile

In the TF approximation, the differential equation of hydrostatic equilibrium determining the density profile of a DM halo is given by Eq. (206). For the logotropic equation of state (55), it becomes

$$A\Delta\left(\frac{1}{\rho}\right) = 4\pi G\rho. \tag{F1}$$

If we define

$$\theta = \frac{\rho_0}{\rho}, \qquad \xi = \left(\frac{4\pi G\rho_0^2}{A}\right)^{1/2} r, \tag{F2}$$

where ρ_0 is the central density and $r_0 = (A/4\pi G\rho_0^2)^{1/2}$ is the logotropic core radius, we find that Eq. (F1) reduces to the Lane-Emden equation of index $n = -1$ [104],

$$\Delta\theta = \frac{1}{\theta} \tag{F3}$$

with the boundary conditions $\theta = 1$ and $\theta' = 0$ at $\xi = 0$.[74] This equation has been studied in detail in [1,103]. There exists an exact analytical solution $\theta_s = \xi/\sqrt{2}$, corresponding to $\rho_s = (A/8\pi G)^{1/2} r^{-1}$, called the singular logotropic sphere. The regular logotropic density profiles must be computed numerically. The normalized density profile $(\rho/\rho_0)(r/r_0)$ is universal.[75] It is plotted in Fig. 18 of [1]. The density profile of a logotropic DM halo has a core ($\rho \to$ cst when $r \to 0$) and decreases at large distances as $\rho \sim r^{-1}$. More precisely, for $r \to +\infty$, we have

$$\rho \sim \left(\frac{A}{8\pi G}\right)^{1/2}\frac{1}{r}, \tag{F4}$$

like for the singular logotropic sphere. This profile has an infinite mass because the density does not decrease sufficiently rapidly with the distance. This implies that, in the case of real DM halos, the logotropic equation of state (55) or the logotropic profile determined by Eq. (F1) cannot be valid at infinitely large distances (corresponding to very low densities).[76] The logotropic profile is expected to be surrounded by an extended envelope where the density decreases more rapidly like,

---

[74]As explained in footnote 66 the Lane-Emden equation of index $n = -1$ cannot be obtained from the equation of state of a polytrope of index $\gamma = 0$ (i.e., $n = -1$) which has a vanishing pressure gradient. One has to consider the limit $\gamma \to 0$ and $K \to \infty$ with $A = K\gamma$ finite, leading to the logotropic equation of state (55). In this sense, Eq. (F3) is a new equation which completes the class of Lane-Emden equations for standard polytrope.

[75]This universality is related to the homology invariance of the solutions of the Lane-Emden equation.

[76]This infinite mass problem does not rule out the logotropic model. Actually, we have the same problem with the isothermal sphere. The isothermal density profile decreases at large distances as $\rho \sim 1/(2\pi G\beta mr^2)$, like the singular isothermal sphere [104]. It has an infinite mass. Despite this problem, the isothermal density profile has often been used to model DM halos because it provides a good fit of their central parts (up to a few halo radii) and it can be justified by Lynden-Bell's statistical theory of violent collisionless relaxation [23,25,99,142]. In reality, the density of DM halos decreases more rapidly at large distances, typically as r^{-3}, like for the Burkert [116] and NFW [115] profiles. This can be explained in terms of incomplete relaxation (see, e.g., Appendix B of [25]). In [1,2] we have suggested that the logotropic model could be justified by a notion of generalized thermodynamics. In this context, the constant A in the logotropic distribution plays the role of a generalized temperature which is the counterpart of the temperature T in the isothermal distribution. This generalized thermodynamical interpretation strengthens the analogy between the isothermal and logotropic models.

e.g., r^{-3} (see footnote 76). In practice, we shall consider the logotropic profile up to a few halo radii r_h (see below).

We note that the density profiles of real DM halos obtained from observations display a core ($\rho \sim r^0$) followed by a region where the density decreases as r^{-1}, similar to the logotropic density profile. This r^{-1} decay can be seen in Fig. 6 (right) of Oh *et al.* [143] and in Fig. 3 (plate U11583) of Robles and Matos [144]. The fact that the slope of the density profile of DM halos close to the core radius r_h is approximately equal to -1 has also been pointed out by Burkert [145] (see in particular the upper right panel of his Fig. 1). These properties are in good agreement with the logotropic model.[77] However, at large distances, the density of real DM halos decreases more rapidly than r^{-1}, typically as r^{-2} or r^{-3}, consistent with the asymptotic behavior of the isothermal sphere [104] or with the asymptotic behaviors of the Burkert [116] and NFW [115] profiles. Now, we note that the logotropic density profile defined by Eqs. (F2) and (F3) has been obtained by neglecting quantum (or wave) effects. If we consider the logotropic GPP equations (219) and (220) it is possible that, like in the case of FDM (see Appendix E), quantum interferences build up a halo whose average density profile decreases as r^{-2} or r^{-3} at large distances [65].[78] It would be interesting to investigate this idea numerically. If this idea is correct, a "quantum" logotropic DM halo would possess a core ($\rho \sim r^0$) + an intermediate logotropic profile ($\rho \sim r^{-1}$) + an extended isothermal ($\rho \sim r^{-2}$) or NFW ($\rho \sim r^{-3}$) envelope, in agreement with the observations (see, e.g., [143–145]). This structure would be obtained in the TF approximation $m \gg m_0 = 3.57 \times 10^{-22}$ eV/c^2 (see Sec. XV F). If we go beyond the TF approximation (which is not satisfied for a boson mass $m \sim 10^{-22}$ eV/c^2), the DM halo should also possess a quantum core (soliton) like in the FDM model (see Appendix E).

Remark.—Using qualitative arguments, Ferreira and Avelino [5] have argued that logotropic DM halos are dynamically unstable. However, the stability of logotropic spheres must be considered carefully due to the fact that they have an infinite mass in an unbounded domain. The stability of box-confined logotropic configurations has been studied in detail in [103]. It is found that they are stable below a critical density contrast and unstable above it. These results are similar to those obtained for box-confined self-gravitating isothermal spheres [111]. Isothermal spheres have been used in many models of DM halos despite the fact that they have an infinite mass and that they are unstable above a critical density contrast leading to core collapse. Similar properties are expected for logotropic spheres.

2. Halo mass

The halo radius r_h is defined as the distance at which the central density ρ_0 is divided by 4. For logotropic DM halos, using Eq. (F2), it is given by

$$r_h = \left(\frac{A}{4\pi G \rho_0^2}\right)^{1/2} \xi_h, \tag{F5}$$

where ξ_h is determined by the equation

$$\theta(\xi_h) = 4. \tag{F6}$$

The normalized density profile $(\rho/\rho_0)(r/r_h)$ of logotropic DM halos is plotted in Fig. 19 of [1]. The halo mass M_h, which is the mass $M_h = \int_0^{r_h} \rho(r')4\pi r'^2 dr'$ contained within the sphere of radius r_h, is given by

$$M_h = 4\pi \frac{\theta'(\xi_h)}{\xi_h} \rho_0 r_h^3. \tag{F7}$$

Solving the Lane-Emden equation of index $n = -1$ [see Eq. (F3)], we numerically find

$$\xi_h = 5.85, \qquad \theta'_h = 0.693. \tag{F8}$$

This yields

$$r_h = 5.85 \left(\frac{A}{4\pi G}\right)^{1/2} \frac{1}{\rho_0} \tag{F9}$$

and

$$M_h = 1.49 \rho_0 r_h^3. \tag{F10}$$

3. Constant surface density

Eliminating the central density between Eqs. (F9) and (F10), we obtain the logotropic halo mass-radius relation

$$M_h = 8.71 \left(\frac{A}{4\pi G}\right)^{1/2} r_h^2. \tag{F11}$$

Since $M_h \propto r_h^2$ we see that the surface density Σ_0 is constant.[79] This is a very important property of logotropic DM halos [1]. From Eq. (F9), we get

---

[77]We note that the logotropic profile $\rho \sim r^{-1}$ may be wrongly interpreted in certain observations as a NFW cusp r^{-1} if the logotropic core is not sufficiently well resolved. Indeed, in that case, we see only the r^{-1} tail of the logotropic distribution, not the core ($\rho \sim r^0$). This may lead to the illusion that certain DM halos are cuspy in agreement with the NFW prediction while they are not [146].

[78]This halo may also be obtained in a purely classical model based on the Euler-Poisson equations with a logotropic equation of state. This corresponds to the TF approximation $\hbar \to 0$ of the logotropic GPP equations.

---

[79]This is consistent with the fact that the density of a logotropic DM halo decreases as r^{-1} at large distances.

$$\Sigma_0 = \rho_0 r_h = 5.85 \left(\frac{A}{4\pi G} \right)^{1/2}. \qquad \text{(F12)}$$

Therefore, all the logotropic DM halos have the same surface density, whatever their size, provided that A is interpreted as a universal constant. With the value of $A/c^2 = 2.10 \times 10^{-26} \text{ g m}^{-3}$ obtained from cosmological considerations (without free parameter) in Sec. VI we obtain $\Sigma_0^{\text{th}} = 133 \, M_\odot/\text{pc}^2$ in very good agreement with the value $\Sigma_0^{\text{obs}} = \rho_0 r_h = 141^{+83}_{-52} \, M_\odot/\text{pc}^2$ obtained from the observations [17]. On the other hand, Eq. (F10) may be rewritten as

$$M_h = 1.49 \, \Sigma_0 r_h^2 = 1.49 \frac{\Sigma_0^3}{\rho_0^2}. \qquad \text{(F13)}$$

We note that the ratio $M_h/(\Sigma_0 r_h^2) = 1.49$ in Eq. (F13) is in good agreement with the ratio $M_h/(\Sigma_0 r_h^2) = 1.60$ obtained from the observational Burkert profile (see Appendix D 4 of [25]). This is an additional argument in favor of the logotropic model.

4. The gravitational acceleration

We can define an average DM halo surface density by the relation

$$\langle \Sigma \rangle = \frac{M_h}{\pi r_h^2}. \qquad \text{(F14)}$$

For logotropic DM halos, we find

$$\langle \Sigma \rangle_{\text{th}} = \frac{M_h}{\pi r_h^2} = \frac{1.49}{\pi} \Sigma_0^{\text{th}} = 63.1 \, M_\odot/\text{pc}^2. \qquad \text{(F15)}$$

This theoretical value is in good agreement with the value $\langle \Sigma \rangle_{\text{obs}} = 72^{+42}_{-27}, M_\odot/\text{pc}^2$ obtained from the observations [147].[80]

The gravitational acceleration at the halo radius is

$$g = g(r_h) = \frac{GM_h}{r_h^2} = \pi G \langle \Sigma \rangle. \qquad \text{(F16)}$$

For logotropic DM halos, we find

$$g_{\text{th}} = \pi G \langle \Sigma \rangle_{\text{th}} = 1.49 G \Sigma_0^{\text{th}} = 2.76 \times 10^{-11} \text{ m/s}^2. \qquad \text{(F17)}$$

Again, this theoretical value is in good agreement with the measured value $g_{\text{obs}} = \pi G \langle \Sigma \rangle_{\text{obs}} = 3.2^{+1.8}_{-1.2} \times 10^{-11} \text{ m/s}^2$ of the gravitational acceleration [147].

---

[80]This measured value is based on the observations and on a fit of the density profile of DM halos by the Burkert profile [147].

The circular velocity at the halo radius is

$$v_h^2 = \frac{GM_h}{r_h}. \qquad \text{(F18)}$$

Using Eqs. (F13)–(F17), we obtain the relation

$$v_h^4 = GgM_h = \pi \langle \Sigma \rangle G^2 M_h = 1.49 \Sigma_0 G^2 M_h, \qquad \text{(F19)}$$

where g and Σ_0 are universal constants. This relation is connected to the Tully-Fisher relation [148] which involves the baryon mass M_b instead of the DM halo mass M_h via the cosmic baryon fraction $f_b = M_b/M_h \sim 0.17$. This yields $(M_b/v_h^4)^{\text{th}} = f_b/(1.49 \, \Sigma_0 G^2) = 46.4 \, M_\odot \, \text{km}^{-4} \, \text{s}^4$ which is close to the observed value $(M_b/v_h^4)^{\text{obs}} = 47 \pm 6 \, M_\odot \, \text{km}^{-4} \, \text{s}^4$ [19]. The Tully-Fisher relation is also a prediction of the modification of Newtonian dynamics (MOND) theory [149]. Using Eqs. (F17) and (208), we obtain

$$g_{\text{th}} = 0.0291 \sqrt{3(1 - \Omega_{\text{m},0})} H_0 c = 0.0419 \, H_0 c. \qquad \text{(F20)}$$

This relation explains why the fundamental constant $a_0 = g/f_b$ that appears in the MOND theory is of order $H_0 c/4 = 1.65 \times 10^{-10} \text{ m/s}^2$ (see the Remark in Sec. 3.3. of [4] for a more detailed discussion). Note, however, that our model is completely different from the MOND theory.

5. Logarithmic density slope

The logarithmic slope of the density profile of a DM halo is defined by

$$\alpha(r) = \frac{d \ln \rho}{d \ln r}. \qquad \text{(F21)}$$

For logotropic DM halos it can be expressed in terms of the Lane-Emden function θ by

$$\alpha(r) = -\frac{\xi \theta'}{\theta} = -v, \qquad \text{(F22)}$$

where $v = \xi \theta'/\theta$ is the Milne variable [104]. The logarithmic density slope $\alpha(r)$ of a logotropic DM halo is plotted in Fig. 23. It starts from $\alpha = 0$ at $r = 0$ (core) and tends to -1 when $r \to +\infty$. It reaches a minimum value $\alpha_{\text{min}} = -1.03$ at $r_* = 1.52 r_h$. We find that $\alpha = -0.3$ (corresponding to the typical logarithmic inner density slope of real DM halos found by [143,144,146]) at $r = 0.186 r_h$. Robles and Matos [144] define the core radius r_h^* by the condition $\alpha(r_h^*) = -1$. In the case of logotropic DM halos, r_h^* is consistent with our definition of the halo radius r_h since we find that $r_h^* = 0.890 r_h \sim r_h$.
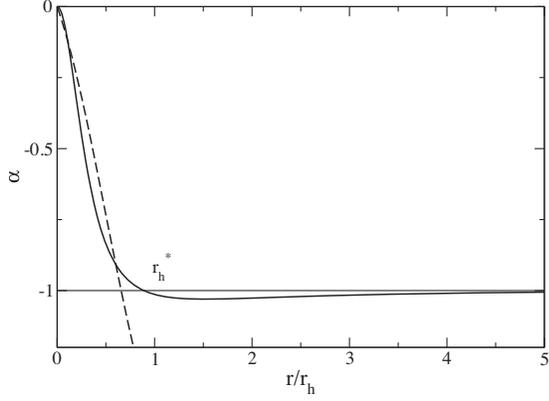
FIG. 23. Logarithmic density slope of the logotropic profile as a function of the radial distance normalized by the halo radius. It is compared to the logarithmic density slope of the Burkert profile (dashed line) from Eq. (D21). The two profiles are relatively close to each other for $r \leq r_h$. At $r \sim r_h$ the Burkert profile has an effective slope $\alpha \sim -1$ like the asymptotic slope of the logotrope. Asymptotically, the Burkert profile has a slope $\alpha \sim -3$, which is out of the frame of the figure.

6. Logarithmic circular velocity slope

The circular velocity of a DM halo is given by

$$v_c^2(r) = \frac{GM(r)}{r}, \qquad \text{(F23)}$$

where $M(r) = \int_0^r \rho(r')4\pi r'^2 dr'$ is the mass contained within the sphere of radius r. The logarithmic slope of the circular velocity profile is defined by

$$\beta(r) = \frac{d \ln v_c}{d \ln r}. \qquad \text{(F24)}$$

Using Eq. (F23) it can be written as

$$\beta(r) = \frac{1}{2}\left(\frac{d \ln M(r)}{d \ln r} - 1\right). \qquad \text{(F25)}$$

For logotropic DM halos, using the Lane-Emden equation (F3), we can establish that

$$\frac{d \ln M(r)}{d \ln r} = \frac{\xi}{\theta\theta'} = u, \qquad \text{(F26)}$$

where $u = \xi/(\theta\theta')$ is the Milne variable [104]. Therefore,

$$\beta(r) = \frac{1}{2}(u - 1). \qquad \text{(F27)}$$

The logarithmic slope $\beta(r)$ of the circular velocity of a logotropic DM halo is plotted in Fig. 24.
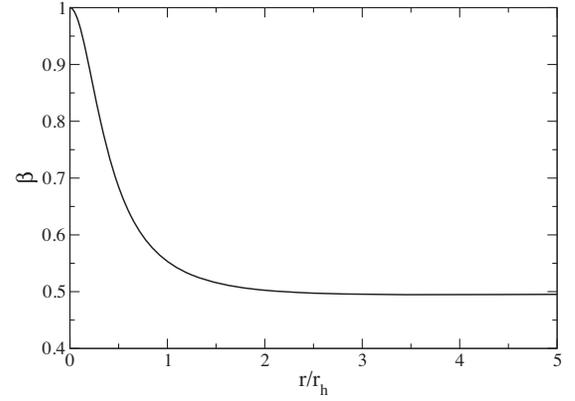
FIG. 24. Logarithmic circular velocity slope of the logotropic profile as a function of the radial distance normalized by the halo radius.

7. Comparison between the logotropic model and the fermionic and bosonic models of DM halos

It is an observational evidence that there is no DM halo below a certain mass and below a certain size. The smallest and most compact DM halos observed in the Universe are dSphs like Fornax. To fix the ideas we shall consider that the smallest halo observed in the Universe (what we call the minimum halo) has a mass[81]

$$(M_h)_{\min} = 10^8 \ M_\odot \quad \text{(Fornax)}. \qquad \text{(F28)}$$

It is also an observational fact that the surface density Σ_0 of DM halos is constant and that it has the universal value [17]

$$\Sigma_0^{\text{obs}} = \rho_0 r_h = 141^{+83}_{-52} \ M_\odot/\text{pc}^2. \qquad \text{(F29)}$$

In the case of fermionic or bosonic models of DM, the minimum halo is expected to correspond to the ground state $(T = 0)$ of the self-gravitating quantum system [105]. We can then combine the mass-radius relation $M_h(r_h)$ of a fermionic or bosonic DM halo at $T = 0$ (ground state) with the universal surface density Σ_0 from Eq. (F29) in order to express the mass $(M_h)_{\min}$, the radius $(r_h)_{\min}$, and the central density $(\rho_0)_{\max}$ of the minimum halo as a function of the characteristics (mass m and scattering length a_s) of the DM particle. For specified values of m and a_s we can thus obtain $(M_h)_{\min}$, $(r_h)_{\min}$, and $(\rho_0)_{\max}$. In practice, we proceed the other way round. We use the observed value of $(M_h)_{\min}$ given by Eq. (F28) to obtain the characteristics (m, a_s) of the DM particle. Once these characteristics are known, we can obtain the radius $(r_h)_{\min}$ and the central density $(\rho_0)_{\max}$ of the minimum halo. We can also plot the density profile of the minimum halo for these different

---

[81]We take this value as a reference in order to be consistent with our previous papers. If a possibly more relevant minimum mass is adopted, our numerical applications should be reconsidered but our main conclusions should not be altered.

models. These calculations are developed in detail in Sec. II of [105] (they are generalized in Sec. VII C of [105] to more complicated models by using a Gaussian ansatz). We can also obtain an estimate of the minimum halo mass and minimum halo radius as a function of m and a_s from the Jeans instability theory (see, e.g., Refs. [67,72] and Appendices H and I of [105]) but this method is less accurate. We note that the fermionic or bosonic models of DM halos are not fully predictive since (i) we have to assume the value of Σ_0 from the observations [see Eq. (F29)] and (ii) we need to know the value of m and a_s to determine $(M_h)_{\min}$, $(r_h)_{\min}$, and $(\rho_0)_{\max}$ theoretically [alternatively, we have to know the value of $(M_h)_{\min}$ to obtain m and a_s, which then yield $(r_h)_{\min}$ and $(\rho_0)_{\max}$].

In the case of the logotropic model, there is no unknown parameter. The universal constant surface density $\Sigma_0 = 133\ M_\odot/\mathrm{pc}^2$ of the DM halos is predicted by this model (see [1] and Appendix F 3). As a result, the characteristics of a logotropic DM halo of mass M_h are fully characterized by Eq. (F13). For $(M_h)_{\min} = 10^8\ M_\odot$, we obtain (without free parameter)

$$(r_h)_{\min} = 710\ \mathrm{pc}, \qquad (\rho_0)_{\max} = 0.187\ M_\odot \mathrm{pc}^{-3}. \quad \text{(F30)}$$

We note, however, that the minimum halo mass $(M_h)_{\min}$ is not directly determined by the logotropic model since the mass-radius relation $M_h(r_h)$ of *all* the logotropic DM halos satisfies the constraint from Eq. (F29).[82]

The density profile of a logotropic DM halo of mass $(M_h)_{\min} = 10^8\ M_\odot$ (minimum halo) is plotted in Fig. 25. It can be compared to the profiles obtained in Sec. II of [105] by assuming that DM is made of fermions (see Fig. 1 of [105]), noninteracting BECs (see Fig. 2 of [105]), or self-interacting BECs in the TF approximation (see

---

[82]In the fermionic or bosonic DM models, the value of the minimum halo mass $(M_h)_{\min}$ results from the combination of the mass-radius relation of the ground state $M_h(r_h)$ with the constraint from Eq. (F29), for given values of m and a_s [105]. For example, for noninteracting bosons of mass $m \sim 10^{-22}\ \mathrm{eV}/c^2$, we get $(M_h)_{\min} \sim 10^8\ M_\odot$ and $(r_h)_{\min} \sim 1\ \mathrm{kpc}$. However, for bigger halos, these purely quantum models cannot account for the observed constant surface density of DM halos (see Sec. XV H). Note that, if we consider the quantum logotropic model (going beyond the TF approximation), the core of DM halos has both a quantum and a logotropic nature. It is possible that the quantum core dominates in small halos [we have indeed seen that the TF approximation is marginally valid in small DM halos of mass $(M_h)_{\min} \sim 10^8\ M_\odot$ for $m \sim m_0 \sim 10^{-22}\ \mathrm{eV}/c^2$] and that the logotropic core dominates in large DM halos. In that case, the mass and size $(M_h)_{\min} \sim 10^8\ M_\odot$ and $(r_h)_{\min} \sim 1\ \mathrm{kpc}$ of the minimum halo could be due to quantum effects (the small boson mass $m \sim 10^{-22}\ \mathrm{eV}/c^2$) like in the FDM model—in agreement with the Jeans study of Sec. XVI D—while the universal surface density $\Sigma_0 = 141\ M_\odot/\mathrm{pc}^2$ of bigger DM halos could be due to logotropic effects (the fundamental constant $A/c^2 = 2.10 \times 10^{-26}\ \mathrm{g\,m}^{-3}$ of our model). This important point is further discussed in Appendix G.
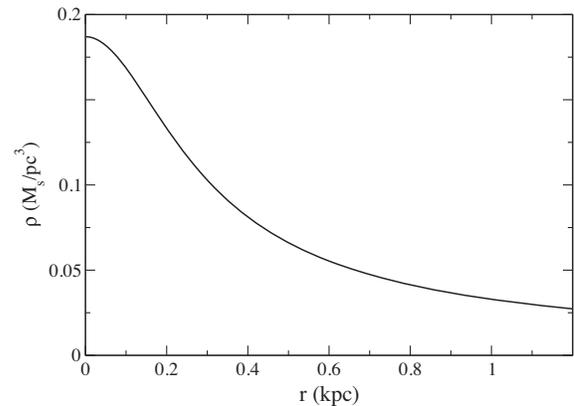
FIG. 25. Density profile of the minimum halo of mass $(M_h)_{\min} = 10^8\ M_\odot$ in the logotropic model.

Fig. 3 of [105]). We see that the density of a logotropic DM halo decreases less rapidly than the density of a fermionic or bosonic DM halo in its ground state. Indeed, it decays as r^{-1} at large distances, while the density profile of noninteracting BECs decreases exponentially rapidly and the density profiles of fermions and BECs in the TF approximation have a compact support. As mentioned previously, the logotropic profile is not valid at large distances because it would have an infinite mass. In reality, the logotropic core is surrounded by an outer envelope where the density decreases more rapidly than r^{-1}, presumably as r^{-3}.

Remark.—As discussed in Appendix F 1, the r^{-1} decay of the logotropic density profile is in agreement with the density profile of real DM halos close to the halo radius. This r^{-1} decay is responsible for the universal surface density of DM halos and the fact that their mass-radius relation behaves as $M_h \propto r_h^2$ in agreement with the observations [17]. By contrast, fermionic and bosonic DM halos do not present a region where the density decreases as r^{-1}. As a result, they do not have a constant surface density Σ_0 and their mass-radius relation is not in agreement with the observations (see the discussion at the end of Sec. XV H). For large fermionic or bosonic DM halos, the constraint from Eq. (F29) could be satisfied by taking into account the presence of an isothermal halo surrounding the quantum core and assuming that the effective "central" density of the halo corresponds to the density at the contact between the quantum core and the halo (see Ref. [25] for details). In that case, we have to identify the halo radius r_h with the isothermal core radius r_0, not with the quantum core radius R_c, and we have to allow the temperature T to change from halo to halo according to Eq. (168) of [25] in order to maintain a constant surface density. Alternatively, if the constraint (F29) cannot be satisfied in all DM halos, the (pure) fermionic and bosonic DM models are in trouble and the logotropic model may be an interesting substitute.

APPENDIX G: THE TYPICAL MASS OF THE DM PARTICLE

Let us assume that DM halos are described by the quantum logotropic model and that dSphs (with typical mass $10^8 M_\odot$) are just at the limit of validity of the TF approximation. This means that they can be marginally described both by the FDM model ($\hbar \neq 0$ and $A = 0$) and by the classical logotropic model ($A \neq 0$ and $\hbar = 0$).

The mass-radius relation of FDM halos is [see Eq. (E17)]

$$M = 9.95 \frac{\hbar^2}{Gm^2 R}. \tag{G1}$$

The mass-radius relation of classical logotropic DM halos is [see Eq. (F13)]

$$M = 1.49 \, \Sigma_0 R^2, \tag{G2}$$

where $\Sigma_0 = 5.85(A/4\pi G)^{1/2} = 133 \, M_\odot/\text{pc}^2$ [see Eq. (F12)] is the universal surface density of DM halos. If we combine these two relations, we get

$$(M_h)_{\min} = 5.28 \left(\frac{\Sigma_0 \hbar^4}{G^2 m^4} \right)^{1/3}. \tag{G3}$$

This formula determines the mass $(M_h)_{\min}$ of the minimum halo as a function of the boson mass m. Inversely, knowing the minimum halo mass from the observations, we can determine the boson mass. Taking $M = 10^8 M_\odot$ we find $m = 3.46 \times 10^{-22}$ eV/c². This explains why the mass $m_0 = 3.57 \times 10^{-22}$ eV/c² determining the domain of validity of the TF approximation in DM halos similar to dSphs happens to coincide with the boson mass $m \sim 10^{-22}$ eV/c² (see Sec. XV F). We then obtain the minimum halo radius

$$(r_h)_{\min} = 1.88 \left(\frac{\hbar^2}{Gm^2 \Sigma_0} \right)^{1/3} = 709 \text{ pc}, \tag{G4}$$

which is in good agreement with the typical size of dSphs.

On the other hand, the Jeans mass in the FDM model is (see Appendix H of [105])

$$M_J = \frac{\pi}{6} \left(\frac{\pi^3 \hbar^2 \rho_{m,0}^{1/3}}{Gm^2} \right)^{3/4}, \tag{G5}$$

where $\rho_{m,0}$ is the present matter density in the homogeneous background. Writing $(M_h)_{\min} = \chi M_J$ with $\chi \sim 10$–100 (see Appendix I of [105]) and using Eqs. (G3) and (G5) we get

$$m = 4.89 \chi^6 \frac{\hbar \rho_{m,0}^{3/2}}{\Sigma_0^2 G^{1/2}}. \tag{G6}$$

Using $\rho_{m,0} = 0.0178\Lambda/G$ and $\Sigma_0 = 0.0207 c\sqrt{\Lambda}/G$ [see Eqs. (155) and (156) of [105]], we finally obtain

$$m = 27.1 \chi^6 \frac{\hbar \sqrt{\Lambda}}{c^2}. \tag{G7}$$

Therefore, the DM boson mass m is equal to the cosmon mass (190) multiplied by a huge prefactor $\sim 10^{11}$ (this is because χ is raised to the power 6). The cosmon mass gives the fundamental mass scale of bosons [49,105].

APPENDIX H: NUMERICAL VALUES FROM OBSERVATIONS

In our numerical applications, we have taken the following values from the Planck Collaboration [34]:

$$H_0 = 2.195 10^{-18} \text{ s}^{-1}, \tag{H1}$$

$$\epsilon_0 = 7.75 \times 10^{-7} \text{ g m}^{-1} \text{s}^{-2}, \tag{H2}$$

$$\epsilon_0/c^2 = 8.62 \times 10^{-24} \text{ g m}^{-3}, \tag{H3}$$

$$\Omega_{\text{de},0} = 0.6911, \tag{H4}$$

$$\Omega_{\text{dm},0} = 0.2589, \tag{H5}$$

$$\Omega_{\text{b},0} = 0.0486, \tag{H6}$$

$$\Omega_{\text{m},0} = 0.3089. \tag{H7}$$

[1] P. H. Chavanis, Eur. Phys. J. Plus **130**, 130 (2015).

[2] P. H. Chavanis, Phys. Lett. B **758**, 59 (2016).

[3] P. H. Chavanis and S. Kumar, J. Cosmol. Astropart. Phys. 5 (2017) 018.

[4] P. H. Chavanis, Phys. Dark Universe **24**, 100271 (2019).

[5] V. M. C. Ferreira and P. P. Avelino, Phys. Lett. B **770**, 213 (2017).

[6] S. Capozziello, R. D'Agostino, and O. Luongo, Phys. Dark Universe **20**, 1 (2018).

[7] S. D. Odintsov, V. K. Oikonomou, A. V. Timoshkin, E. N. Saridakis, and R. Myrzakulov, Ann. Phys. (Amsterdam) **398**, 238 (2018).

[8] S. Capozziello, R. D'Agostino, R. Giambò, and O. Luongo, Phys. Rev. D **99**, 023532 (2019).

[9] K. Boshkayev, R. D'Agostino, and O. Luongo, Eur. Phys. J. C **79**, 332 (2019).

[10] A. Al Mamon and S. Saha, Int. J. Mod. Phys. D **29**, 2050097 (2020).

[11] K. Boshkayev, T. Konysbayev, O. Luongo, M. Muccino, and F. Pace, Phys. Rev. D **104,** 023520 (2021).

[12] H. Benaoum, P. H. Chavanis, and H. Quevedo, Universe **8,** 468 (2022).

[13] R. R. Caldwell, M. Kamionkowski, and N. N. Weinberg, Phys. Rev. Lett. **91,** 071301 (2003).

[14] P. H. Frampton, K. J. Ludwick, and R. J. Scherrer, Phys. Rev. D **84,** 063003 (2011).

[15] J. Kormendy and K. C. Freeman, in *Proceedings of the IAU Symposium 220, Dark Matter in Galaxies*, edited by S. D. Ryder, D. J. Pisano, M. A. Walker, and K. C. Freeman (Astronomical Society of the Pacific, San Francisco, 2004), p. 377.

[16] M. Spano, M. Marcelin, P. Amram, C. Carignan, B. Epinat, and O. Hernandez, Mon. Not. R. Astron. Soc. **383,** 297 (2008).

[17] F. Donato, G. Gentile, P. Salucci, C. Frigerio Martins, M. I. Wilkinson, G. Gilmore, E. K. Grebel, A. Koch, and R. Wyse, Mon. Not. R. Astron. Soc. **397,** 1169 (2009).

[18] L. E. Strigari , J. S. Bullock, M. Kaplinghat, J. D. Simon, M. Geha, B. Willman, and M. G. Walker, Nature (London) **454,** 1096 (2008).

[19] S. S. McGaugh, Astron. J. **143,** 40 (2012).

[20] A. Suárez and P. H. Chavanis, Phys. Rev. D **95,** 063515 (2017).

[21] P. H. Chavanis, arXiv:2109.05963.

[22] P. H. Chavanis, Phys. Rev. D **106,** 043502 (2022).

[23] P. H. Chavanis, M. Lemou, and F. Méhats, Phys. Rev. D **92,** 123527 (2015).

[24] P. H. Chavanis, Eur. Phys. J. Plus **132,** 248 (2017).

[25] P. H. Chavanis, Phys. Rev. D **100,** 083022 (2019).

[26] A. Burkert, Astrophys. J. **904,** 161 (2020).

[27] H. Deng, M. P. Hertzberg, M. H. Namjoo, and A. Masoumi, Phys. Rev. D **98,** 023513 (2018).

[28] B. Li, T. Rindler-Daller, and P. R. Shapiro, Phys. Rev. D **89,** 083536 (2014).

[29] A. Suárez and P. H. Chavanis, Phys. Rev. D **92,** 023510 (2015).

[30] A. Suárez and P. H. Chavanis, J. Phys. Conf. Ser. **654,** 012008 (2015).

[31] P. H. Chavanis and T. Matos, Eur. Phys. J. Plus **132,** 30 (2017).

[32] A. H. Guth, Phys. Rev. D **23,** 347 (1981).

[33] Planck Collaboration, Astron. Astrophys. **571,** A66 (2014).

[34] Planck Collaboration, Astron. Astrophys. **594,** A13 (2016).

[35] S. Weinberg, *Gravitation and Cosmology* (John Wiley, New York, 2002).

[36] A. Arbey, J. Lesgourgues, and P. Salati, Phys. Rev. D **65,** 083514 (2002).

[37] J.-A. Gu and W.-Y. P. Hwang, Phys. Lett. B **517,** 1 (2001).

[38] L. A. Boyle, R. R. Caldwell, and M. Kamionkowski, Phys. Lett. B **545,** 17 (2002).

[39] M. S. Turner, Phys. Rev. D **28,** 1243 (1983).

[40] L. H. Ford, Phys. Rev. D **35,** 2955 (1987).

[41] P. J. E. Peebles and A. Vilenkin, Phys. Rev. D **60,** 103506 (1999).

[42] T. Matos and L. A. Ureña-López, Phys. Rev. D **63,** 063506 (2001).

[43] M. Joyce, Phys. Rev. D **55,** 1875 (1997).

[44] N. Bilic, G. B. Tupper, and R. D. Viollier, Phys. Lett. B **535,** 17 (2002).

[45] M. Makler, S. Q. Oliveira, and I. Waga, Phys. Lett. B **555,** 1 (2003).

[46] A. Kamenshchik, U. Moschella, and V. Pasquier, Phys. Lett. B **511,** 265 (2001).

[47] S. Weinberg, Rev. Mod. Phys. **61,** 1 (1989).

[48] T. Padmanabhan, Phys. Rep. **380,** 235 (2003).

[49] P. H. Chavanis, Phys. Dark Universe **37,** 101098 (2022).

[50] P. Steinhardt, in *Critical Problems in Physics*, edited by V. L. Fitch and D. R. Marlow (Princeton University Press, Princeton, NJ, 1997).

[51] I. Zlatev, L. Wang, and P. J. Steinhardt, Phys. Rev. Lett. **82,** 896 (1999).

[52] P. H. Chavanis, Eur. Phys. J. Plus **129,** 38 (2014).

[53] A. Arvanitaki, S. Dimopoulos, S. Dubovsky, N. Kaloper, and J. March-Russell, Phys. Rev. D **81,** 123530 (2010).

[54] A. S. Goldhaber and M. M. Nieto, Rev. Mod. Phys. **82,** 939 (2010).

[55] S. Tsujikawa, Classical Quantum Gravity **30,** 214003 (2013).

[56] P. S. Wesson, Mod. Phys. Lett. A **19,** 1995 (2004).

[57] C. G. Böhmer and T. Harko, Found. Phys. **38,** 216 (2008).

[58] R. D. Peccei, J. Sola, and C. Wetterich, Phys. Lett. B **195,** 183 (1987).

[59] C. Wetterich, Nucl. Phys. **B302,** 668 (1988).

[60] J. Sola, Phys. Lett. B **228,** 317 (1989).

[61] J. Sola, Int. J. Mod. Phys. A **05,** 4225 (1990).

[62] I. L. Shapiro and J. Sola, Phys. Lett. B **475,** 236 (2000).

[63] A. S. Eddington, Proc. R. Soc. A **133,** 605 (1931).

[64] E. Madelung, Z. Phys. **40,** 322 (1927).

[65] P. H. Chavanis, Eur. Phys. J. B **95,** 48 (2022).

[66] P. H. Chavanis (to be published).

[67] A. Suárez and P. H. Chavanis, Phys. Rev. D **98,** 083529 (2018).

[68] P. H. Chavanis, Phys. Rev. D **84,** 043531 (2011).

[69] P. H. Chavanis, Astron. Astrophys. **537,** A127 (2012).

[70] S. Dodelson, *Modern Cosmology* (Academic Press, New York, 2003).

[71] P. H. Chavanis, Universe **6,** 226 (2020).

[72] P. H. Chavanis, Phys. Rev. D **103,** 123551 (2021).

[73] J. C. Fabris, S. V. B. Gonçalves, and P. E. de Souza, Gen. Relativ. Gravit. **34,** 53 (2002).

[74] J. C. Fabris, S. V. B. Gonçalves, and P. E. de Souza, Gen. Relativ. Gravit. **34,** 2111 (2002).

[75] H. B. Sandvik, M. Tegmark, M. Zaldarriaga, and I. Waga, Phys. Rev. D **69,** 123524 (2004).

[76] D. Carturan and F. Finelli, Phys. Rev. D **68,** 103501 (2003).

[77] L. Amendola, F. Finelli, C. Burigana, and D. Carturan, J. Cosmol. Astropart. Phys. 07 (2003) 005.

[78] P. P. Avelino, L. M. G. Beça, J. P. M. de Carvalho, C. J. A. P. Martins, and P. Pinto, Phys. Rev. D **67,** 023511 (2003).

[79] A. Dev, J. S. Alcaniz, and D. Jain, Phys. Rev. D **67,** 023515 (2003).

[80] J. S. Alcaniz, D. Jain, and A. Dev, Phys. Rev. D **67,** 043514 (2003).

[81] T. Multamäki, M. Manera, and E. Gaztañaga, Phys. Rev. D **68,** 023004 (2003).

[82] R. Bean and O. Doré, Phys. Rev. D **68,** 023515 (2003).

[83] L. M. G. Beça, P. P. Avelino, J. P. M. de Carvalho, and C. J. A. P. Martins, Phys. Rev. D **67,** 101301(R) (2003).

[84] N. Bilic, R. J. Lindebaum, G. B. Tupper, and R. D. Viollier, J. Cosmol. Astropart. Phys. 11 (2004) 008.

[85] N. Bilic, G. B. Tupper, and R. D. Viollier, Phys. Rev. D **80,** 023515 (2009).

[86] N. Bilic, G. B. Tupper, and R. D. Viollier, in *Physics Beyond the Standard Models of Particles, Cosmology and Astrophysics*, edited by H. V. Klapdor-Kleingrothaus, I. V. Krivosheina, and R. Viollier (World Scientific Publishing, Singapore, 2011), pp. 503–510.

[87] P. P. Avelino, L. M. G. Beça, J. P. M. de Carvalho, C. J. A. P. Martins, and E. J. Copeland, Phys. Rev. D **69,** 041301(R) (2004).

[88] P. P. Avelino, K. Bolejko, and G. F. Lewis, Phys. Rev. D **89,** 103004 (2014).

[89] A. Abdullah, A. A. El-Zant, and A. Ellithi, arXiv:2108.03260.

[90] W. Hu, Astrophys. J. **506,** 485 (1998).

[91] R. R. R. Reis, I. Waga, M. O. Calvão, and S. E. Jóras, Phys. Rev. D **68,** 061302 (2003).

[92] R. R. R. Reis, M. Makler, and I. Waga, Phys. Rev. D **69,** 101301 (2004).

[93] R. Maartens, Living Rev. Relativity **7,** 7 (2004).

[94] J. E. Kim, G. B. Tupper, and R. D. Viollier, Phys. Lett. B **593,** 209 (2004).

[95] R. Jackiw, *Lectures on Fluid Dynamics. A Particle Theorist's View of Supersymmetric, Non-Abelian, Non-commutative Fluid Mechanics and d-Branes* (Springer, New York, 2002).

[96] P. Creminelli, G. D'Amico, J. Norena, and F. Vernizzi, J. Cosmol. Astropart. Phys. 02 (2009) 018.

[97] S. Kumar and A. A. Sen, J. Cosmol. Astropart. Phys. 10 (2014) 036.

[98] T. Padmanabhan and T. Roy Choudhury, Phys. Rev. D **66,** 081301(R) (2002).

[99] D. Lynden-Bell, Mon. Not. R. Astron. Soc. **136,** 101 (1967).

[100] E. Seidel and W. M. Suen, Phys. Rev. Lett. **72,** 2516 (1994).

[101] B. Carvente, V. Jaramillo, C. Escamilla-Rivera, and D. Núñez, Mon. Not. R. Astron. Soc. **503,** 4008 (2021).

[102] P. H. Chavanis, Phys. Rev. D **98,** 023009 (2018).

[103] P. H. Chavanis and C. Sire, Physica (Amsterdam) **375A,** 140 (2007).

[104] S. Chandrasekhar, *An Introduction to the Study of Stellar Structure* (Dover, New York, 1958).

[105] P. H. Chavanis, Phys. Rev. D **100,** 123506 (2019).

[106] H. Anton and P. C. Schmidt, Intermetallics **5,** 449 (1997).

[107] P. Debye, Ann. Phys. (N.Y.) **344,** 789 (1912).

[108] E. Grüneisen, Ann. Phys. (N.Y.) **344,** 257 (1912).

[109] P. H. Chavanis, Eur. Phys. J. Plus **130,** 181 (2015).

[110] P. H. Chavanis, Phys. Rev. D **92,** 103004 (2015).

[111] P. H. Chavanis, Astron. Astrophys. **381,** 340 (2002).

[112] C. M. Müller, Phys. Rev. D **71,** 047302 (2005).

[113] P. P. Avelino, L. M. G. Beca, J. P. M. de Carvalho, and C. J. A. P. Martins, J. Cosmol. Astropart. Phys. 09 (2003) 002.

[114] J. C. Fabris, S. V. B. Gonçalves, and R. de Sá Ribeiro, Gen. Relativ. Gravit. **36,** 211 (2004).

[115] J. F. Navarro, C. S. Frenk, and S. D. M. White, Mon. Not. R. Astron. Soc. **462,** 563 (1996).

[116] A. Burkert, Astrophys. J. **447,** L25 (1995).

[117] G. F. R. Ellis and M. S. Madsen, Classical Quantum Gravity **8,** 667 (1991).

[118] T. Padmanabhan, Phys. Rev. D **66,** 021301 (2002).

[119] E. J. Copeland, M. Sami, and S. Tsujikawa, Int. J. Mod. Phys. D **15,** 1753 (2006).

[120] K. Bamba, S. Capozziello, S. Nojiri, and S. D. Odintsov, Astrophys. Space Sci. **342,** 155 (2012).

[121] P. H. Chavanis, Eur. Phys. J. Plus **129,** 222 (2014).

[122] V. Gorini, A. Kamenshchik, U. Moschella, and V. Pasquier, Phys. Rev. D **69,** 123512 (2004).

[123] W. Hu, R. Barkana, and A. Gruzinov, Phys. Rev. Lett. **85,** 1158 (2000).

[124] H. Y. Schive, T. Chiueh, and T. Broadhurst, Nat. Phys. **10,** 496 (2014).

[125] H. Y. Schive, M.-H. Liao, T.-P. Woo, S.-K. Wong, T. Chiueh, T. Broadhurst, and W-Y. Pauchy Hwang, Phys. Rev. Lett. **113,** 261302 (2014).

[126] B. Schwabe, J. Niemeyer, and J. Engels, Phys. Rev. D **94,** 043513 (2016).

[127] P. Mocz, L. Lancaster, A. Fialkov, F. Becerra, and P. H. Chavanis, Phys. Rev. D **97,** 083519 (2018).

[128] J. Veltmaat, J. C. Niemeyer, and B. Schwabe, Phys. Rev. D **98,** 043509 (2018).

[129] P. Mocz *et al.*, Phys. Rev. Lett. **123,** 141301 (2019).

[130] P. Mocz *et al.*, Mon. Not. R. Astron. Soc. **494,** 2027 (2020).

[131] J. Veltmaat, B. Schwabe, and J. C. Niemeyer, Phys. Rev. D **101,** 083518 (2020).

[132] P. Mocz, M. Vogelsberger, V. H. Robles, J. Zavala, M. Boylan-Kolchin, A. Fialkov, and L. Hernquist, Mon. Not. R. Astron. Soc. **471,** 4559 (2017).

[133] M. Membrado, A. F. Pacheco, and J. Sanudo, Phys. Rev. A **39,** 4207 (1989).

[134] P. H. Chavanis and L. Delfini, Phys. Rev. D **84,** 043532 (2011).

[135] P. H. Chavanis, Phys. Rev. D **101,** 063532 (2020).

[136] B. Eggemeier and J. C. Niemeyer, Phys. Rev. D **100,** 063528 (2019).

[137] N. Bar, D. Blas, K. Blum, and S. Sibiryakov, Phys. Rev. D **98,** 083027 (2018).

[138] L. Hui, J. Ostriker, S. Tremaine, and E. Witten, Phys. Rev. D **95,** 043541 (2017).

[139] B. Bar-Or, J. B. Fouvry, and S. Tremaine, Astrophys. J. **871,** 28 (2019).

[140] B. Bar-Or, J. B. Fouvry, and S. Tremaine, Astrophys. J. **915,** 27 (2021).

[141] P. H. Chavanis, Eur. Phys. J. Plus **136,** 703 (2021).

[142] P. H. Chavanis, M. Lemou, and F. Méhats, Phys. Rev. D **91,** 063531 (2015).

[143] S.-H. Oh *et al.*, Astrophys. J. **142,** 24 (2011).

[144] V. H. Robles and T. Matos, Mon. Not. R. Astron. Soc. **422,** 282 (2012).

[145] A. Burkert, Astrophys. J. **808,** 158 (2015).

[146] W. J. G. de Blok, S. S. McGaugh, A. Bosma, and V. C. Rubin, Astrophys. J. **552,** L23 (2001).

[147] G. Gentile, B. Famaey, H. Zhao, and P. Salucci, Nature (London) **461,** 627 (2009).

[148] R. B. Tully and J. R. Fisher, Astron. Astrophys. **54,** 661 (1977).

[149] M. Milgrom, Astrophys. J. **270,** 365 (1983).